RECONCILING HIGH EFFICIENCY WITH LOW LATENCY IN THE DATACENTER

A DISSERTATION
SUBMITTED TO THE DEPARTMENT OF ELECTRICAL ENGINEERING
AND THE COMMITTEE ON GRADUATE STUDIES
OF STANFORD UNIVERSITY
IN PARTIAL FULFILLMENT OF THE REQUIREMENTS
FOR THE DEGREE OF
DOCTOR OF PHILOSOPHY

David Lo
June 2015

This dissertation is online at: http://purl.stanford.edu/yb021pv0010

I certify that I have read this dissertation and that, in my opinion, it is fully adequate in scope and quality as a dissertation for the degree of Doctor of Philosophy.

Christos Kozyrakis, Primary Adviser

I certify that I have read this dissertation and that, in my opinion, it is fully adequate in scope and quality as a dissertation for the degree of Doctor of Philosophy.

Oyekunle Olukotun

I certify that I have read this dissertation and that, in my opinion, it is fully adequate in scope and quality as a dissertation for the degree of Doctor of Philosophy.

Mendel Rosenblum

Approved for the Stanford University Committee on Graduate Studies.

Patricia J. Gumport, Vice Provost for Graduate Education

This signature page was generated electronically upon submission of this dissertation in electronic format. An original signed hard copy of the signature page is on file in University Archives.

Abstract

Web services are an integral part of today's society, with billions of people using the Internet regularly. The Internet's popularity is in no small part due to the near-instantaneous access to large amounts of personalized information. Online services such as web search (Bing, Google), social networking (Facebook, Twitter, LinkedIn), online maps (Bing Maps, Google Maps, NavQuest), machine translation (Bing Translate, Google Translate), and webmail (GMail, Outlook.com) are all portals to vast amounts of information, filtered to only show relevant results with sub-second response times. The new services and capabilities enabled by these services are also responsible for huge economic growth.

Online services are typically hosted in warehouse-scale computers located in large datacenters. These datacenters are run at a massive scale in order to take advantage of economies of scale. A single datacenter can comprise of 50,000 servers, draw tens of megawatts of power, and cost hundreds of millions to billions of dollars to construct. When considering the large numbers of datacenters worldwide, the total impact of datacenters is quite significant. For instance, the electricity consumed by all datacenters is equivalent to the output of 30 large nuclear power plants. At the same time, demand for additional compute capacity of datacenters is on the rise because of the rapid growth in Internet users and the increase in computational complexity of online services.

This dissertation focuses on improving datacenter efficiency in the face of latency-critical online services. There are two major components of this effort. The first is to improve the energy efficiency of datacenters, which will improve the operational expenses of the datacenter and help mitigate the growing environmental footprint of operating datacenters. The first two systems we introduce, autoturbo and PEGASUS, fall under this category. The second efficiency opportunity we pursue is to increase the resource efficiency of datacenters by enabling higher utilization. Higher resource efficiency leads to significantly increased capabilities without increasing the capital expenses of owning a datacenter and is critical to future scaling of datacenter capacity. The third system we describe, Heracles, targets the resource efficiency opportunity for current and future datacenters.

There are two avenues of improving energy efficiency that we investigate. We examine methods of improving energy efficiency of servers when they are running at peak load and when they are not. Both cases are important because of diurnal load variations on latency-critical online services that can cause the utilization of servers to vary from idle to full load in a 24 hour period. Latency-critical workloads present a

unique set of challenges that have made improving their energy efficiency difficult. Previous approaches in power management have run afoul of the performance sensitivity of latency-critical workloads. Furthermore, latency-critical workloads do not contain sufficient periods of idleness, complicating efforts reduce their power footprint via deep-sleep states.

In addition to improving energy efficiency, this dissertation also studies the improvement of resource efficiency. This opportunity takes advantage of the fact that datacenters are chronically run at low utilizations, with an industry average of 10%-50% utilization. Ironically, the low utilization of datacenters is not caused by a lack of work, but rather because of fears of performance interference between different workloads. Large-scale latency-critical workloads exacerbate this problem, as they are typically run on dedicated servers or with greatly exaggerated resource reservations. Thus, high resource efficiency through high utilization is obtained by enabling workloads to co-exist with each other on the same server without causing performance degradation.

In this dissertation, we describe three practical systems to improve the efficiency of datacenters. Autoturbo uses machine learning to improve the efficiency of servers running at peak load for a variety of energy efficiency metrics. By intelligently selecting the proper power mode on modern CPUs, autoturbo can improve Energy Delay Product by up to 47%. PEGASUS improves energy efficiency for large-scale latency-critical workloads by using a feedback loop to safely reduce the power consumed by servers at low utilizations. An evaluation of PEGASUS on production Google websearch yields power savings of up to 20% on a full-sized production cluster. Finally, Heracles improves datacenter utilization by performing coordinated resource isolation on servers to ensure that latency-critical workloads will still meet their latency guarantees, enabling other jobs to be co-located on the same server. We tested Heracles on several production Google workloads and demonstrated an average server utilization of 90%, opening up the potential for integer multiple increases in resource and cost efficiency.

Acknowledgements

First and foremost, I would like to thank my thesis advisor, Christos Kozyrakis. Christos has been a wonderful source of advice, mentorship, guidance, and support ever since I started working with him the summer after my sophomore year as an undergraduate. This thesis would not have been possible if not for Christos's insights into future challenges facing computer architects and his percipient advice throughout my academic career. It has been a great pleasure doing research with him.

I would also like to thank other Stanford faculty for their advice and guidance. Thanks to the Pervasive Parallelism Lab (PPL) faculty and the Stanford Experimental Datacenter Lab (SEDCL) faculty for fostering a productive research environment: Mendel Rosenblum, Kunle Olukotun, Mark Horowitz, Bill Dally, John Ousterhout, Alex Aiken, Balaji Prabhakar, and Pat Hanrahan.

A significant portion of my dissertation is based on research that I performed while at Google. This was made possible only with the support of Liqun Cheng, Rama Govindaraju, Partha Ranganathan, Luiz Barroso, Chris Johnson, Alex Kritikos, Mahesh Palekar, Nadav Eiron, and Peter Dahl. It was only through their assistance that I was able to run real-world experiments with production Google workloads on Google hardware, a feat that cannot be replicated anywhere else.

I would like to thank my fellow graduate students in Christos's research group, both past and present: Daniel Sanchez, Jacob Leverich, Christina Delimitrou, Adam Belay, Richard Yoo, Mike Dalton, Hari Kannan, Woongki Baek, Raghu Prabhakar, Grant Ayers, Mingyu Gao, Sam Grossman, Ana Klimovic, Camilo Moreno, Rakesh Ramesh, Greg Kehoe, and Felipe Munera. Daniel introduced me to research when he was supervising my REU project that fateful summer after sophomore year, and his dedication as a mentor was responsible for setting me on the path to a PhD. It's been a pleasure collaborating and co-authoring papers with Daniel and Richard, as well as with Krishna Malladi and Jeremy Sugerman. Jacob was an excellent sysadmin, and I am envious of the sparsity of cluster downtime under his watch.

I also want to thank Mendel Rosenblum and Kunle Olukotun for taking the time to be my dissertation readers, Mark Horowitz for being the fifth examiner on my defense committee, and Eric Darve for chairing said committee. I would like to extend appreciation to our wonderful admins, Sue George and Teresa Lynn. I am grateful to Google, which has supported research that became a critical component of my dissertation through two internships and a Google PhD Fellowship.

Many others contributed to my personal growth and well-being throughout my studies at Stanford. I

would like to thank Mom, Dad, and Michael for their love, encouragement, and support even when I was half a world away. I would also like to thank my friends for their unquestionable role in maintaining my sanity. Finally, I want to thank Caroline Suen for her love, understanding, and support.

It's been a good ride.

Contents

List of Tables

List of Figures

List of Algorithms

Chapter 1

Introduction

1.1 Importance of datacenters

Web services are an integral part of today's society, with billions of people using the Internet regularly. The Internet's popularity is in no small part due to the near-instantaneous access to large amounts of personalized information. Online services such as web search (Bing, Google), social networking (Facebook, Twitter, LinkedIn), online maps (Bing Maps, Google Maps, NavQuest), machine translation (Bing Translate, Google Translate), and webmail (GMail, Outlook.com) are all portals to vast amounts of information, filtered to only show relevant results with sub-second response times. The new services and capabilities enabled by these services are also responsible for huge economic growth, with studies estimating that the Internet is responsible for contributing $1.7 trillion towards the global GDP and a 21% growth in the GDP of developed nations [103].

Large-scale datacenters hosting Warehouse-Scale Computers (WSCs) are responsible for hosting the vast majority of these online services. Microsoft in 2013 announced that it has 1 million servers, while studies have estimated that Google owned approximately 1 million servers in 2011. These servers are spread out across the world for locality and redundancy reasons into many datacenters, with a single datacenter containing around 50,000 servers. These millions of servers in datacenters worldwide cost significant amounts of money to build and operate, and also consume considerable amounts of electricity for power and cooling. In 2015, Apple was reported to invest $2 billion into the construction of a single datacenter alone [157]. World-wide, datacenters were estimated to consume the equivalent power output of 30 large nuclear power plants [38]. Put another way, datacenters consume approximately 1% of the total amount of electricity generated world-wide. Though both the scale of datacenters and the scale of their resource requirements are daunting, datacenters are very efficient in terms of compute capability per dollar. Through economies of scale, the cost per unit computation is far cheaper for a datacenter than a commodity PC. In addition, very large application such as search and social networking require large clusters of hundreds to thousands of servers: there is too much data and computation for such an application to fit on a single server or even a small rack of servers [6].

While datacenters are already large, complex, and power-hungry, they are projected to grow in the future due to increasing demand for Internet services. Global Internet penetration in 2014 is currently estimated at around 40%, leaving significant room for growth. In addition, online services are becoming more computationally intensive over time to provide more personalized access to information. Large-scale data-mining and machine learning are being used more widely in various web applications, such as using deep learning to improve the accuracy of online maps [39]. The growth of users combined with the increasing computational complexity of workloads translates to growing demand for datacenters. A study performed by Cisco in 2013 estimates that the number of workloads running in datacenters will nearly double from 2013 to 2018 [20].

1.2 Scaling challenges for datacenters

Large-scale datacenters have been enabled by the economics of co-locating massive amounts of compute, networking, and storage in a single facility. By taking advantage of economies of scale while purchasing equipment for datacenters, large datacenter operators are able to negotiate for bulk-volume discounts on hardware. In addition, the large scale of datacenters and the associated electricity consumption enables datacenter operators to obtain better pricing on electricity by purchasing it at wholesale rates. The growth in datacenter computing has been fueled by the favorable economics of building and operating large datacenters, as the marginal costs of performing computation is far outstripped by the profits of operating popular web services.

Unfortunately, there are several challenges for the continued scaling of the capabilities of datacenters. The growth of datacenters have been driven by two factors. The first is the cost reduction of operating a datacenter, and the second is the increasing capability of datacenters. However, previous approaches to scale datacenters are either one-time tricks or are encountering scaling issues. On the cost reduction side, a technique was to build the servers in-house and to strip out unnecessary components to reduce cost, but this was a one-time trick. Another cost reduction technique was to improve the efficiency of power delivery and cooling of datacenters, but this approach is facing diminishing returns as better datacenter designs have pushed the amount of wasted electricity to a very small fraction of total datacenter power.

On the other hand, methods to continue scaling of the compute capabilities of datacenters are also running out of steam. There are two ways to grow the amount of computational capacity: either increase the number of datacenters or increase the computational power of a single datacenter. Increasing the number of datacenters is a very expensive proposition, given that a large datacenter can cost billions of dollars to build. Scaling the capability of a datacenter by adding additional servers is economically infeasible, due to the costs of scaling power delivery infrastructure above approximately 50MW for a single datacenter facility [88]. The last tool in scaling the capability of datacenters has been that of Moore's Law combined with Dennard scaling, where shrinking the node size leads to a 2.8$\times$ increase in the compute capability without a substantial increase in cost or power consumption [88]. However, Dennard scaling has greatly slowed past the 90nm node [30], thus greatly reducing the inter-generational intrinsic growth rate of CPU compute capability for future datacenters.

With the increasing difficulty of reducing the costs of datacenters and improving the capabilities of datacenters, new approaches for scaling are needed. One promising avenue is to examine today's datacenters and to improve the efficiency of the servers and the applications running on datacenters. Previous approaches of improving the economics of datacenters have mostly ignored the internals of servers and workloads, instead focusing on externals such as power delivery or on the economy of purchasing additional servers. Since previous approaches are no longer providing the same scaling benefits that they once did, a fresh look at improving the efficiency of servers and workloads is warranted. There are two opportunities we focus on in this dissertation: improving efficiency of components that contribute to the operational expenses (OpEX) and the efficient use of costs that comprise the capital expenses (CapEX) of datacenters.

1.3 Datacenter efficiency

A promising avenue of increasing the capabilities of future datacenters is to improve the efficiency of datacenters. By making better use of resources such as servers and electricity, improved efficiency can lead to increased capability without raising costs. Thus, higher datacenter efficiency is key to enabling the growth of datacenters for the expanding number of Internet users as well as the increasing computational demand placed on datacenters. There are three sources of efficiency that we examine in this thesis: **peak energy efficiency**, **energy proportionality**, and **resource efficiency**. The first two, peak energy efficiency and energy proportionality, are a direct way of improving the OpEX of a datacenter. The last one, resource efficiency, will improve the CapEX of datacenters.

Peak energy efficiency is about reducing the amount of electrical power used when servers are running at peak load. By lowering the peak electricity consumption of servers, datacenters can be provisioned for less peak power, lowering the power infrastructure costs as well as the maximum electricity bill. Alternatively, more servers can be packed into the same power footprint, leading to increased computational density. An example of this technique is the exploration of low-power architectures, such as ARM cores, in the datacenter. Datacenter operators are primarily interested in the amount of power consumed to meet a certain performance target, which is captured by composite energy efficiency metrics that combine power/energy with latency or performance. Ironically, the use of low-power cores alone can actually hurt energy efficiency, as shown in a study that examined the use of Intel Atom cores for Bing search [71].

While peak energy efficiency focuses on reducing the amount of power used at peak load, **energy proportionality** focuses on improving the power used at lower loads. Ideal energy proportionality behavior is that a server consumes X% power when running at X% load. In other words, a server consumes no power when idle, peak power when running at maximum load, and the power vs. load curve would be a straight line between those two points. Unfortunately, servers in datacenters are both un-energy proportional and underutilized, leading to massive amounts of wasted electricity [98]. By improving energy proportionality, the electricity costs of operating a datacenter will be reduced by a significant amount. Previous approaches on improving energy proportionality in datacenters have focused on putting idle machines into a deep sleep

state to reduce idle power while running active machines at high load [109].

Finally, **resource efficiency** looks at improving the utilization of resources within a datacenter. Today's datacenters are operated at a low average utilization, ranging from 10% in Amazon's EC2 [95] to 20% for Twitter [29] and 30% for Google [7]. This underutilization represents a significant fraction of wasted compute capability and the associated costs in purchasing said capability. Thus, increasing resource efficiency leads to an increase in both capability and cost efficiency for datacenters. Furthermore, improving resource efficiency is the only way to improve cost efficiency, as the only way to recoup infrastructure costs is to make use of the infrastructure. Prior work on improving resource efficiency has been through improved cluster management and scheduling techniques, such as Borg [155] and Mesos [51] that perform bin-packing of workloads.

1.4 Challenges for latency-critical applications

Many online services, such as websearch, social networking, webmail, etc. fall under a category of workloads called **large-scale latency-critical** workloads. These workloads all share two common characteristics. The first is that the data is sharded across many servers, thus requiring an architecture where all individual servers must respond before a final result can be generated. The second common characteristic is that the workload is ultimately user-facing and thus has a strict end-to-end latency constraint on the order of hundreds of milliseconds. Thus, large-scale latency critical workloads place very tight latency constraints on the tail-latency of each individual server, as the slowest server in the entire ensemble determines the overall query time.

Due to the strict latency constraints, large-scale latency-critical workloads pose a unique set of challenges towards increasing efficiency of the datacenter. This is because of the fundamental trade-off between efficiency and low latency. On the energy efficiency side, it is well understood that there is a Pareto frontier representing the trade-offs between latency and energy, where speeding up a computation to achieve lower latency requires larger and larger amounts of energy. Furthermore, investigating composite energy efficiency metrics shifts the optimum point on the Pareto frontier even further, complicating efforts to identify the most efficient operating point.

On the energy proportional side, recent research [98] has shown that servers running latency-critical workloads are terribly energy inefficient when running at low loads, with efficiencies lower than what previous models that account for idle power suggest [6]. By improving energy proportionality to match the linear power models, significant energy savings can be achieved at lower utilizations. However, there are significant challenges in reducing the energy consumed by the server without negatively impacting the latency guarantees of the latency-critical workload. Previous work has attempted to use active low-power modes for CPUs to reduce power at low loads, but this approach causes unacceptable latency violations. This is because previous approaches are designed for batch or real-time workloads, which have a vastly different set of performance assumptions compared to latency-critical workloads.

Finally, latency-critical workloads also pose many challenges for increasing resource efficiency. Latency-critical workloads, because of their user-facing nature, are subject to diurnal load variations and thus are not

fully utilized throughout the entire day. Moreover, latency-critical workloads are typically run on dedicated servers or with greatly exaggerated resource reservations in order to avoid inter-workload interference [28]. This is because existing techniques to mitigate interference, such as OS process scheduling and process isolation via containers or virtual machines, do not protect against performance degradation. Remaining sources of interference in the system, such as in shared caches and network links, can cause latency-critical workloads to miss their latency targets even when they are under low load. Thus, the typical approach used by cluster managers to handle interference is to make the problem go away by throwing resources at latency-critical workloads until interference is no longer an issue.

1.5 Summary of contributions

In this dissertation, we show that there exists a huge opportunity to expand the capabilities of datacenters by increasing the efficiency of existing datacenters. We demonstrate that large improvements in efficiency can be obtained by combining information about workloads with the intelligent use of hardware. We focus on the three efficiency metrics described earlier: peak energy efficiency, energy proportionality, and resource efficiency.

First, we present *autoturbo*, a dynamic controller that uses machine learning to improve energy efficiency for both batch and latency-critical workloads at peak loads. Autoturbo chooses the best setting of TurboMode, an opportunistic overclocking mechanism found on modern multi-core processors, to optimize for a given energy efficiency metric. Through controlling TurboMode, autoturbo essentially manages the frequency and voltage of CPUs, two critical parameters for determining the performance and power consumption for CPUs. By using an efficiency model trained on a small set of benchmarks, autoturbo can optimize for both energy efficiency and composite efficiency metrics such as throughput per Watt and Energy Delay Squared Product (ED^2) without a priori knowledge of new workloads. We show that autoturbo can select the proper setting of TurboMode the vast majority of the time, realizing gains of up to 68% on ED^2 compared to statically leaving TurboMode off while avoiding losses of 25% that are caused by statically enabling TurboMode. We further demonstrate the generalizability of autoturbo to different generations of CPUs from several processor vendors.

Second, we investigate the unexpectedly poor energy efficiency of latency-critical workloads at low utilizations. We show that a significant amount of energy is wasted to process queries faster than the Service Level Objective (SLO) for latency-critical workloads at low loads. We then demonstrate that the failure of previous approaches, such as schemes managing active low power modes for CPUs, is due to the lack of end-to-end latency information from the workload and the lack of a fine-grained power control mechanism. We finally show that using latency information from the workload to manage a fine-grained power control mechanism will lead to significant improvements in energy proportionality. This is achieved thorough an *iso-latency* power management policy that slows down the CPU while keeping the latency-critical workload running just fast enough to meet its SLO. We then implement *PEGASUS*, a dynamic real-time controller that

realizes the iso-latency policy. An evaluation of PEGASUS on production hardware at Google with various latency-critical workloads show a potential power savings of up to 40% during periods of low load while maintaining without violating the latency SLO.

Finally, we extend the concept of iso-latency to improving resource efficiency. In large datacenters, there is an abundance of work that can be done, yet the average utilization of the datacenter is low because of latency-critical workloads. We characterize all potential interference sources for several production latency-critical workloads at Google, and demonstrate the need for a dynamic controller that isolates all shared resources on each server. We then describe an implementation of such a controller, *Heracles*, which uses latency feedback from the latency-critical workload in order to simultaneously manage several shared resources in real-time using both hardware and software mechanisms. Heracles is then able to raise utilization by filling in idle resources with best-effort batch jobs while ensuring that the latency-critical workload meets its SLO. We evaluate Heracles on production Google hardware with several mixes of high-priority latency-critical and low-priority batch jobs and demonstrate an average utilization of 90% without violating the latency guarantees of the latency-critical application.

Chapter 2

Motivation and background

2.1 Datacenters

Web services are an integral part of today's society, with the International Telecommunications Union estimating that there 3 billion regular users of the Internet in 2014 [66]. The Internet's popularity is in no small part due to the near-instantaneous access to large amounts of personalized information. Online services such as web search (Bing, Google), social networking (Facebook, Twitter, LinkedIn), online maps (Bing Maps, Google Maps, NavQuest), machine translation (Bing Translate, Google Translate), and webmail (GMail, Outlook.com) are all portals to vast amounts of information, filtered to only show relevant results with sub-second response times. As an example of the daunting scale of online services, there are estimates that show that the size of Google's search index in 2015 encompasses over 45 billion webpages [24]. The new services and capabilities enabled by these services are also responsible for huge economic growth, with studies estimating that the Internet is responsible for contributing $1.7 trillion towards the global gross domestic product (GDP) and a 21% growth in the GDP of developed nations in 2009. Furthermore, Internet services account for 3.4% of GDP across large economies that make up 70% of the world's GDP. If the Internet was a single sector, its contribution would outweigh that of agriculture and utilities [103].

Large-scale datacenters housing Warehouse-Scale Computers (WSCs) are responsible for hosting the vast majority of these online services. These datacenters are favored by the economies of scale that come with building and operating tens of thousands of servers in a single facility. The large capacities of datacenters are driven by the dual necessities of operating over an extremely large dataset with near instantaneous response times. For example, Google web search stores its document index in DRAM for low latency responses, but an index of tens of billions of webpages cannot possibly fit on a single machine. Thus, a single Google websearch instance spans across thousands of machines [98]. When scaled to handle multiple online services to handle load for a global audience, the scale of resources invested in datacenters worldwide is breathtaking. Microsoft in 2013 announced that it has 1 million servers, while studies have estimated that Google owned approximately 1 million servers in 2011. These servers are spread out across the world for locality and

redundancy reasons into many datacenters, with a single datacenter containing around 50,000 servers. These millions of servers in datacenters worldwide cost significant amounts of money to build and operate, and also consume considerable amounts of electricity for power and cooling. In 2015, Apple was reported to invest $2 billion into the construction of a single datacenter alone [157]. World-wide, datacenters were estimated to consume the equivalent power output of 30 large nuclear power plants [38]. Put another way, datacenters consume approximately 1% of the total amount of electricity generated world-wide.

2.1.1 Total Cost of Ownership

The move towards consolidating computation into dense datacenters is driven by the financial bottom line for operators of online services. By concentrating servers into datacenters, economies of scale are achieved for purchasing and operating servers, networking equipment, power distribution infrastructure, cooling equipment, and other facilities. In addition, datacenters also consolidate the consumption of electricity from the electrical grid, enabling operators to purchase electricity at wholesale rates.

One common metric for measuring the cost of datacenters it the Total Cost of Ownership, or TCO. Datacenter TCO is broken down into two components, **CapEX** and **OpEX**. CapEX, or capital expenditures, are the sum total of the costs of purchasing capital equipment for the datacenter. CapEX includes the costs of servers, networking gear (such as routers and switches), cooling infrastructure (such as chillers and air handlers), power delivery infrastructure (such as power distribution units at the racks, backup batteries, and emergency generators), and the actual facility itself (such as real-estate costs). The costs of operating the equipment (such as electricity for the servers, networking gear, cooling infrastructure, and power lost in inefficiencies of the power delivery infrastructure), interest on loans used to pay for capital equipment, and salary for employees working in datacenters are included in OpEX.

To illustrate the TCO breakdown of a datacenter between its various CapEX and OpEX parts, we use the TCO model from James Hamilton [46]. We show the assumptions used in Hamilton's model in Table 2.1 and the TCO breakdown resulting from that model in Figure 2.1. Hamilton's model suggests that the vast majority of costs in a datacenter is related to the costs of buying servers, with energy accounting for only 31% of the TCO of the datacenter and networking a mere 8%. Of the energy costs, 18% goes to CapEX for cooling and power delivery and the remaining 13% going to OpEX costs for the electricity bill. Improving peak energy efficiency improves the entire 31% portion of TCO, while energy proportionality would only improve the OpEX portion for energy costs. In addition, improving the energy efficiency of datacenters skews the cost distribution more heavily towards CapEX for servers and networking, which comprise the other 70% of TCO for a datacenter.

2.2 Scaling for datacenters

Projections for future demand on the computational capabilities indicate a continued growth for the already staggering capabilities of datacenters. This is due to several factors. The first is that there is still ample room

(a) Basic Datacenter Assumptions

Size of facility (critical load)	8,000,000 W
Cost of power ($/kW-hr)	$0.07
Cost per critical watt in $/W	$9
Watts per server	165
Cost per server	$1,450
Average critical load usage	80%
Power usage effectiveness (PUE)	1.45
Power and cooling costs as a percentage of facility costs	82%

(b) Financial Assumptions

Annual interest rate	5%
Facility amortization	10 years
Server amortization	3 years
Network amortization	4 years
Networking gear discount	60%

(c) Networking Gear

Layer	Equipment	Count	Price	Power
Border	Cisco 7609	2	$362,000	5,000 W
Core	Cisco 6509E	2	$500,000	5,000 W
Aggregation	Juniper Ex8216	22	$750,000	10,000 W
Access	Cisco 3560-48TD	1,150	$11,995	151 W
Total			$12,807,300	413,650 W

(d) Monthly Expenses

Servers	$1,998,097
Networking	$294,943
Power/Cooling	$626,211
Energy	$474,208
Other	$137,461

Table 2.1: James Hamilton's datacenter TCO model [46]. Basic assumptions are provided by Hamilton based on his experience working for Amazon Web Services and Microsoft Foundation Services. Monthly expenses are simple monthly payments given an amortization period and annual interest rate.

for the number of Internet users to grow. Global Internet penetration in 2014 is around 40%, meaning that that number of potential Internet users can more than double. In addition, online services are becoming more computationally intensive in order to provide more relevant and personalized access to information for users. Recently, large-scale data-mining and machine learning techniques are being integrated into various web applications. For instance, large-scale facial recognition is being used by Facebook for automatic tagging of friends in uploaded photos. Google has started using deep learning to improve the accuracy of online maps by reading street numbers from Street View imagery [39]. Future algorithms, such as automatic captioning of images [77, 156], would require even more computational power.

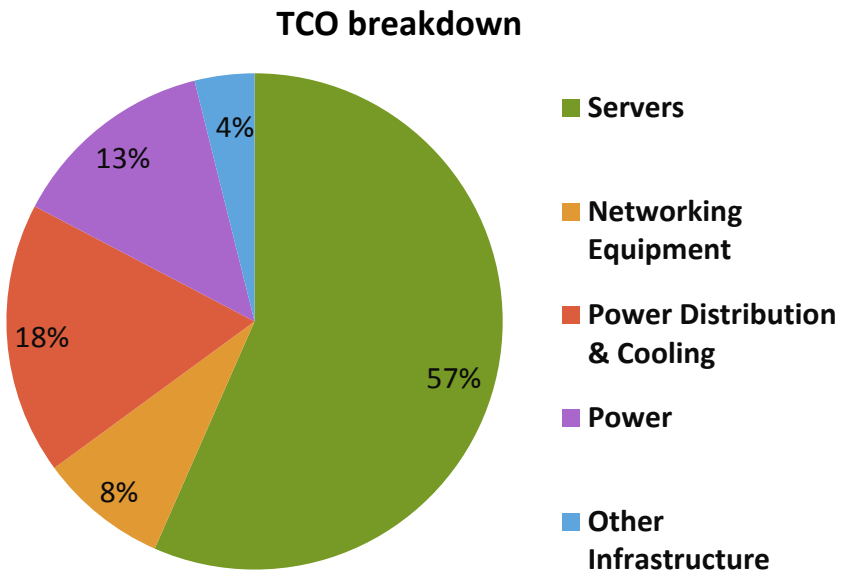

Figure 2.1: Breakdown of TCO by category based on assumptions in Table 2.1.

Up until the present, economically scaling the capabilities of datacenters has primary relied on computation becoming cheaper over time. Historically, the growth of datacenters have been driven by reductions in the CapEX or OpEX of the datacenter or by relying on chip vendors to produce CPUs with better performance for the same cost and power budget.

Since servers are the single largest contributor to TCO (57% in Hamilton's model), operators of large datacenters have found ways of reducing the costs of servers. The singularly most effective cost reduction technique for servers was to switch from purchasing servers from vendors such as Dell or HP to buying commodity servers from original design manufacturers. This approach was first widely used at Google and has seen wide adoption in the industry as well, with Facebook and Microsoft releasing their server designs to the Open Compute project. By designing their own servers, datacenter operators are able to strip out unnecessary components such as optical drives and front panel bezels to minimize component costs. In addition, purchasing servers directly from original design manufacturers remove the server vendors as middlemen, further streamlining costs. The switch to commodity servers has proven quite effective at reducing TCO. In a hypothetical case study, Barroso et al. calculate that using commodity servers can achieve a 42% savings on amortized 3-year TCO compared to high end servers from Dell [6]. The switch to commodity servers, while extremely effective at reducing CapEX, is nevertheless a trick that can only be used once.

Reductions in the OpEX of datacenters have revolved around improving the energy efficiency of datacenters, as the costs for operational staff in a datacenter are negligible. Historically, much power in a datacenter

is "wasted" on equipment that do not directly contribute to computation, namely on power distribution infrastructure and facility cooling. For example, a traditional datacenter architecture for backup power involving a centralized Uninterruptible Power Supply (UPS) adds an extra 17% power overhead [49]. The amount of power wasted on non-compute power is typically captured in terms of Power Utilization Efficiency, or PUE. PUE is defined as the total power consumed by the datacenter facility divided by the total critical power. For example, a hypothetical datacenter sized for 5MW of critical power may consume a total of 8MW when power delivery losses and cooling is included, leading to a PUE ratio of $\frac{8MW}{5MW} = 1.6$. While the industry average PUE is 1.8-1.9, modern large datacenters are able to achieve a PUE of almost 1.1 [6, 42]. This is due to techniques such as distributing backup batteries to each server, isolating hot/cold aisles for cooling, and situating datacenters in naturally cool climates so cooling the datacenter is as simple as "opening the windows" [6]. Given that PUEs are already so low for large datacenters, there is diminishing returns for improving PUE further: a PUE of 1.1 means that there can be at most a 10% gain in improving facility efficiency.

Scaling the capabilities of datacenters can be done by onlining additional datacenters or by increasing the capacity of existing datacenters. Both of these propositions have their own set of challenges. Large datacenter tend to be sited in locations with cool climates for energy efficiency, proximity to base-load generating power stations for cheaper electricity rates, as well as closeness to major fiber nodes. Locations with these desirable properties are rare, and so scaling up the number of datacenters might lead to suboptimal placements of future datacenters. In addition, there is significant financial and regulatory risk in the placement of new datacenters [27]. The challenges with scaling up the capacity of datacenters lie in the difficulty of provisioning additional space and power within an existing datacenter. Unless the existing datacenter was already provisioned for additional capacity, adding new servers will incur costs of purchasing new racks, PDUs, and networking equipment; furthermore, the new servers will also need power delivery and cooling equipment. Finally, there are practical limits to the size of datacenters due to physical, regulatory, and power utility considerations [27].

One elegant technique used to scale the capability of datacenters is to rely on processor vendors to produce CPUs with higher performance but with the same cost and power budget. Historically, this trend has been enabled by a combination of Moore's Law and Dennard scaling. Every two years, Moore's Law yields a doubling of transistor count, which we can optimistically assume yields a doubling of performance due to more cores. In the same period of time, Dennard scaling also yields a frequency multiplier of $1.4\times$, a gate capacitance multiplier of $0.7\times$, and a threshold voltage multiplier of $0.7\times$ due to smaller feature size [30]. These multipliers combine to produce a performance increase of $2.8\times$, but the smaller capacitance and threshold voltages cancel out the power cost of achieving higher performance. This allows datacenter operators to have a longer-term amortization schedule for datacenter facilities compared to servers, as a newer generation of servers will feature $2.8\times$ the performance with the same power budget. Unfortunately, Dennard scaling has challenges past the 90nm node due to sub-threshold leakage becoming a dominant power term at lower supply voltages [30]. This means that for the foreseeable future, new generations of CPUs can at best

achieve a 40% increase in compute capability for the same power budget [88].

2.2.1 Future scaling opportunities

With the slowdown in capacity scaling from previous techniques, we need to find new ways of increasing datacenter capacity to handle the projected growth in datacenter load. One such opportunity is to increase the efficiency of the servers themselves. PUEs of large datacenters are approaching 1.0, indicating that the vast majority of energy used by a datacenter is going to the servers themselves. In addition, the hardware cost of servers is the single largest component of datacenter TCO, implying that servers ought to be used at high utilization to be cost efficient. There are many ways for the efficiency of servers to be improved from the perspective of energy efficiency and resource efficiency.

There are several energy efficiency metrics to capture the efficiency of servers. We first look at a group of metrics that capture *peak load efficiency*. Intuitively, these metrics measure the energy efficiency of the server when the server is running at 100% load, which leads to maximum power consumption of the server. Peak load energy efficiency metrics include simple metrics such as throughput per Watt, which is equivalent to computations per Joule and measures the amount of energy that is spent on processing a single task. In addition to these simple metrics, there are also composite metrics such as Energy Delay Product (ED) and Energy Delay Squared Product (ED^2). ED and ED^2 are used when the latency of the computation needs to be factored into the total energy cost. These metrics are appropriate when users interact with the system, as users would like to have their batch jobs finish somewhat quickly and to have results to their websearch queries in less than a second. Improving peak energy efficiency would improve both the CapEX and OpEX portions of energy's contribution to datacenter TCO.

Peak load efficiency is important for large scale batch systems, which can be run at very high utilizations with distributed computation frameworks such as Hadoop [151] or Spark [149]. Applications running on these frameworks can be scaled to run on all cores across many servers, resulting in high utilization. Unfortunately, large datacenters are not actually utilized at high loads. Studies that look at individual server utilization in an entire fleet over time at large datacenter operators show that the vast majority of servers are lightly utilized. Average utilizations of 20%-30% (Figure 2.2) are the norm, where it is the exception rather than the rule for servers to run at utilizations above 90%.

Thus, in addition to peak energy efficiency, we must also examine the energy efficiency of servers at other operating points. The widely accepted standard for measuring this efficiency is to compare the power consumed by servers to an idealized *energy proportional* model. The power used by a server can be broken into two components: static power and dynamic power. Static power is composed of power that is needed to keep an idle server powered on and ready to execute work at a moment's notice, such as fan power, DRAM refresh, and static leakage of CMOS circuits in the CPU, cache, and memory. Dynamic power is the amount of power actually spent in performing work, such as power consumed in the CPU to execute instructions, power to read and write data from DRAM and disk, and power spent by the network interface to receive and transmit packets.

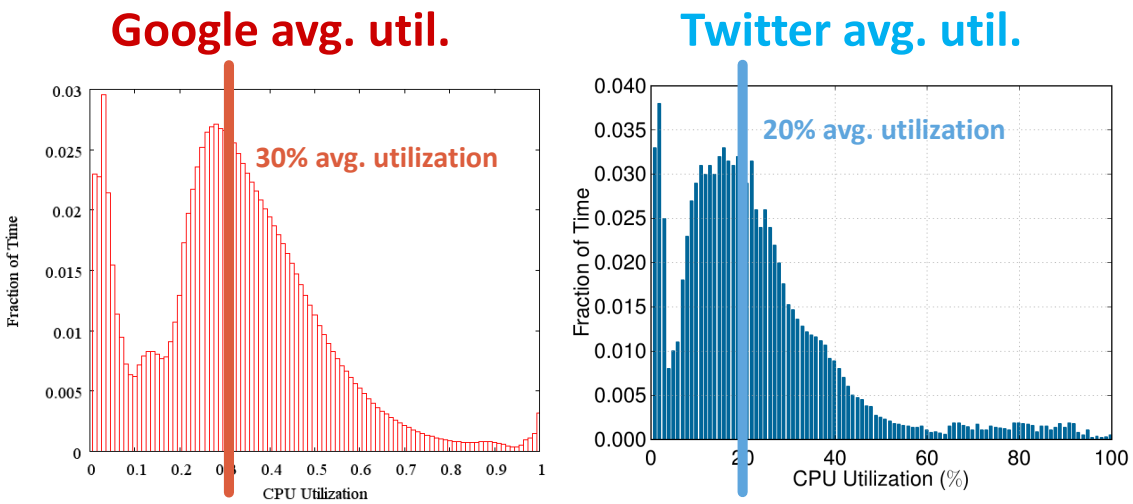

(a) Average CPU utilization at Google [6]

(b) Average CPU utilization at Twitter [29]

Figure 2.2: Average CPU utilizations for large-scale clusters

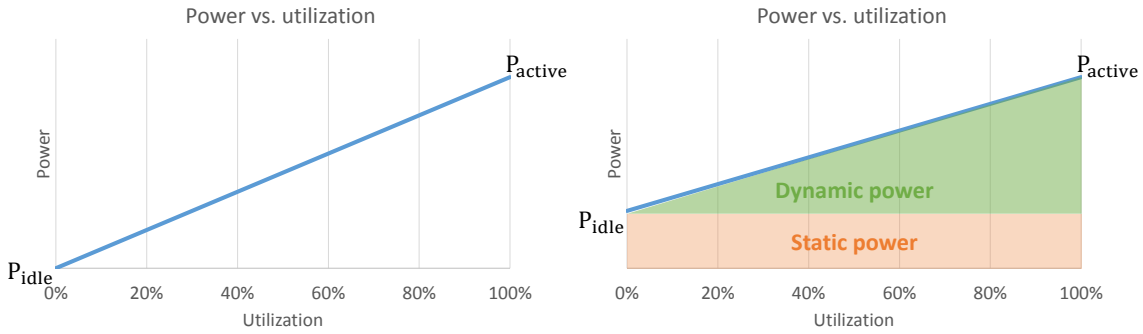

(a) Ideal energy proportionality

(b) Model for an example server

Figure 2.3: Power as a function of utilization

An ideal energy proportional server would have no static power component ($P_{idle} = 0$), and thus its power consumption vs. load would be a straight line ($Power \propto Load$) as in Figure 2.3a. However, real servers have a fairly substantial idle power component, as shown in Figure 2.3b. This is because of the large amount of power needed to keep a server on standby. Servers with large fractions of idle static power (e.g. $P_{idle} = 0.5P_{active}$) are not uncommon [6, 88]. Because of the low utilization of servers, static power can come to dominate the overall energy consumption of a datacenter. Thus, improving the energy proportional behavior of servers can lead to large savings in total energy. A study that simulated the energy consumption of a cluster demonstrated that a reduction of P_{idle} from $0.5P_{active}$ to $0.1P_{active}$ can save up to 35-40% on datacenter energy [34]. Thus, improving the energy proportionality of servers can yield a substantial savings in OpEX through a reduction in electricity consumption.

Finally, there exists a significant opportunity to improve the resource efficiency of datacenters. Resource efficiency is a measure of how well the compute capacity of the datacenter is actually utilized in a day-to-day setting, and is directly measured as the utilization of the servers. Therefore, low utilization of servers in the datacenter has a direct negative impact on the realized capacity of a datacenter. Even if a datacenter can theoretically handle a large amount of work, the theoretical peak utilization is a moot point if it cannot be practically achieved. Thus, improving the utilization of servers in a datacenter corresponds to a one-to-one increase of the realized capability of a datacenter. Recall from Figure 2.2 that the average utilization of servers is 20-30%. Thus, assuming conservatively that utilization can be raised to 90%, the computing power of the datacenter has effectively tripled or quadrupled. From an economic standpoint, improving the utilization of existing servers in a datacenter is equally desirable. In the analysis of datacenter TCO, increasing the utilization of servers is the only way to recover the money invested into the CapEX of the datacenter. From Hamilton's model, CapEX accounts for 87% of the TCO of a datacenter. An average utilization of 20%-30% translates to an approximate wastage of 70%-80% of CapEX, for a total waste of 60%-70% of datacenter TCO. When a single large datacenter can cost $2 billion to build [157], wasting over $1 billion is very difficult to ignore. Furthermore, improving the utilization of servers also positively impacts overall datacenter energy efficiency. This is because of the poor energy proportionality of modern servers, meaning that servers are more energy efficient when running at higher loads. Thus, improving the resource efficiency of servers by raising utilization is very advantageous, as it improves both the capability and the energy efficiency of the datacenter.

Related work for improving efficiency

Improving the efficiency of servers, and of computers in general, is not a new field. On the energy efficiency side, a significant amount of work has gone into designing more energy efficient architectures, such as low-power mobile cores [71]. In addition, there is significant work on improving overall energy efficiency by managing an "ensemble" of servers together [131]. To improve energy proportionality, several systems have been proposed to coalesce long periods of idleness where the servers can be put into deep sleep modes, effectively removing the idle power term [109]. Another approach to improve energy proportionality is to use Dynamic Voltage Frequency Scaling (DVFS), where components of the server are operated at lower performance to save power during periods of low load. DVFS has been shown to work well on throughput-oriented batch jobs [37, 62, 81, 84, 129, 142, 160] as well as real-time workloads [4, 93, 122, 135, 141]. Finally, for resource efficiency, there are several cluster managers used in production systems that attempt to maximize the utilization of servers by bin-packing work into them, such as Google's Borg and the open-source Mesos project [51, 155]. There is also substantial work on improving these cluster managers with interference-aware scheduling techniques, as found in Paragon, Quasar, BubbleUp, and BubbleFlux [28, 29, 104, 163]. Unfortunately, these many techniques to improve efficiency do not interact well with a large-class of datacenter workloads: that of large-scale latency-critical workloads, which we will describe in Section 2.3.

At first blush, it may seem this dissertation is yet another thesis on improving efficiency of computer

systems. However, we note that previous efforts to improve efficiency do not directly deal with large-scale latency-critical workloads running on warehouse scaling computers. Large-scale latency-critical workloads have a unique set of requirements that render previous techniques ineffective, which we will describe in Section 2.3. This dissertation expands upon previous work to to unlock huge efficiency gains for latency-critical workloads, a class of emerging workloads that was once written off as hopelessly inefficient.

2.3 Large-scale latency critical workloads

Many online services, such as websearch, social networking, webmail, etc. fall under a category of workloads called **large-scale latency-critical** workloads. These workloads all share two common characteristics. The first is that data is sharded across many servers, thus requiring an architecture where all individual servers must respond before a final result can be generated. For instance, Google websearch is structured as a hierarchical fan-out tree (Figure 2.4) where a single incoming search query is distributed to all the leaf nodes in the tree, and the final search result is obtained after aggregating and sorting the results from each leaf node [25]. The second common characteristic is that the workload is ultimately user-facing and thus has a strict latency service level objective (SLO) on the order of hundreds of milliseconds. If the SLO is defined on an individual server level, the target could be that the 99.9%-ile tail latency needs to be less than tens of milliseconds; while a SLO for the entire end-to-end latency could be closer to $\sim$ 100 milliseconds. The strict SLO is due to studies that show that users treat "slow" response times as unacceptable degradation in user experience. One recent study at Google demonstrated that a page render time greater than 400 milliseconds has a measurable impact on ad-revenue [137]. Thus, large-scale latency critical workloads place very tight latency constraints on the tail-latency of each individual server, as the slowest server in the entire ensemble determines the overall query time. The strict latency SLO of large-scale latency-critical workloads differentiates it from large batch jobs that may also access a large amount of data stored on many separate servers. Batch jobs, due to their non-interactive nature, are much more tolerating of small disturbances compared to large-scale latency-critical workloads. Users who submit batch jobs will hardly notice a 1 second increase in processing times, while the same increase in end-to-end latency for a user of an online service is considered unacceptable. Ultimately, both the *latency-critical* and *large-scale* aspects of large-scale latency-critical workloads combine to make this class of workloads very challenging to achieve high efficiency on.

Not only are large-scale latency-critical workloads difficult to achieve high efficiency on, they are also the primary reason behind the underutilization of datacenters. These workloads are user-facing, and thus the load on them is dictated by the number of users currently using the online service. This behavior is apparent as *diurnal* load variation. We measure an example diurnal load for Google websearch over a 24 hour period and plot it in Figure 2.5. Due to coarse-grained load balancing at the front-end, websearch is utilized at nearly peak load for approximately half of the day. However, during the other half of the day, namely when users are asleep in the middle of the night, the load on websearch drops to approximately 25%. Because to geo-locality considerations (web services steer traffic to the closest datacenter to the user) and a non-uniform distribution

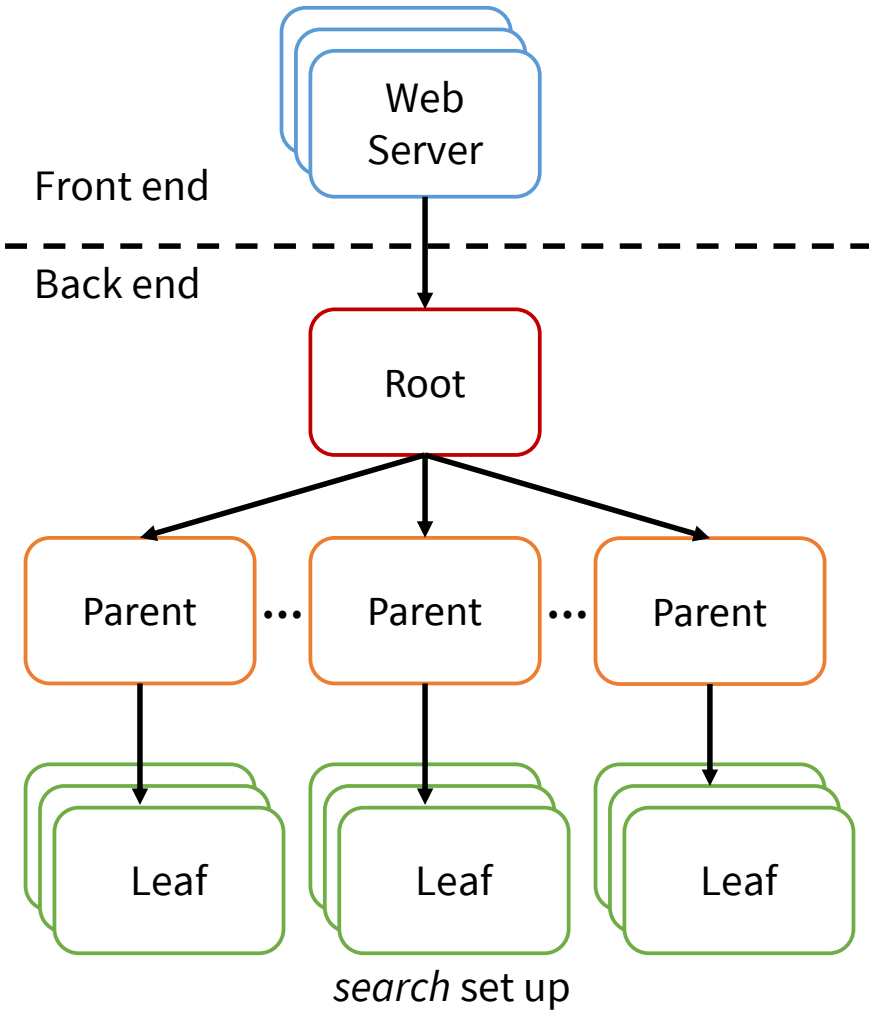

Figure 2.4: Example topology of Google websearch, from [25].

of the world's population across timezones (there are more people in Asia than in the middle of the Pacific), there will always be instances of online services that operate below capacity because of diurnal user patterns.

Paradoxically, large datacenters have a near endless supply of jobs that can be executed. These jobs typically take the form of best-effort batch jobs, such as analytics, log processing, machine learning, etc. For instance, training a neural network to better recognize images would fall under this category of batch jobs. In theory, one would expect that the servers in the datacenter would always be highly utilized, as there should always be a job ready to fill in any idleness. In practice, the actual utilization of a datacenter is fairly low, even with advanced cluster management software. Figure 2.6 shows the CPU utilization of a cluster of servers at Google, as well as the number of CPUs requested by jobs [132]. The CPU utilization rarely rises above 50%, but the amount of CPUs reserved is always at 100%. Furthermore, most of the exaggerated

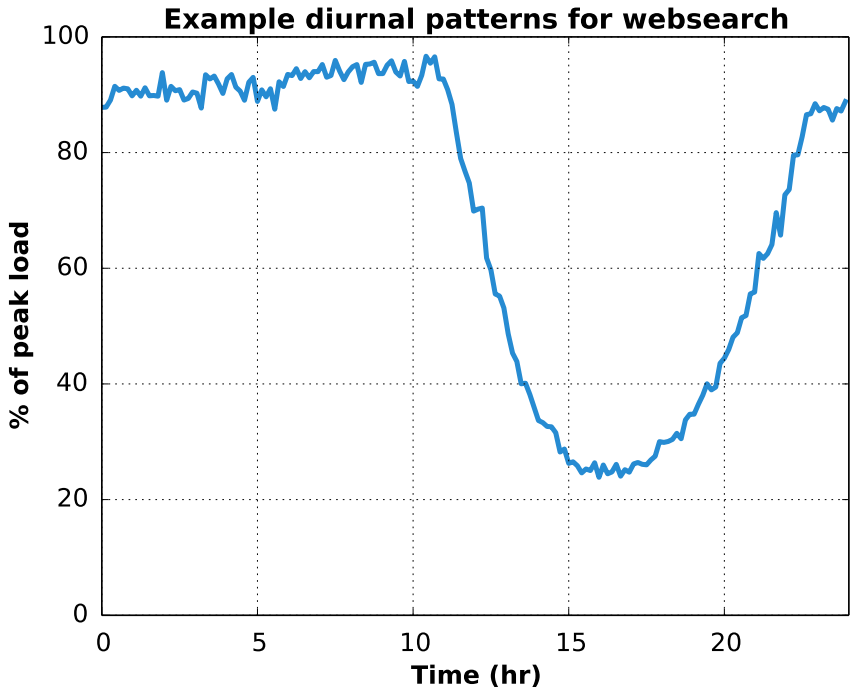

Figure 2.5: Diurnal user load variation for Google websearch. Time is an offset from the start of the trace, not absolute time.

resource reservations are due to high priority (i.e. latency-critical) jobs, where on average high priority jobs reserve more than twice the amount of CPUs than they actually consume. Naturally, this exaggeration of resource requirements leads to poor utilization of the datacenter in a way that the cluster manager cannot fix. While over-exaggerated resource reservations seem wasteful, there are good reasons for specifying such reservations, which we will describe shortly in Section 2.3.2.

We now discuss the difficulties of achieving high efficiency for large-scale latency-critical workloads. The common underlying theme is that various techniques that worked for other workloads do not work for latency-critical workloads because of the strict latency SLO that latency-critical workloads must meet.

2.3.1 Energy proportionality challenges

A previous approach to achieving energy proportionality in the datacenter proposes using deep sleep states to reduce idle power, such as in PowerNap [109]. However, large-scale latency-critical workloads do not expose enough idleness to take advantage of these deep sleep states. A study of latency-critical workloads at Google showed that even at very low loads (10%), the distribution of the periods of idleness in various system components prohibit the use of the lowest power sleep states [110]. In addition, the same study concluded that attempting to create long enough periods of idleness by batching requests causes latency SLO

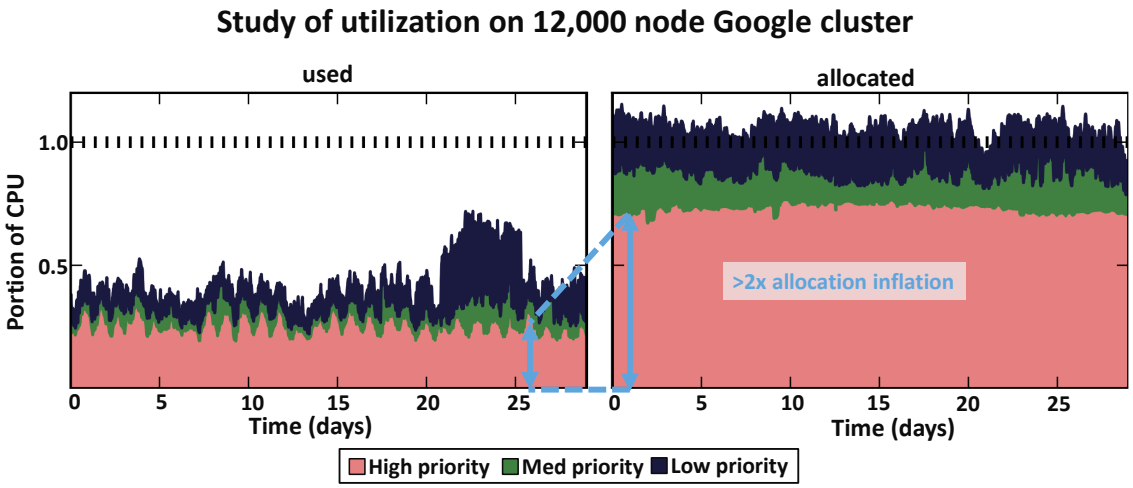

Figure 2.6: Fraction of CPUs across a Google cluster that is utilized and reserved.

violations, making batching a non-starter. Another approach advocates consolidating load onto fewer servers and turning off the idle servers during periods of low load [85]. However, the large distributed state that needs to be available for OLDI workloads prevents load consolidation and makes this approach impractical. For instance, websearch shards its search index in DRAM across thousands of nodes and there is not enough free DRAM available in any single node to hold more index data (otherwise the index would have been made larger to begin with).

To improve energy proportionality for a single node, there have been attempts to use DVFS to reduce server power at low load. Unfortunately, previous DVFS controllers were designed for throughput-oriented or real-time workloads and not latency-critical workloads. Namely, these DVFS control schemes use CPU utilization as the primary control input and completely ignore additional latency requirements of the workload. This mismatch in assumptions leads to latency SLO violations for the latency-critical workload, rendering such DVFS schemes unusable. Previous experiments have yielded conclusive evidence that such DVFS schemes are not suitable for latency-critical workloads. For instance, using the *cpufreq* power governor, a DVFS scheme found in Linux that is used to extend the battery life of laptop computers, causes large latency violations for websearch as seen in Figure 2.7.

Given the difficulties of adapting previous approaches for achieving energy proportionality to latency-critical workloads, the standard solution has been to simply give up. Operators of latency-critical online services would rather deal with the wasted energy than to cause latency violations that could result in a poor end-user experience and a subsequent loss of revenue. However, since datacenters are becoming limited by the amount of power they consume, improving energy proportionality is of paramount importance for future datacenter scaling.

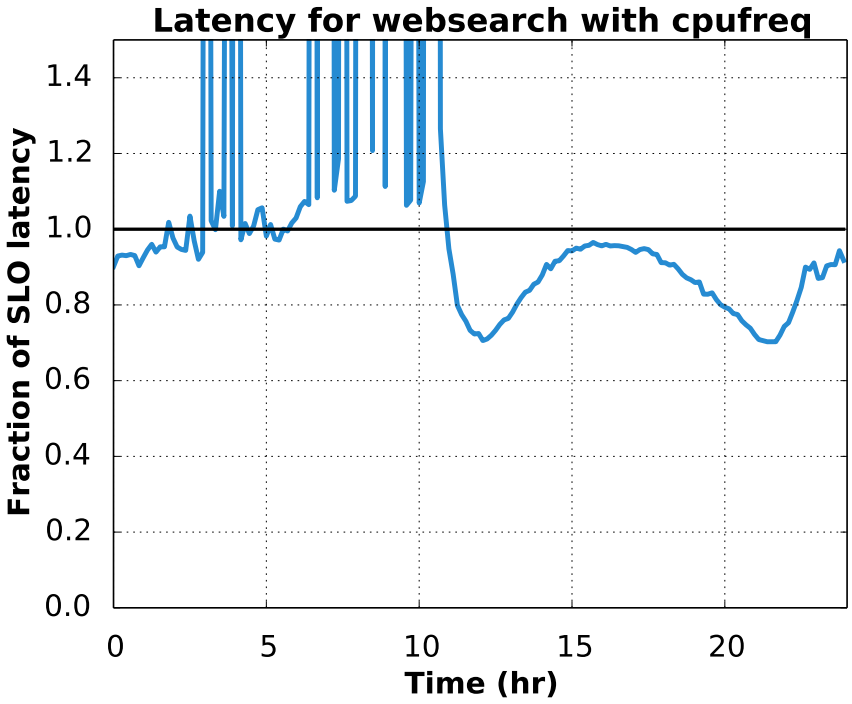

Figure 2.7: Latency of websearch with *cpufreq*, showing latency SLO violations. The solid horizontal line shows the target SLO latency.

2.3.2 Resource efficiency challenges

The only way to improve resource efficiency is to make better use of compute resources. Recall from earlier that in many large datacenters, there is an abundance of jobs that can be run. Thus, the challenge for resource efficiency is not on the supply side; in fact, the cluster manager in Figure 2.6 believes that the cluster is being highly utilized. We previously alluded to the fact that the paradox of high allocations and low usage is caused by the exaggeration of resources in the requirements of the job. This resource exaggeration is a product of the extreme sensitivity of latency-critical workloads to inter-workload interference. Inter-workload interference occurs when two jobs are running on the same server and contend for shared resources.

Any shared resource on the server can be a source of interference. For example, two jobs co-scheduled on the same logical CPU will necessarily be multiplexed, and thus the performance of each job will suffer compared to the case where each job has its own CPU. To make matters worse, latency-critical workloads are by nature exquisitely sensitive to any performance degradations because of the strict latency SLOs. This sensitivity effectively means that interference from any single source could be enough to cause a latency SLO violation. Thus, in order to mitigate interference from a co-located workload, every single source of shared resource contention must have interference mitigation mechanisms. The large numbers of shared resources in a server (cores, caches, DRAM, network, power, etc.) makes this a daunting requirement.

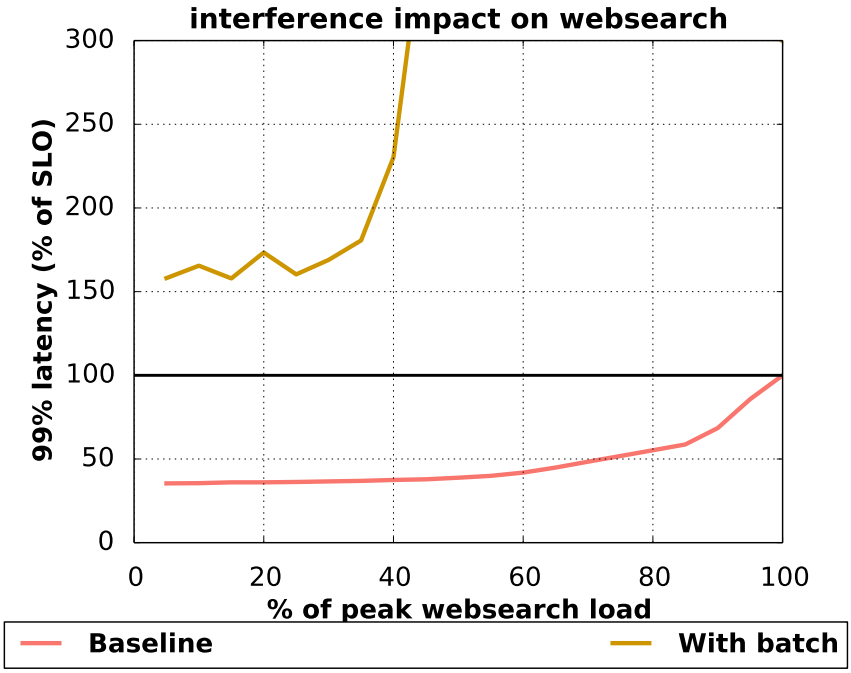

Figure 2.8: Latency of websearch with a low-priority batch workload, showing latency SLO violations. The solid horizontal line shows the target SLO latency.

Up until recently, the lack of hardware support for shared resource isolation has made achieving high resource efficiency quite challenging. Using only software mechanisms to achieve high resource efficiency for latency-critical workloads while guaranteeing their tight latency SLOs has been very difficult. For example, using the priority scheduling parameter alone in Linux's Completely Fair Scheduler is woefully inadequate in preventing latency violations. To demonstrate this point, we conducted an experiment where a batch job was co-schedule with Google websearch on the same server. The scheduling parameters were set so that the batch job was marked as low priority, and websearch as high priority. The latency was then measured and shown in Figure 2.8. It is immediately clear that OS scheduling priorities could not guarantee that websearch will meet its latency requirements. Even more concerning is that websearch failed to meet its latency SLO at any offered load, even at very low loads. Unfortunately, even interference-aware schedulers such as Paragon [28], BubbleUp [104], or CPI2 [164] are unable to improve resource efficiency in this case, as such schedulers will conclude that such a co-location is impossible and will schedule websearch onto dedicated servers.

The widely adopted workaround to the sensitivity of latency-critical workloads to interference has been to either run those workloads on dedicated servers or to greatly exaggerate their resource requirements. In the dedicated server case, having no other workloads on the same server guarantees that there cannot be any interference. Greatly exaggerating the resource requirements of latency-critical workloads is a slightly more nuanced approach, the idea being that the exaggerated resource reservation will only allow small jobs unlikely

to cause interference to be co-scheduled with the latency-critical one. In either case, resource efficiency suffers greatly, as a significant fraction of the server will be left idle when the latency-critical workload is not being used at high load.

2.4 Questions this dissertation explores

This dissertation will explore opportunities to improve both energy efficiency and resource efficiency for datacenters. There are several questions that we use to guide this exploration. The first is to examine whether there exists opportunities to achieve huge efficiency gains in existing systems. We choose to focus on existing systems to achieve wider immediate applicability for today's datacenters. We specifically focus our inquiry on finding acceptable trade-offs that can lead to efficiency improvements, as the vast majority of "free" efficiency gains, such as PUE improvement and commodity servers, have already been exploited.

First, we examine peak CPU power consumption. At peak load, CPU power consumes 70% of total system power, making it an attractive target for efficiency optimization. We therefore analyze whether or not running the CPU at full power actually translates to significantly improved performance for different workloads and different efficiency metrics. We also apply this analysis to large-scale latency-critical workloads, and ask if there exists power and performance trade-offs at lower utilizations. Specifically, we ask the question of whether or not there exists unused performance at lower utilizations that can be turned into energy savings. Finally, we investigate what kinds of mechanisms and the granularity of said mechanisms needed to realize potential energy savings as well as the magnitude of energy savings.

We then turn our focus to determining how we can use increase the resource efficiency of servers in the face of latency-critical workloads. We begin by asking the same question of whether there is unused performance at lower utilizations for latency-critical workloads, and how we can turn performance slack into increased server utilization. We then investigate the necessary mechanisms needed to perform resource partitioning to guarantee performance isolation between workloads running on the same server. Finally, we apply what we learned from the previous questions to answer the question of how high the utilization of servers can be raised to without violating the SLOs of latency-critical workloads.

Chapter 3

Dynamic Management of TurboMode in Modern Multi-core Chips

We begin the technical portion of this dissertation by examining opportunities to improve peak energy efficiency for CPUs. We examine the dynamic overclocking of CPUs, or TurboMode, a feature recently introduced on all x86 multi-core chips. It leverages thermal and power headroom from idle execution resources to overclock active cores to increase performance. TurboMode can accelerate CPU-bound applications at the cost of additional power consumption. Nevertheless, naive use of TurboMode can significantly increase power consumption without increasing performance. Thus far, there is no strategy for managing TurboMode to optimize its use across all workloads and efficiency metrics.

In this chapter, we analyze the impact of TurboMode on a wide range of efficiency metrics (performance, power, cost, and combined metrics such as QPS/W and ED^2) for representative server workloads on various hardware configurations. We determine that TurboMode is generally beneficial for performance (up to +24%), cost efficiency ($QPS/\$$ up to +8%), energy-delay product (ED, up to +47%), and energy-delay-squared product (ED^2, up to +68%). However, TurboMode is inefficient for workloads that exhibit interference for shared resources. We use this information to build and validate a model that predicts the optimal TurboMode setting for each efficiency metric. We then implement *autoturbo*, a background daemon that dynamically manages TurboMode in real time without any hardware changes. We demonstrate that *autoturbo* improves $QPS/\$$, ED, and ED^2 by 8%, 47%, and 68% respectively over not using TurboMode. At the same time, *autoturbo* virtually eliminates all the large drops in those same metrics (-12%, -25%, -25% for $QPS/\$$, ED, and ED^2) that occur when TurboMode is used naively (always on).[1]

[1] This chapter is based on work that was originally published in [100].

3.1 Introduction

There is a constant need for higher performance in computer systems. This is particularly the case for large-scale datacenters (DCs) that host demanding popular services such as social networking, webmail, streaming video, websearch, and cloud computing. These applications demand both high throughput to support large number of users and low latency to meet Quality of Service constraints for each user. Nevertheless, performance is not the only efficiency metric. A large concern for datacenter operators is the total cost of ownership (TCO) for a certain level of service, including both capital and operational expenses. The two largest TCO components are the cost of servers and the cost to power them, which can be 53% and 19% respectively [47]. Therefore, any optimization should also target metrics that capture energy and cost efficiency such QPS/W or $QPS/\$$ for throughput workloads and energy-delay products (ED or ED^2) for latency sensitive applications.

This chapter focuses on dynamic CPU overclocking (TurboMode) as a method to increase the efficiency of server computers. While this chapter focuses on server workloads, the techniques we present can be used in any kind of computer system that uses TurboMode. TurboMode has been recently introduced on x86 multi-core chips from Intel and AMD. It overclocks a cores by utilizing available thermal headroom from idle execution resources [1, 58]. Current chips can dynamically overclock a core by up to 40% or more, which can lead to an increase in performance by up to 40%. As the number of cores per chip increases over time, the overclocking range and the performance implications of TurboMode will also increase. TurboMode is controlled by firmware using an embedded hardware controller that sets the exact clock frequency based on the thermal headroom available and the expected performance benefits. Software has little control over TurboMode, except for the ability to enable/disable it.

Unfortunately, TurboMode is not always beneficial and deciding when to enable it is quite complex. As seen in Section 3.3, the optimal TurboMode setting varies across different applications, hardware platforms, and efficiency metrics. There is no clear static setting or simple heuristic for TurboMode management. Naively turning on TurboMode (i.e., relying solely on the firmware controller) can actually lead to energy waste of up to 28% and decrease cost efficiency in some cases. At the same time, disabling TurboMode all the time misses opportunities for huge gains in energy and cost efficiency. We need an automatic system that manages TurboMode intelligently, maximizing its benefits when applicable and masking its impact otherwise.

Towards this goal, we make the following contributions:

1. We characterize the impact of TurboMode on performance, power, cost and energy efficiency metrics for various server workloads on several hardware platforms (Intel and AMD). We demonstrate that turning on TurboMode can greatly improve such metrics (ED^2 up to 68%) but can also significantly degrade the same metrics in the presence of workload interference (ED^2 up to 25%). The wide variability in TurboMode's efficiency necessitates a dynamic control scheme.

2. We develop a predictive model that utilizes machine learning to predict the proper TurboMode setting. We demonstrate that our modeling technique is effective for a wide range of efficiency metrics and

different hardware configurations. It can accurately predict the optimal TurboMode setting for various application configurations.

3. We implement *autoturbo*, a daemon that uses the model to dynamically control TurboMode. The daemon requires neither hardware modifications nor a priori knowledge of the workload. We demonstrate that it improves both energy efficiency (ED by 47% and ED^2 by 68%) and cost efficiency ($QPS/\$$ by 8%). More importantly, it eliminates nearly all the cases where TurboMode causes efficiency drops.

We expect the utility of *autoturbo* to be even greater with future multi-core chips. With more cores per chip, the frequency range and potential of TurboMode will be larger. At the same time, there will be increased interference for shared resources such as caches, memory channels, and on-chip or off-chip interconnects.

The rest of this chapter will be organized as follows. Section 3.2 describes TurboMode and current implementations of it from x86 server CPU vendors. Section 3.3 analyzes the impact of TurboMode for various workloads, metrics, and machine configurations. Section 3.4 describes our implementation of *autoturbo* and Section 3.5 evaluates its efficacy. Section 3.6 presents related work and Section 3.7 concludes this chapter.

3.2 TurboMode Background

TurboMode (TM) is a form of dynamic voltage frequency scaling (DVFS). Unlike prior applications of DVFS which decrease CPU clock frequency and voltage to save power, TM operates in the opposite direction. Namely, TM *increases* CPU clock frequency in the active cores when a multi-core processor has idle resources. Thus, previous DVFS control schemes ([62, 113]) are inadequate in managing TM, as they do not account for the dependency between CPU clock frequency and the presence of idle resources. The processor is able to overclock active cores because the CPU's thermal design power (TDP) is the worst case power at maximum load. When a workload idles some resources of a core, there will be thermal and power headroom available. Since in practice applications do not fully utilize all execution units of a core, TM functions even if all cores are active. TM exploits this available headroom by increasing the operating frequency of the processor [1, 58]. Increasing the CPU's frequency will then speed up the applications running on the CPU, potentially leading to better performance. The frequency boost enabled by TM is already significant on current processors. In one of our evaluation machines, TM can boost the CPU from a nominal frequency of 2.50GHz to 3.60GHz, a 44% gain that could lead to a 44% performance increase.

All current implementations of TM are controlled via a feedback controller implemented in firmware. The firmware controller monitors the CPU to determine the frequency boost that should be applied. The final operating frequency of the processor is determined by several factors that include CPU power consumption, the number of idle cores, and CPU temperature.

The only way for software to manage TM for all modern x86 server CPUs is to enable/disable its use. One way to do so is to statically enable/disable TM from the BIOS. However, this approach is extremely coarse-grained, as turning on TM from a disabled state would require a machine reboot. Instead, we use

an online approach by utilizing the operating system to dynamically enable or disable TM through existing ACPI power management functions. In our work, we use the Linux kernel's built-in CPU frequency scaling support to set the maximum frequency allowed for the CPU. By setting the maximum CPU frequency at the nominal frequency, or one step lower, the CPU will be prevented from entering the TM regime. However, the CPU frequency scaling facility *cannot* set the maximum allowable TM frequency. For instance, if a CPU can scale from a nominal 2.50GHz to 3.60GHz, setting the maximum CPU frequency to 3.20GHz will not prevent the firmware TM controller from setting the CPU frequency to 3.60GHz. However, for the same processor, setting the maximum frequency at 2.50GHz will prevent TM from activating. We will show later in this chapter that adjusting this one simple switch can have profound performance, power, and cost implications.

Both major x86 server CPU vendors, AMD and Intel, have implemented TM in their latest generation processors. AMD's version is named Turbo CORE, while Intel's version is called TurboBoost. In this chapter, we use "TM" as an umbrella term for both versions. At a high level, both implementations are quite similar. Both overclock the processor beyond its base frequency when there is thermal and power headroom, and both have a maximum TM boost frequency that is prescribed by the number of active cores. At the hardware level, there are significant differences between AMD's and Intel's TM controller. AMD's implementation reacts to current and temperature sensors on the CPU die to adjust the frequency boost. Intel's version predicts the power utilization based on the instruction mix and uses that information to determine the frequency boost. Intel's TM is also subject to thermal throttling, but unlike AMD's version, it is not the primary method to control frequency gain. Theoretically, Intel's implementation has a more repeatable TM boost, while AMD's implementation is more sensitive to external factors such as ambient temperature. However, in our experiments, we have observed that the frequency boost from AMD's TM does not experience wide variance between experiment runs. This is due to our test machines being situated in a climate controlled environment that would be found in a datacenter. Finally, we also observe that TM appears to be frequency limited and not power limited.

Another difference between Intel's and AMD's TM controllers is that Intel's version attempts to address energy efficiency. It does this by applying differing amounts of frequency boost depending on the "memory scalability" of the workload and a user configurable parameter for the aggressiveness of TM (*MSR_IA32_ENERGY_PERF_BIAS*) [134]. In practice, we find that this setting is hard to use effectively. We have observed that setting the parameter to "energy efficient" can still lead to degradation in energy efficiency metrics. Therefore, in our study, we leave this parameter at the setting for "highest performance" to avoid interference between the firmware controller and our software controller for TM. Intel also exposes a MSR that allows software to control the maximum achievable TM boost (*MSR_TURBO_RATIO_LIMIT*); however, we do not evaluate it because there is no equivalent MSR for the AMD platform.

A software TM controller is motivated further by the fact that improving the firmware TM controller does not guarantee improvements in energy efficiency. This is because it is infeasible to pre-program firmware to be aware of the impact of TM on all workloads and workload combinations. In addition, the firmware does not have information on the other aspects of the system that affect cost and power (e.g. cooling system,

component costs, etc.), nor does it know which metric to optimize for. Thus, an entire system needs to be assembled and operated before it can be determined whether TM will improve efficiency metrics.

3.3 TurboMode Analysis

We now examine the highly variable impact of TM on performance, energy, and cost efficiency for a variety of workloads on a wide-range of hardware platforms.

3.3.1 Methodology

Hardware We selected several very different hardware platforms that represent a wide selection of server parameters that are seen in practice [19,71] in order to reach conclusions that are not specific to one hardware configuration. We use real hardware for our evaluation in order to accurately capture the complex behavior of TM.

1. Sandy Bridge Server (*SBServer*) has a Sandy Bridge EP (Core i7 3930k) processor with 6 cores that share a 12MB L3 cache. The granularity of TM control is chip-wide. This configuration is representative of a low-end Sandy Bridge server.

2. Interlagos Server (*ILServer*). This system contains an AMD Opteron 6272 processor, mimicking a low-end Interlagos based server. The processor can logically be viewed as a dual socket part, since it is composed of two dies that share a package. Each die has 4 modules, where each module has 2 integer cores that share a front-end. All modules on the same die share 8MB of L3 cache. We lower the base frequency from 2.1GHz to 1.9GHz in order to be able to dynamically control TM. Unlike Sandy Bridge and Ivy Bridge CPUs, the Interlagos architecture allows for control of TM at the module level.

3. Sandy Bridge Laptop (*SBMobile*). The laptop contains an Intel Core i7 2860QM processor with 4 cores that share a 8MB L3 cache. We use a mobile part in order to understand the implications of TM on a more energy-proportional system. In addition, the larger frequency boost of this CPU gives insight into future CPUs with a larger TM frequency swing.

4. Ivy Bridge Server (*IBServer*) and Haswell Server (*HServer*). We also performed a partial evaluation on Ivy Bridge (Xeon E3-1230v2) and Haswell (Xeon E3-1220v3) CPUs. Due to space constraints we do not present a full evaluation of TM on these platforms; however, we will demonstrate that our dynamic controller works well on these platforms.

All machines use Ubuntu 12.04 LTS as the operating system with Linux 3.2.0-26. We summarize the machine configurations used in this study in Table 3.1. For our experiments, we disable HyperThreading on both Intel CPUs and the second core in each Interlagos module to avoid performance counter interference.

We monitor the frequency of the CPU throughout our experiments using *turbostat* to verify that TM is functioning as expected. We measure the total system power by interposing a power meter between the

Name	Base Freq.	Max TM boost	HW Cost	CPU TDP
SBServer (Intel)	3.20GHz	19%	$2000	130W
ILServer (AMD)	1.90GHz	59%	$1700	115W
SBMobile (Intel)	2.50GHz	44%	$1300	45W
IBServer (Intel)	3.30GHz	12%	$1500	69W
HServer (Intel)	3.10GHz	13%	$1500	80W

Table 3.1: Machine configuration summary.

power supply and the power plug. This enables us to determine the impact of TM on total system power, which is important to DC operators. In addition, we also measure the power of the system when idle in order to approximate the system active power for a completely energy-proportional system (e.g. $ActivePower \approx TotalPower - IdlePower$). We apply the energy-proportional approximation to *SBServer*, *ILServer*, and *SBMobile* and denote the resulting theoretical configurations as *SBServer*†, *ILServer*†, and *SBMobile*†. We make energy-proportional approximations because scenarios that are not energy-proportional heavily favor the use of TM. This is because high system idle power masks the power increase from TM. The idle power of *SBServer*, *ILServer*, and *SBMobile* is 83W, 60W, and 25W, respectively. Utilizing a single core is a non-energy-proportional scenario because it adds approximately 50W, 30W, and 20W to the power consumed by *SBServer*, *ILServer*, and *SBMobile*, respectively. $ActivePower$ is underestimated due to the inclusion of CPU active idle power in $IdlePower$. Since TM will always increase $TotalPower$, the ratio $ActivePower_{TM}/ActivePower_{baseline}$ will be overestimated. Thus QPS/W, $QPS/\$$, ED, and ED^2 results for the energy-proportional approximation conservatively underestimate the benefits of TM.

Workloads We evaluate the performance, power, and cost implications for a variety of applications on each of the different hardware configurations. A wide ranging set of benchmarks were chosen in order to capture the behavior of TM for compute-driven datacenter applications. For our study, we focus mainly on the CPU and the memory subsystem and ignore interactions with the disk, network, and I/O subsystems. We use SPECCPU2006 applications (SPECCPU) as single-threaded workloads and mixes of SPECCPU applications to emulate multi-programmed workloads. SPECCPU application mixes are chosen similar to the process used in [136]. Applications are categorized based on cache sensitivity, and a mix is created by randomly choosing categories and then randomly choosing an application for each category. The number of applications in a mix is 4, 6, 8, 4, and 4 for *SBMobile*, *SBServer*, *ILServer*, *IBServer*, and *HServer* respectively. We generate 35 random application mixes for each hardware configuration. We use PARSEC [9] as a multi-threaded benchmark application. We evaluate all PARSEC applications for all thread counts from 1 to the number of cores on each machine.

For enterprise class workloads, we use SPECpower_ssj2008 that is run with enough threads to utilize the entire machine. We also construct websearch, a representative latency-critical web application, by using the query serving component of Nutch [35, 79] with an in-memory index. The index for websearch is generated by indexing a 250GB dump of 14.4 million pages from 2005 Wikipedia, which generates a 37GB index. We then use a 4GB portion of that index, which captures approximately 27GB and 1.6 million pages of the

original data. Websearch is driven by simulated search queries that are generated by a model that uses an exponential distribution for query arrival times and a query term model that is representative of web search queries seen at search engines [162]. Websearch must also satisfy a Quality of Service (QoS) constraint that 95% of the queries must be processed in less than 500ms [91]. Nutch is configured such that at 100% utilization it will use all available CPU cores.

Single SPECCPU workloads and application mixes from SPECCPU can be considered to be either throughput-oriented or latency-oriented. These benchmarks represent throughput-oriented applications if the number of benchmarks executed per second is the primary metric. Similarly, if the metric of interest is how long each benchmark takes to execute, then SPECCPU is an analogue for latency-oriented applications. SPECpower_ssj2008 is a throughput-oriented benchmark that scores the system by how many queries per second it can handle. Thus, we do not compute latency metrics for SPECpower_ssj2008. Finally, while websearch is both sensitive to throughput and latency, it can be optimized for either one. To optimize websearch for throughput, one would measure the maximum sustained QPS that can be achieved without violating QoS. To optimize for latency, one would reduce the 95%-ile latencies for a fixed QPS rate. In addition, since SPECpower_ssj2008 and websearch are request-driven workloads, we sweep the input QPS rate from 10% to 100% of the maximum QPS rate on each server configuration. This is done because datacenters are not always utilized at 100%.

3.3.2 TurboMode for Different Metrics

There are many metrics that are useful when dealing with performance, power, and cost. All of the metrics that we examine are legitimate metrics when applied to different workload scenarios. For instance, under periods of high load, the metric of interest will be performance, but under normal load conditions, $QPS/\$$ is more important. Even the same workload can have different metrics of interest. Take websearch for example. If one has a fixed 95%-ile latency target, the metric of interest is QPS/W or $QPS/\$$. On the other hand, if one wants to optimize for a lower 95%-ile target, then ED and ED^2 are more relevant. We list the metrics that we analyze below:

1. *Performance* measures the raw performance of a workload and is useful when application throughput and latency is critical. This metric will obviously be improved by the use of TM, and we include other metrics to see the true cost of using TM.

2. *Power* measures the total system power consumed while executing the workloads. This metric is for situations where minimal power is needed, even at the expense of performance.

3. *Energy Delay Product and Energy Delay Squared Product*: Energy Delay Product is calculated as the product of the energy it takes to complete an operation with the time it takes to complete the operation, and Energy Delay Squared Product is found in a similar way. These metrics are commonly used as a way of finding the optimal trade-off between performance and energy. This trade-off is important for latency sensitive applications in an energy constrained environment. [14]

	Workload	$\frac{QPS}{W}$	$\frac{QPS}{\$}$	ED	ED^2
SBServer	**SPECCPU**	On	On	On	On
	SPECCPU mixes	Off	?	Off	?
	PARSEC	Off	?	Off	?
	SPECpower_ssj2008	Off	On	N/A	N/A
	websearch	Off	On	On	On
SBServer†	**SPECCPU**	Off	On	On	On
	SPECCPU mixes	Off	Off	Off	?
	PARSEC	Off	Off	Off	?
	SPECpower_ssj2008	Off	On	N/A	N/A
	websearch	Off	On	On	On
ILServer	**SPECCPU**	On	On	On	On
	SPECCPU mixes	On	On	On	On
	PARSEC	On	On	On	On
	SPECpower_ssj2008	Off	On	N/A	N/A
	websearch	On	On	On	On
ILServer†	**SPECCPU**	Off	On	On	On
	SPECCPU mixes	Off	Off	?	On
	PARSEC	Off	On	?	On
	SPECpower_ssj2008	Off	On	N/A	N/A
	websearch	On	On	On	On
SBMobile	**SPECCPU**	Off	On	On	On
	SPECCPU mixes	Off	?	?	?
	PARSEC	Off	On	?	?
	SPECpower_ssj2008	Off	On	N/A	N/A
	websearch	Off	On	On	On
SBMobile†	**SPECCPU**	Off	On	Off	?

Table 3.2: Optimal TM settings for each metric/workload class/hardware configuration. On/Off indicates a static optimal TM setting of On/Off. ? indicates that there is no optimal static TM setting. The results for SPECpower_ssj2008 are reported at 100% QPS rate achieved with TM on. The QPS/W and $QPS/\$$ for websearch are reported at 100% QPS rate with TM on, and ED and ED^2 metrics are reported at 100% QPS rate with TM off. *SBMobile*† only has SPECCPU listed because all other workloads are energy-proportional on *SBMobile*.

4. *Queries Per Second Over Power (QPS/W)*: The efficiency of throughput-oriented batch workloads running on power constrained systems are best measured by this metric. QPS/W is inversely proportional to the amount of energy needed to execute one job; thus, this metric is the same as energy efficiency which is important in a large-scale DC [7].

5. $QPS/\$$ is a direct measure of cost efficiency. The fiscally conscious system operator will find this metric to be most relevant for throughput-oriented workloads. We use a standard 3 year depreciation

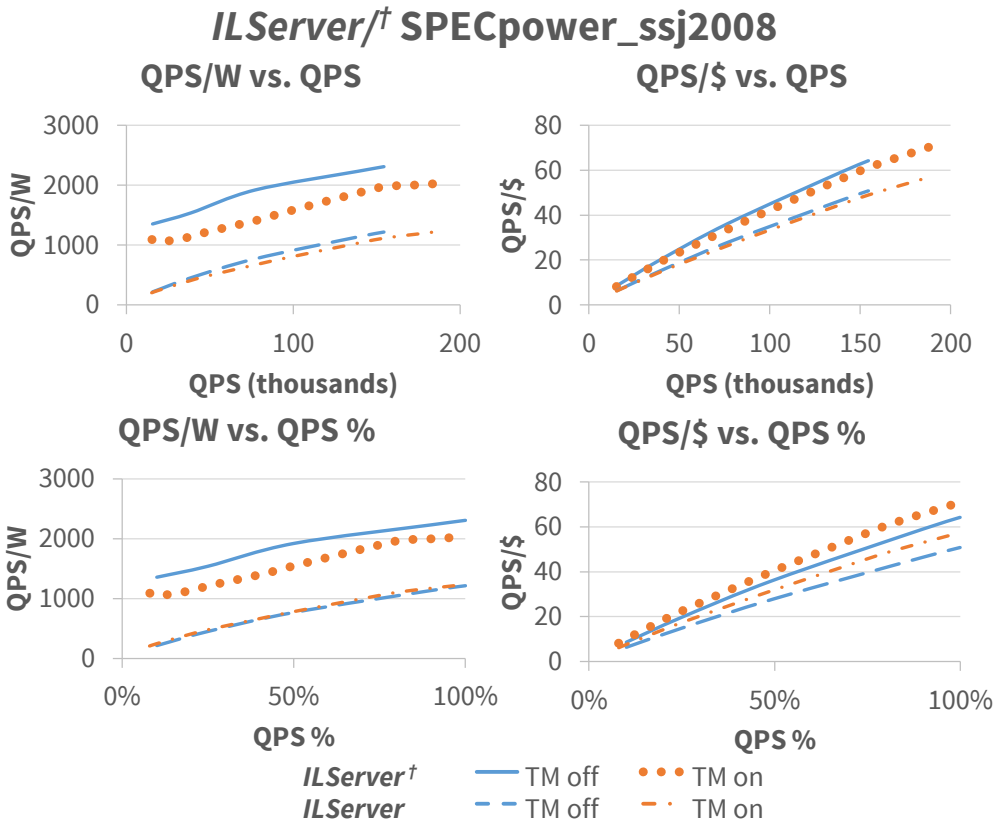

Figure 3.1: Impact of TM on QPS/W and $QPS/\$$ for SPECpower_ssj2008 on *ILServer* and *ILServer*†. The graphs in the upper half are for absolute QPS numbers, while the graphs in the lower half are for QPS numbers relative to the maximum QPS rate that can be supported for each setting of TM. Higher numbers are better for QPS/W and $QPS/\$$.

cycle, and we assume an electricity cost of \$0.15/kWHr. We use the cost model found in [119, 120] in our calculations. This metric is commonly used to measure the cost-efficiency of large-scale DCs [7].

We measured the changes in performance and power caused by the use of TM and calculated the above metrics the workloads on various hardware platforms. In Figure 3.2, we show the impact of TM on the various metrics for a subset of applications. For completeness, we show TM's impact on all metrics in Table 3.2.

Using TM will always have a positive impact on performance, as speeding up the clock frequency of the processor should not degrade application performance. Similarly, TM will certainly increase power consumption. As a case study of the optimal TM setting for QPS/W and $QPS/\$$ for a throughput driven workload, we examine SPECpower_ssj2008's behavior on *ILServer* and *ILServer*† as illustrated in Figure 3.1. SPECpower_ssj2008 is amenable to the use of TM, as enabling TM increases the maximum QPS rate by 25%. To optimize for both relative and absolute QPS/W, TM should be kept off. This is because QPS will typically scale only as much as frequency, but the power consumed scales faster than frequency. This is

due to the fact that $P \propto V^2 f$ and that higher frequencies require increased supply voltage [17]. Figure 3.1 shows this effect when idle power is removed (*ILServer*†), as QPS/W when TM is on always falls below the QPS/W for when TM is off.

On the other hand, if TM can produce a performance gain, then it should almost always be enabled to optimize for $QPS/\$$. This effect can be explained in a straightforward manner by reviewing the hardware and energy costs associated with the TCO. For *ILServer*, the cost of the hardware is about the same as the cost of electricity and infrastructure for power delivery and cooling. Since the use of TM does not increase power consumption by an inordinately large factor, it is always more advantageous to enable TM if it enables more performance out of the same piece of hardware. In Figure 3.1, the $QPS/\$$ for absolute QPS numbers seems to show that TM degrades this metric. However, in reality, if each machine can handle more work, then fewer machines need to be provisioned. Thus, TM improves $QPS/\$$ not for an individual machine, but rather for the entire datacenter, as reflected in the graph for $QPS/\$$ vs. relative QPS.

Table 3.2 shows that our observations for QPS/W and $QPS/\$$ based on SPECpower_ssj2008 running on *ILServer* also generalizes to many other workloads and platforms. There are some exceptions to the rule. Using TM can actually improve QPS/W in situations that are not energy-proportional, such as when running only a single instance of a SPECCPU application. When the idle power is removed (e.g., *SBServer*† and *ILServer*†), then the optimal TM setting for QPS/W for the single SPECCPU application workload is to turn TM off. In addition, there are times when TM should be disabled to optimize for $QPS/\$$, such as when TM does not appreciably increase the QPS rate.

TM has a variable effect on applications for ED and ED^2 in energy-proportional scenarios. In the single application workload scenario, ED and ED^2 always benefit from the use of TM; but trade-offs emerge when the energy-proportional approximation is applied. When multiple cores are being utilized, there is no optimal setting for ED and ED^2 across all workloads. As we will discuss in Section 3.3.3, the optimal TM setting for ED and ED^2 depends on whether the workload exhibits interference for shared resources. In Section 3.4, we will combine our observations from this section to build an effective system to select the optimal TM setting for ED, ED^2, and $QPS/\$$.

3.3.3 TurboMode for Different Workloads

As seen in Table 3.2, the optimal TM setting depends on the workload. We now focus on ED and ED^2 as a case study for how TM can affect those metrics depending on workload. In Figure 3.2, we show a subset of workloads that exhibit large swings for ED and ED^2 on the different machine configurations.

We study the ED and ED^2 metrics for websearch on *SBMobile*; the conclusions we arrive at also apply to *SBServer*†. *ILServer*† can mostly be explained in the same way as well, except for TM's large positive effect on QPS/W and $QPS/\$$. We sweep the QPS rate for websearch from 10% to 100% of the maximum QPS that it can support with both TM on and TM off and plot the effect of TM on various metrics in Figure 3.3, 3.4. 95%-ile latency is improved by 30%-35% across the same QPS range that websearch can support if TM is not enabled. The reason why the 95%-ile latency is reduced by a factor larger than the QPS gain can be

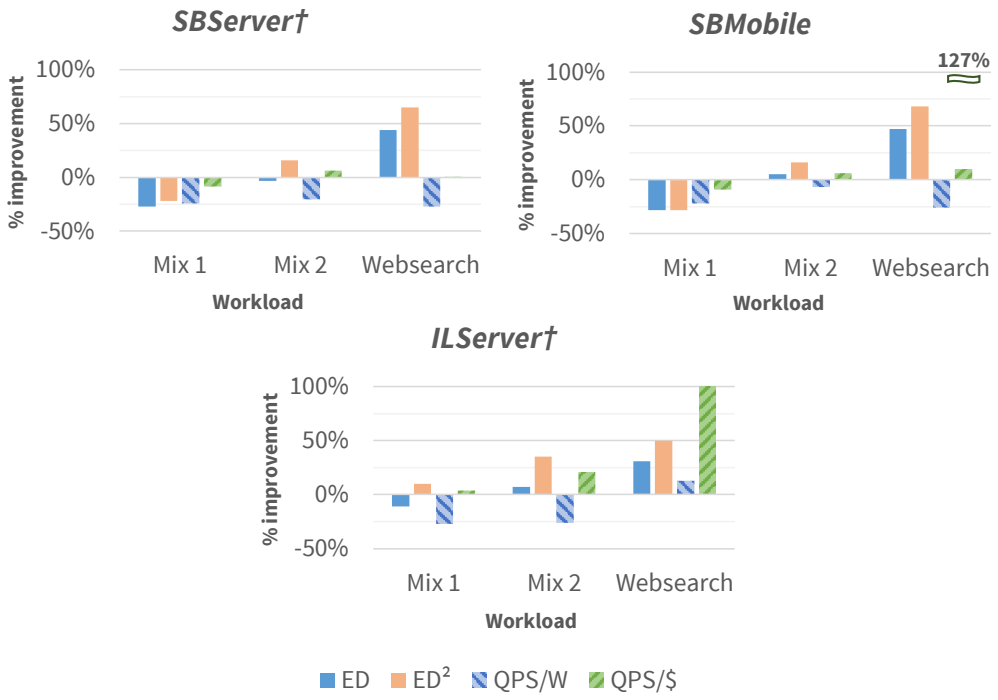

Figure 3.2: TM impact on ED, ED^2, QPS/W, and $QPS/\$$ metrics for a subset of workloads.

explained by queuing theory. A significant component of 95%-ile latency is due to a query being held up by earlier queries; thus, reducing the processing time for an individual query will have an amplified effect on reducing 95%-ile latency. Due to this effect, the ED and ED^2 metrics, which are based on 95%-ile latency, are always improved significantly through the use of TM. However, on the relative QPS graph, it may appear that enabling TM degrades ED and ED^2 when the utilization of the machine goes over 80%. This is misleading, because running websearch at that same *absolute* QPS rate with TM disabled will violate the QoS constraint. Thus, a direct comparison is invalid beyond that point. TM also provides a 24% boost to the maximum QPS, and its behavior for QPS/W and $QPS/\$$ mirrors that of SPECpower_ssj2008 and are explained in the same way. On *ILServer*, TM actually increases the maximum QPS by 180%, due to *ILServer* struggling to meet the QoS constraint when running with TM off. Because of the queuing delay effect, increasing the clock frequency leads to a large increase in maximum QPS, QPS/W, and $QPS/\$$. If the QoS constraint was relaxed to 1 second, then the large increase in maximum QPS vanishes and TM no longer benefits QPS/W or $QPS/\$$ as much.

We now turn our attention to the SPECCPU application mixes. Mix 1 is composed of lbm, xalancbmk, lbm, and milc. Mix 2 is composed of namd, hmmer, gobmk, and bzip2. These mixes were created by a random process as previously described. On *SBMobile*, using TM on Mix 1 increases the CPU frequency by 20%, but only produces an average performance increase of 0.2% with a 29% increase in power. On the other hand, enabling TM for Mix 2 boosts the core frequency by 13% for a 13% increase in performance and a

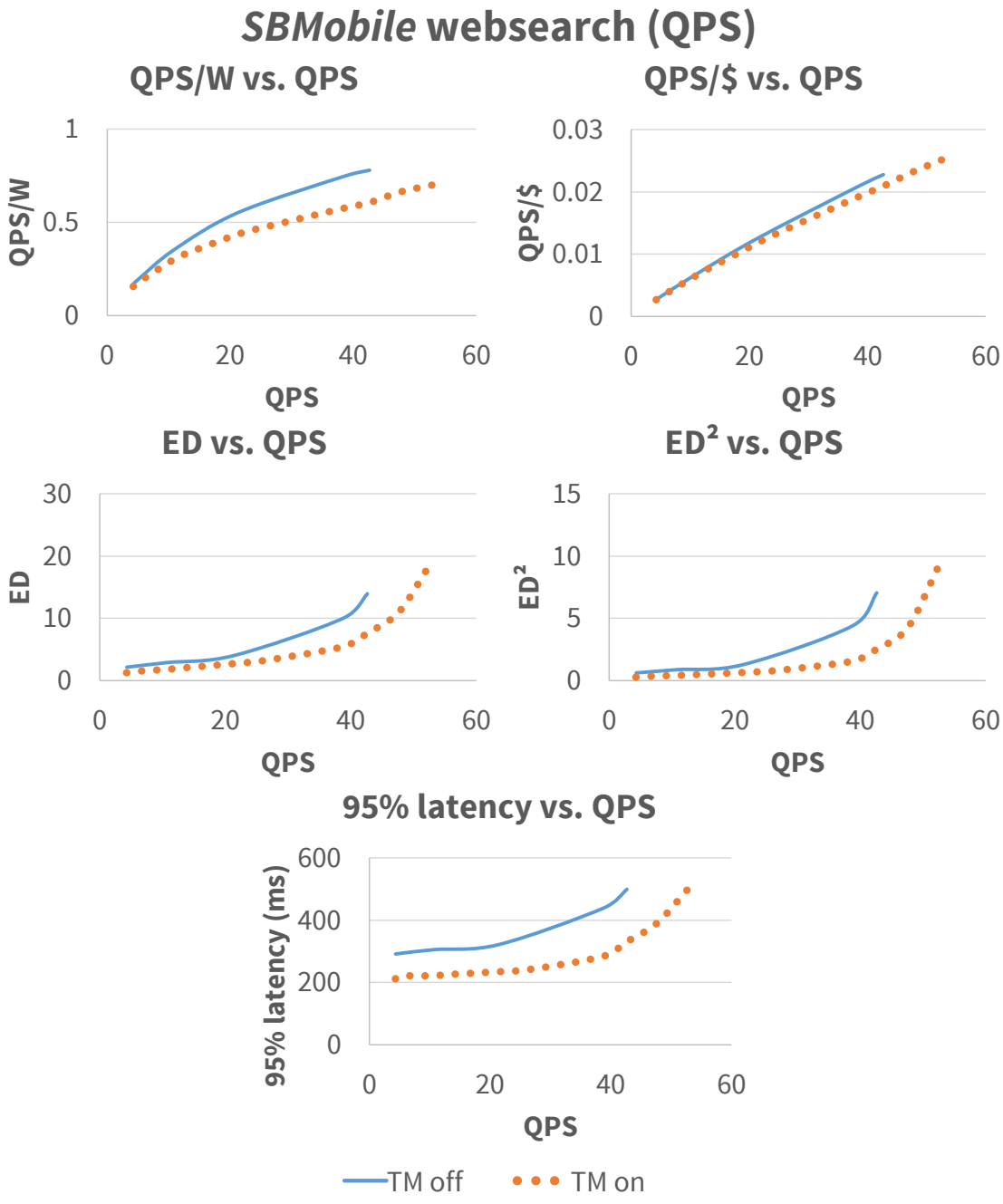

Figure 3.3: TM impact on various efficiency metrics and 95%-ile latency for websearch on *SBMobile*. The 95%-ile latency, ED, and ED^2 numbers are absolute, meaning that lower is better. QPS numbers are absolute in this figure.

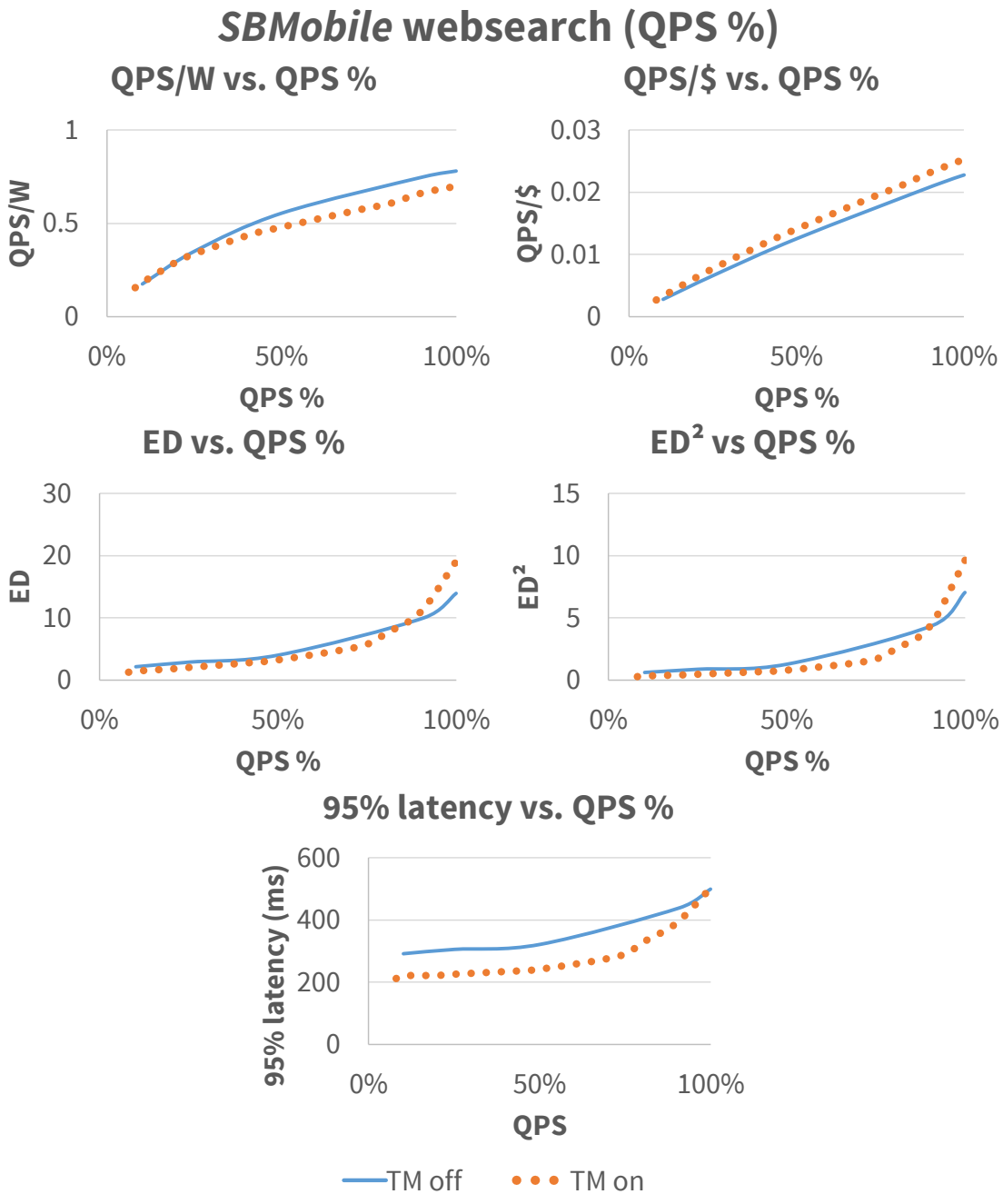

Figure 3.4: TM impact on various efficiency metrics and 95%-ile latency for websearch on *SBMobile*. The 95%-ile latency, ED, and ED^2 numbers are absolute, meaning that lower is better. QPS is normalized to peak QPS in this figure.

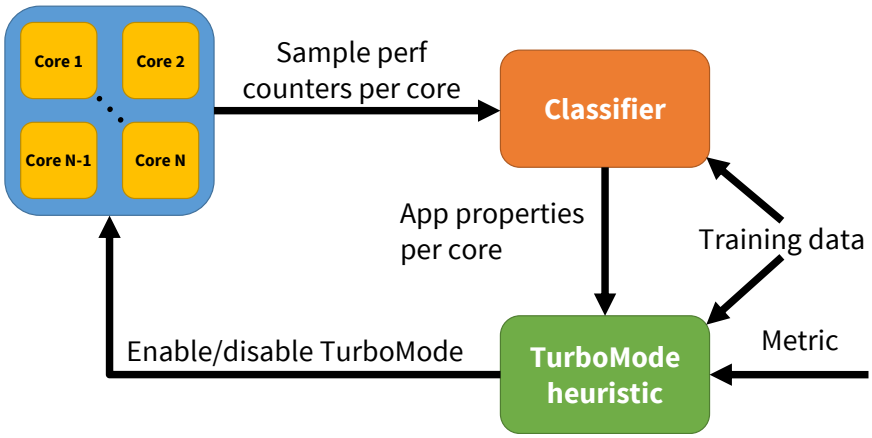

Figure 3.5: Block diagram of online component *autoturbo*.

22% increase in power. The reason for the disparate behavior is due to the composition of the mixes. Mix 1 is composed of applications that either fit in the last level cache, or exhibit cache thrashing behavior, while Mix 2 is composed of applications that are classified as cache insensitive or cache friendly [136]. Mix 1 incurs interference in the LLC and is a completely memory-bound workload that cannot benefit from TM. Enabling TM increases the CPU's power consumption, even if that increase does not translate into a performance gain. For workloads not dominated by memory accesses (e.g., Mix 2), TM will speed up the workload with modest power increases, resulting in a win for $QPS/\$$, ED, and ED^2. However, interference can occur in other shared resources external to the CPU, such as disk, network, and I/O. We expect that workloads that interfere in those resources will also experience large efficiency degradations when TM is enabled, and we leave the handling of those cases to future work. TM has many benefits but also runs the risk of increasing energy consumption without realizing gains in performance. This strongly motivates the construction of an intelligent controller that determines when TM should be enabled. In Section 3.4, the observation that significant memory interference causes TM to burn extra energy will be leveraged to build an intelligent TM controller.

3.4 Dynamic TurboMode Management

3.4.1 Overview

We have demonstrated earlier that the use of TM can significantly increase efficiency for some workloads while also causing major degradations for others. We want the best of both worlds, where the system intelligently uses TM only in situations that produce an efficiency improvement. To achieve this goal, we implement a software controller for TM named *autoturbo*.

The block diagram for *autoturbo* is shown in Figure 3.5. It runs as a periodic background daemon in order to minimize resource usage. *autoturbo* starts by collecting system wide per-core performance counters

Machine	Accuracy	Metric	Classifier	Features
SBServer†	100.0%	ED^2	Naive Bayes	% cycles w/ mem. requests
SBMobile†	96.8%			

Table 3.3: Classifier building results for metrics of interest on various hardware configurations.

for a configurable fixed time period, set to 5 seconds in our experiments. After it has collected counters, it uses a machine learning classifier to predict application characteristics for the workload on each active core. These results are then used by heuristics to determine whether TM should be enabled or disabled to optimize for a certain metric. The heuristic can be as simple as enabling TM if the classifier predicts that the workload benefits from the use of TM for a certain metric, to a more complicated heuristic that is used when several workloads are running at the same time. The TM setting from the heuristic is applied, and the process repeats from the beginning.

Since TM impacts each metric differently, we build a classifier and heuristic for each metric of interest. Every metric requires a separate classifier since TM will affect each metric differently. The process to build the classifier and heuristic can be automated and is described in Section 3.4.2. As *autoturbo* is an open-loop controller, having accurate models is very important.

3.4.2 Offline Classifier Training

The online component of *autoturbo* uses models that are generated offline for the various metrics. The modeling parameters only need to be generated once per server type. The offline training can be done by the system integrator, who then provides this information to all their customers for a plug-n-play solution that works right out of the box. The offline training can also be done by the DC operator for a more customized solution, as they can use their own metrics and workloads for the training phase. Another advantage of the DC operator performing offline training is that they can provide a more accurate TCO model for their infrastructure and cooling costs.

Classifying Individual Workloads Creating a model that predicts the impact of TM on individual workloads for a specific machine is fairly straightforward. We first use SPECCPU and two other memory intensive benchmarks, *stream* and *lmbench-lat_mem*, as the training applications. *stream* and *lmbench-lat_mem* are selected because they exhibit streaming and cache thrashing behaviors. These applications are then run on the machine that we wish to model, and performance, power, and various performance counters are measured when TM is on and when it is off. We then calculate the effect TM has on the power, performance, and cost metrics of interest.

As seen earlier, an application tends to benefit from TM if it is not memory bound. Therefore, to predict if an individual workload benefits from TM, we need only predict if it is memory bound. We build such a predictor by applying machine learning techniques on a wide array of performance counters that capture memory boundness, such as IPC, L3 loads/misses, TLB misses, memory requests, etc. We first use feature

	Machine	Classifier	Counters used	Accuracy
Sensitive	**SBServer**	Logistic Regression	% cycles with outstanding memory requests % cycles front end is idle	83.9%
	ILServer	Naive Bayes	L2-load-misses / instruction	93.5%
	SBMobile	Naive Bayes	% cycles with outstanding memory requests % cycles front end is idle	87.1%
Interfering	**SBServer**	Logistic Regression	% cycles with outstanding memory requests	87.1%
	ILServer	Naive Bayes	L3-misses # requests to memory / instruction	93.5%
	SBMobile	Logistic Regression	% cycles with outstanding memory requests	87.1%

Table 3.4: Classifier building and validation results for *Sensitive* and *Interfering* on various hardware configurations.

Property	SPECCPU apps with property
Sensitive	mcf, milc, cactusADM, soplex, GemsFDTD, libquantum, lbm, omnetpp, astar, sphinx3, xalancbmk
Interfering	bwaves, milc, leslie3d, soplex, GemsFDTD, libquantum, lbm

Table 3.5: SPECCPU application properties on *SBServer* and *SBMobile*. *ILServer* is the same as *SBServer* except that leslie3d is also in *Sensitive*.

selection to find the performance counters that best capture memory boundness, and to reject performance counters that have poor signal to noise ratio or that simply don't function correctly. Then, we train a model based on those features to pick the proper parameters for the model. We fit a model to each metric and machine, due to cost/hardware variation between different configurations. We use the Orange data mining package [23] for this because manually tuning the model is both time consuming and error prone. The model is then used in an online classifier that predicts whether TM will benefit a metric. The results of the feature selection and the accuracy of the classifiers are shown in Table 3.3. We show the results for the ED^2 metric on *SBServer*† and *SBMobile*† only since these are the only configurations where the optimal setting for TM varies depending on application. All other metrics on other hardware configurations have a static optimal setting, e.g., TM should always be off to optimize for QPS/W on *SBServer*†. For the remaining hardware configurations and metric, we show that using a single performance counter that tracks the fraction of time there is a memory request outstanding provides excellent prediction power.

Classifying Application Mixes Predicting the optimal TM setting for a given metric on a mix of applications is more complicated. The naive approach would be to model the interactions between workloads running on every core in the system. However, this approach is unscalable for large core counts, as the number of parameters for the classifier would scale with the square of the number of cores. Training such a classifier would also require a prohibitively large training set of application mixes.

Instead, we use a heuristic approach to determine the optimal TM setting for application mixes. In Section 3.3.3 we observe that memory interference (L3 for *ILServer*, main memory for *SBServer* and *SBMobile*)

causes TM to consume extra power without a corresponding performance gain. Thus, we developed a heuristic that dynamically detects excessive memory interference and disables TM. While we examine only memory interference for this work, extending the heuristic to detect other types of interference is straightforward. To aid in the detection of memory interference, we build classifiers using the same process previously discussed to predict if a workload is sensitive to memory interference (*Sensitive*) and if it causes memory interference (*Interfering*). This classification scheme was inspired by [70]. These two properties are independent from each other. For example, a workload that is memory latency bound but causes the prefetcher to trash the L3 cache is *Interfering*, but not *Sensitive*. To build each machine-specific classifier for *Interfering* and *Sensitive*, we run each SPECCPU application in tandem with the *stream* benchmark and measure the performance degradation for the SPECCPU application and for *stream*. Applications that degrade significantly when run in parallel with *stream* are marked as *Sensitive*, and applications that significantly slow down *stream* are marked as *Interfering*. The results of the application classification are shown in Table 3.5. We then build predictors using this data and show the results in Table 3.4. Misclassifications occur when applications with different properties have similar inputs to the classifier, which is caused by the use of indirect features (e.g., performance counters) to measure memory behavior. However, these cases are rare, as seen by the high classification accuracy.

The performance counters automatically selected by feature selection are intimately related to the architectures of the different CPUs. For *SBServer* and *SBMobile*, applications that are frequently stalled on memory (a high portion of cycles with a memory request pending and a high portion of cycles where the front end is stalled) are sensitive to memory interference. Similarly, applications that have intensive memory activity, as measured by a large fraction of cycles with pending memory requests, cause significant amounts of memory interference. For *ILServer*, since the L3 cache is exclusive of the L2, applications with high L2 MPKI are sensitive to memory interference. Similarly, applications with high L3 MPKI and memory access intensity cause memory interference. Since the best performance counters vary by processor architecture, it would have been difficult to manually pinpoint the precise performance counters to use even if the general theme of "performance counters related to memory" is known.

For *SBServer*, the *Sensitive* model misclassifies 5 SPECCPU applications: 434.zeusmp, 436.cactusADM, 437.leslie3d, 482.sphinx3, 483.xalancbmk. 434.zeusmp and 437.leslie3d are false positives. 434.zeusmp is misclassified due to the high percentage of cycles where the front end is idle, whereas 437.leslie3d is misclassified due to the high percentage of cycles where there is an outstanding memory request. 436.cactusADM, 482.sphinx3, 483.xalancbmk are false negatives. 436.cactusADM is misclassified because it has a relatively low percentage of cycles where there is an outstanding memory request, 482.sphinx3 because it has a relatively low percentage of cycles where the CPU front end idle, and 483.xalancbmk because it has low counts for both outstanding memory request time and front end idle time. 410.bwaves, 429.mcf, 470.lbm, 471.omnetpp for Interfering. 410.bwaves, 470.lbm are false negatives. 429.mcf, 471.omnetpp are false positives. The *Sensitive* and *Interfering* models for *SBMobile* behave similarly to *SBServer*, with the only exception being that 483.xalancbmk is classified correctly by the *MemSensitve* classifier. The similarity of the classifiers

between *SBMobile* and *SBSever* is expected, as both are based on the Sandy Bridge microarchitecture.

The *Sensitive* classifier for *ILServer* misclassifies 410.bwaves and 482.sphinx3. 410.bwaves is a false positive and 482.sphinx3 is a false negative. Both are misclassified because both have similar IPC and L2 load MPKI, but one application is sensitive while the other is not. Thus, during LOOCV, the 410.bwaves data causes the misprediction of 482.sphinx3, and vice versa. The *Interfering* classifier mispredicts both 429.mcf and 471.omnetpp as false positives. 429.mcf is not an interfering application despite having a high L3 MPKI and number of main memory request per instruction, while 471.omnetpp has a high L3 MPKI. Adding more performance counters to the classifiers causes the prediction accuracy to drop, indicating that all other performance counters have poor signal to noise ratios. In addition, measuring too many performance events would require sampling over a limited number of physical hardware event counter registers, degrading their accuracy.

The next step is to determine the maximum amount of interference before TM no longer provides a win. This process is controlled via static policy, which is determined by the maximum number of interfering workloads that can be co-located before the use of TM degrades a metric. To find the proper policy for each metric, we measure the power and performance increase caused by TM for different numbers of active cores. For example, TM increases power by 23% for a 4 core workload on *SBMobile* with a 12% frequency boost. Thus TM must significantly increase the performance of applications running on at least 2 cores in order to not degrade the ED^2 metric for *SBMobile*. This heuristic applies TM conservatively, as it pessimistically assumes that *Sensitive* workloads will not benefit at all from TM in the presence of memory interference. To determine the number of applications that will be degraded, the heuristic looks at the application properties of the workload on each core in a NUMA node. If there is more than one *Interfering* application, then the number of degraded applications will be the number of *Sensitive* applications. If there is one *Interfering* application, the number of degraded applications is the number of *Sensitive* applications on cores other than the one hosting the *Interfering* workload, as a workload cannot interfere with itself.

3.4.3 Online *autoturbo* Operation

We implement the online component of *autoturbo* as a Python program to have convenient access to the Orange machine learning library. However, this portion could also be implemented in the CPU firmware to offload the computational load of the classifier. This would require the CPU firmware to expose an interface to input training data and to declare the metric that *autoturbo* should be optimizing for. The pseudocode for *autoturbo* is given in Algorithm 3.1.

First, the system operator sets the system type and the metric that *autoturbo* should be optimizing for. This loads the appropriate models that were generated by the training phase as described in Section 3.4.2. Next, *autoturbo* samples the appropriate performance counters available on the system for 5 seconds. From this data, it can determine the number of cores that were active in the sampling period. If there were no active cores, then there is nothing to optimize for. If there is one active core, then the single application classifier is used to predict the optimal TM setting for that application. If there is more than one active core, then the

```
1 loadModels(systemType, metric)
2 while True:
3 |   perfCounters = sampleCounters()
4 |   if numCoresActive() == 1:
5 |   |   setTM(singleAppModel(perfCounters))
6 |   elif numCoresActive() > 1:
7 |   |   setTM(multipleAppModel(perfCounters))
```

Algorithm 3.1: autoturbo control loop.

multiple application classifier is used to predict if there is significant workload interference that would negate the benefits of TM. The predicted optimal TM setting is then set via *cpufreq-set*, and the process repeats.

The choice of a 5 second sampling period was done after considering the trade-off between increased reactiveness of *autoturbo* at shorter sampling periods and lower power consumption of *autoturbo* at longer sampling periods. Running the predictive classifiers, like any other application, consumes CPU resources and power. When there is a workload present, each sampling period will invoke at least one classifier, and so increased sampling increases the overhead of *autoturbo*. However, if the sampling period is too long, then changes in the workload composition or changes in the workload phase will not be quickly detected. We chose 5 seconds as a time period that is long enough to not increase CPU utilization or power by an appreciable amount, while being short enough such that the typical workload will not change drastically within most sampling windows.

As *autoturbo* runs as a background daemon, it can be easily deployed across the entire datacenter by standard application deployment procedures. *autoturbo* can be easily extended with remote management features, such as providing real-time reporting on when TM is enabled and the frequency boost of TM. The architecture of *autoturbo* also allows for real time switching of metrics to be optimized for, which is useful for large virtualized datacenters where workloads with different optimization targets can shift between physical machines. In addition, *autoturbo* can also be extended to manually disable TM on a node, which is invaluable in case of a thermal or power emergency in the datacenter. While remote management is currently not available in *autoturbo*, it is planned as future work.

Sandy Bridge implementation details All relevant performance counters can be conveniently obtained from *perf stat*. TM can only be controlled at a chip level granularity; thus, the optimal heuristic for workloads that utilize multiple cores is the same as the one previously described.

Interlagos implementation details In addition to per-core performance counters obtained from *perf stat*, the classifiers for the Interlagos platform also require counters from the North Bridge performance monitoring unit (NBPMU) that provides performance counters for each NUMA node that includes 8 cores. Since *perf stat* for our Linux distribution did not support using the NBPMU, we wrote our own application that gets and sets that appropriate MSRs for the NBPMU by using the msr kernel module. Using the NBPMU poses a challenge because the performance counters obtained from the NBPMU are not per-core counters. Thus, we approximate the contribution from core c to a NBPMU counter by the following formula:

$NBPMU\ counter_c = \frac{(NBPMU\ counter)(L2\ load\ misses_c)}{All\ L2\ load\ misses\ on\ same\ NUMA\ node}$. This method works under the assumption that the probability of a L3 miss is independent of the requesting core. While this assumption is not guaranteed to be true for a set-associative cache, we find it to hold for our benchmark applications. Nevertheless, the ideal solution would be to implement an analogue of the L3 misses and # of main memory request performance counters in the per-core PMU.

While TM can be controlled at a module granularity, in practice we find that controlling TM at such a fine granularity on the Interlagos platform is not worthwhile. This is due to the Interlagos chip not being energy-proportional. For example, if two cores (on two separate dies) are active with TM on, the power draw is 53W above idle power. If TM is disabled on one core, then the power draw only drops by 3W. However, disabling TM on both cores drops the power by an additional 20W. Thus, *autoturbo* controls TM on *ILServer* at a chip-level granularity.

3.5 Evaluation

We evaluate *autoturbo* for all workloads on all hardware platforms across all metrics by running *autoturbo* on top of the workload. We measure the power consumption of the machine and the performance of the workload to determine how effectively *autoturbo* can use TM to optimize for a given metric. We show the results of using *autoturbo* on a subset of workloads/metrics/hardware platforms in Figures 3.6, 3.7. Each line shows the metric of interest for the workload, normalized to the baseline case of when TM is always off. We compare *autoturbo* against two other management strategies for TM. The Naive manager naively uses TM all the time. The Static Oracle has prior knowledge of which setting of TM should be applied for the *entire duration* of the workload to optimize for a given metric. The Static Oracle required several profiling runs and as such is not practical for scheduling unknown workloads. For each line, the workloads (X axis) are sorted by the improvement achieved in ascending order. The behavior of *autoturbo* on the single SPECCPU workload running on *SBMobile*† is similar to *SBServer*†. In addition, *autoturbo* also has the same behavior for websearch and SPECpower_ssj2008 for all metrics measured on all machines. We compare the performance of *autoturbo* on websearch and SPECpower_ssj2008 against naively enabling TM, as that is the optimal setting for those workloads. Even though *autoturbo* was trained on SPECCPU applications, we can still use them as test applications because *autoturbo* was trained on performance counters for the *entire run*, while the classifier uses counters obtained from 5 second windows as its inputs.

SBMobile *autoturbo* is able to use TM to intelligently improve $QPS/\$$ and ED^2 for the workload consisting of SPECCPU application mixes. We show results for when all cores are used and when half the cores are used in Figure 3.6. When all cores are used, the naive approach can improve the $QPS/\$$ ratio and ED^2 metrics for approximately 40% of the mixes compared to the baseline. However, the other 60% of the time it will cause degradations for those metrics. This degradation can be severe, up to 8% for $QPS/\$$ and 25% for ED^2. These degradations are due to applications within the mix interfering with each other, causing the naive use of TM to consume extra power to provide a frequency boost that does not translate into

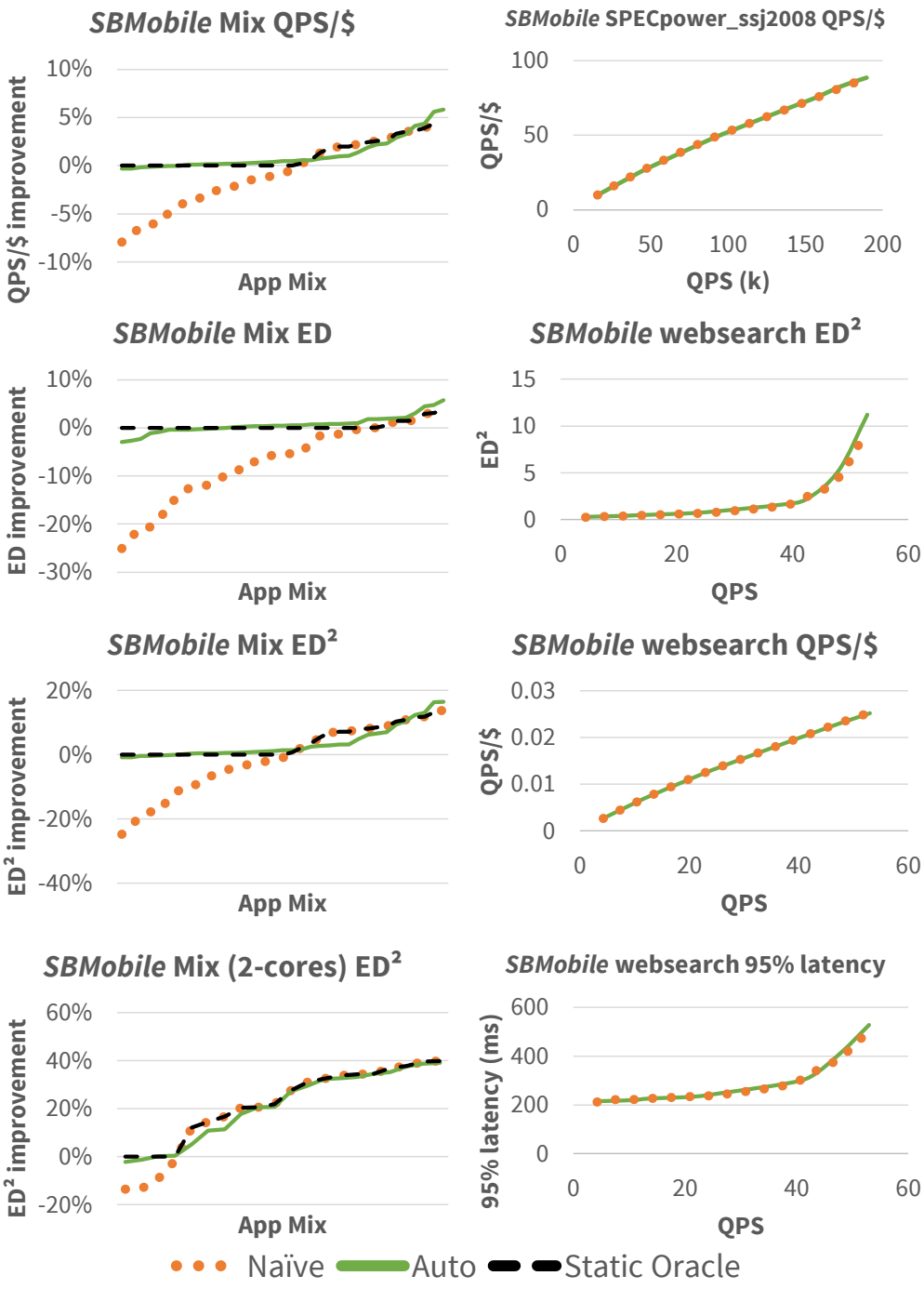

Figure 3.6: *autoturbo*'s effect on various workloads for SBMobile.

improved performance. *autoturbo*'s heuristic to avoid the use of TM in such interference scenarios is clearly

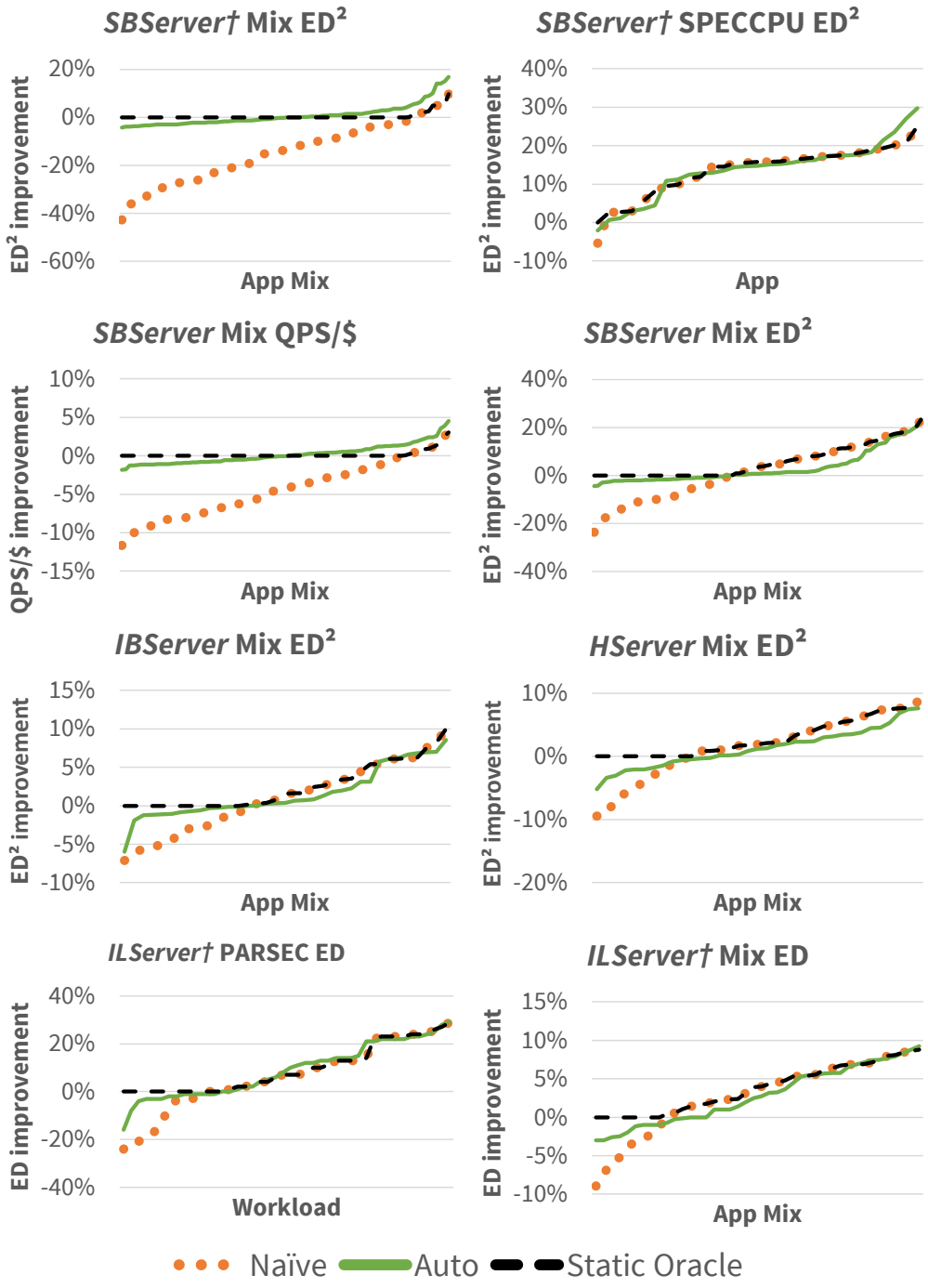

Figure 3.7: *autoturbo*'s effect on various workloads for ILServer/SBServer/HServer.

effective, as *autoturbo* virtually eliminates all cases of metric degradation. However, the heuristic trades off a

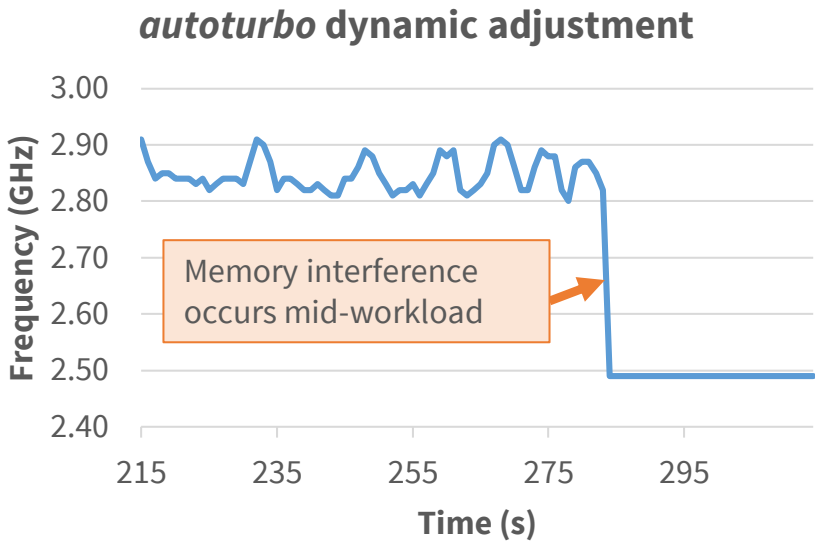

Figure 3.8: *autoturbo* detecting a phase change and adjusting TM for a SPECCPU mix made of gromacs, bwaves, gromacs, and GemsFDTD. *autoturbo* is optimizing for ED^2 on *SBMobile*.

low rate of false positives for a low rate of false negatives. *autoturbo's* heuristic is conservative in managing interference, as it preemptively disables TM in the face of predicted interference even if that interference turns out to be mild. This effect is shown by *autoturbo* failing to match the same level of metric improvement as the Static Oracle. One avenue of future work is to build a regression model that predicts the amount of interference and to only disable TM if that interference is above a threshold. Interestingly, there are also cases where *autoturbo* outperforms the Static Oracle. This occurs in situations where the SPECCPU application has phases in its execution that vary between CPU-intensive and memory-intensive. The Static Oracle cannot take advantage of this dynamism, since it chooses a TM setting for the entire workload duration. On the other hand, *autoturbo* can detect and account for these phase changes, as seen in Figure 3.8. When half the cores are used, we see larger gains in ED^2 because TM provides a larger frequency boost. *autoturbo* functions properly in this case, and is able to enable TM when ED^2 is improved while disabling it for mixes with heavy memory interference.

For SPECpower_ssj2008, not only is *autoturbo* able to properly apply TM, but its CPU footprint is small enough such that it does not interfere with it. Even as QPS is swept from low to high, *autoturbo* does not have a detrimental effect on the efficiency of SPECpower_specssj2008, as the $QPS/\$$ for *autoturbo* closely tracks the behavior of naive TM. For websearch, the use of *autoturbo* generally does not degrade performance or efficiency metrics compared to the naive use of TM. The only exception is when websearch is run at 100% QPS and *autoturbo* slightly degrades the 95%-ile latency and the associated ED^2 metric. When *autoturbo* wakes up to classify the applications, it will cause the OS to switch out a websearch thread, degrading the response latency. If the classifier component of *autoturbo* is integrated into firmware, then this performance penalty will disappear. *autoturbo* is also able to properly optimize for the ED^2 metric for the

single application SPECCPU workload for *SBMobile*†, disabling TM for the one workload (milc) that does not benefit from TM.

While not shown, we observed that *autoturbo* is able to improve $QPS/\$$ and ED^2 for PARSEC as well.

SBServer *autoturbo* is also able to optimize the SPECCPU application mixes for $QPS/\$$ and ED^2 for *SBServer* and ED^2 for *SBServer*†, as shown in Figure 3.7. While the degradation of TM for $QPS/\$$ can be -12%, *autoturbo* is able to select the proper TM setting to ensure that it only degrades $QPS/\$$ by a maximum of -3%. Likewise, *autoturbo* is also able to disable TM in cases where workload interference would degrade ED^2 significantly. *autoturbo* is quite successful at preventing significant degradation of metrics, as it has strictly better worse case performance compared to the Naive TM manager. However, like *SBMobile*, the interference heuristic in TM is overly conservative, causing *autoturbo* to miss some opportunities for improving ED^2. For ED^2 on *SBServer*†, where there is no idle power to buffer the ED^2 of workloads with interference, the conservative heuristic in *autoturbo* pays off by being strictly better than the Naive use of TM to improve ED^2. *autoturbo* does have a few minor false positives that degrade ED^2 by at most -7%. These false positives arise when *autoturbo* misclassifies applications as not being *Sensitive* or *Interfering* when they actually are. *autoturbo* also is able to successfully optimize the single application SPECCPU workload running *SBServer*† for ED^2. It successfully tracks the performance of the Static Oracle, demonstrating that the theoretical accuracy of the single workload ED^2 classifier is realized in a practical setting. While not shown, *autoturbo* successfully optimizes PARSEC for ED^2 on *SBServer*† as well. Like *SBMobile*, *autoturbo* also correctly turns on TM for SPECpower_ssj2008 and websearch to take advantage of TM improving $QPS/\$$, ED, and ED^2 while exhibiting negligible interference with those workloads.

ILServer We show the results of running *autoturbo* on *ILServer* in Figure 3.7. For the SPECCPU application mix workload, we use *autoturbo* to optimize the ED metric on *ILServer*†, since all other metrics on *ILServer*† and all metrics on *ILServer* have a statically optimal TM setting. This is because an 8 application SPECCPU mix fails to saturate memory bandwidth, a result of the low clock frequency and the low IPC on the *ILServer*. Thus, running many interfering applications together still leads to a small but non-negligible speedup for SPECCPU mixes for a relatively small increase in power. Like *SBServer*†, *autoturbo* successfully eliminates major degradations in ED but also misses some opportunities to improve ED. For PARSEC on *ILServer*†, *autoturbo* is able to eliminate most of the degradations to ED while keeping the benefits of TM. The only case where it failed to do so was when *autoturbo* activated TM for *streamcluster* at low thread counts, because it could not predict that the performance gain was too small to be worthwhile. *autoturbo* is also able to successfully optimize SPECpower_ssj2008 for $QPS/\$$ and websearch for $QPS/\$$, ED, and ED^2 by turning on TM consistently and by not interfering with those workloads.

IBServer and HServer We observe the generality of *autoturbo* by demonstrating that it functions across several generations of architectures from the same CPU vendor, as seen in Figure 3.7. A surprising result for HServer is that while Haswell has independent frequency domains for each core, once TM is activated, all cores will run at the same frequency, thus *autoturbo* is still useful. Due to space constraints, we omit the results from the entire metric and workload evaluation and only show results for *autoturbo* optimizing the

ED^2 metric for SPECCPU application mixes. Just like with the other hardware configurations, *autoturbo* intelligently enables TM to optimize for ED^2. However, *autoturbo* will occasionally disable the use of TM even when it is optimal to use TM. Again, this is because of the conservative heuristic used to determine if there is too much interference.

3.6 Related Work

While the management of TM is a developing field, there is much prior work on dynamic power management for CMPs. [62] proposes the use of a global manager that selects the proper power mode with the help of DVFS to minimize power with respect to a given performance target. However, they assume that the underlying hardware supports software managed per-core DVFS, which is not available from current implementations of TM. [80] studies the use of on-chip regulators for DVFS and conclude that CMPs can benefit greatly from its use. Per-core DVFS would allow *autoturbo* to selectively enable TM for cores hosting workloads that benefit from the extra frequency boost. [33] proposes a hardware mechanism that can be used to accurately model the profitability of DVFS at various operating points. If this hardware mechanism was available on our evaluation hardware, then we could accurately use it to predict the optimal setting of TM as opposed to using our ML model to approximate the benefits of TM. [63] also proposes using performance counters to decide when to use low-power and high-power DVFS states. We use a machine learning to extend this idea to create a more robust predictor that can handle workload interference from executing several workloads on the same CMP. A key enabler for TM is per-core power gating [87], which creates large amounts of thermal and electrical headroom that is used to boost the frequency of the remaining active cores. Another enabling technology is for the CPU to estimate its power consumption when deciding if there is sufficient headroom to activate TM [64]. Computational sprinting [127] utilizes thermal capacitance to temporarily overclock the CPU to achieve increased performance for a short period of time. This is different from TM in that TM can achieve sustained overclocking if there are idle resources on the CPU.

The field of evaluating and managing TM is nascent, as the technology was only recently introduced. [17] evaluate TM on an Intel Nehalem processor and determine that TM improves execution time at the cost of power. We extend their work by demonstrating that although QPS/W is not improved, the use of TM can still improve other metrics of interest. In addition, we also implement a software TM controller that is able to prevent the activation of TM in suboptimal scenarios.

There has been much prior work on detecting and managing workload interference caused by memory contention. [69] quantifies destructive interference between separate processes on CMPs and concludes that most of the performance penalty comes from contention for the shared memory bus, supporting our strategy for detecting workload interference. [105] propose Cross-core interference Profiling Environment (CiPE) as a way of directly detecting cross-core interference in an accurate fashion, as opposed to indirect detection of *autoturbo*. CiPE uses offline profiling, which is infeasible for DCs that can accept any workload, such as

Amazon EC2. However, CiPE is a viable method for characterizing applications as *Sensitive* and/or *Interfering* during the offline training phase for *autoturbo*. [113] also deals with resource contention with an eye towards optimizing for the ED metric. Their focus is more on scheduling, although they also use DVFS as a fallback attempt to deal with energy inefficiency in the case of memory contention that scheduling cannot resolve. *autoturbo* complements this work, as it can optimize for energy efficiency in the newly introduced TM regime that cannot be controlled in the same way as DVFS. [136] proposes Vantage, an effective cache partitioning scheme. *autoturbo* can use Vantage to partition the last level cache to shield *Sensitive* applications from *Interfering* applications to maximize the benefit of TM. [50] manages interference between contending workloads on a CMP by using clock modulation, which is another knob *autoturbo* can use to selectively enable TM for workloads that benefit from a faster clock.

3.7 Conclusions

Modern servers must carefully balance performance gains against energy consumption and cost increases. We showed that TurboMode, the dynamic overclocking of multi-core chips when thermal and power headroom exists, can greatly improve performance. However, its impact on efficiency metrics that include energy and cost is not always positive and depends significantly on the characteristics of the application and underlying hardware. We developed *autoturbo*, a software daemon that utilizes predictive models to understand the impact of TurboMode on the current workload and to decide if TM should be turned on or off. *autoturbo* allows workloads to get the maximum benefit from TurboMode when possible (up to 68% efficiency increase for ED^2), while eliminating virtually all the cases where TurboMode leads to efficiency drop (up to -25% for ED^2). We also demonstrate that *autoturbo* is a general solution that works for many different hardware configurations.

Chapter 4

Towards Energy Proportionality for OLDI Workloads

After finding opportunities to improve peak energy efficiency, we turn our attention to improving energy efficiency during periods of low utilization. This is critical for large-scale latency-critical workloads running in warehouse-scale computers (WSCs). Reducing the energy footprint of WSCs systems is key to their affordability, yet difficult to achieve in practice. The lack of energy proportionality of typical WSC hardware and the fact that important workloads (such as search) require all servers to remain up regardless of traffic intensity renders existing power management techniques ineffective at reducing WSC energy use.

We present PEGASUS, a feedback-based controller that significantly improves the energy proportionality of WSC systems, as demonstrated by a real implementation in a Google search cluster. PEGASUS uses request latency statistics to dynamically adjust server power management limits in a fine-grain manner, running each server just fast enough to meet global service-level latency objectives. In large cluster experiments, PEGASUS reduces power consumption by up to 20%. We also estimate that a distributed version of PEGASUS can nearly double these savings.[1]

4.1 Introduction

Warehouse-scale computer (WSC) systems support popular online services such as search, social networking, webmail, online maps, automatic translation, and software as a service (SaaS). We have come to expect that these services provide us with instantaneous, personalized, and contextual access to petabytes of data. To fulfill the high expectations for these services, a rapid rate of improvement in the capability of WSC systems is needed. As a result, current WSC systems include tens of thousands of multi-core servers and consume tens of megawatts of power [6].

[1] This chapter is based on work that was originally published in [98].

The massive scale of WSC systems exacerbates the challenges of energy efficiency. Modern servers are not energy proportional: they operate at peak energy efficiency when they are fully utilized, but have much lower efficiencies at lower utilizations [5]. While the average utilization of WSC systems for continuous batch workloads can be around 75%, the average utilization of shared WSC systems that mix several types of workloads, including online services, may be between 10% and 50% [6]. At medium and low utilizations, the energy waste compared to an ideal, energy proportional system is significant. To improve the cost effectiveness of WSC systems, it is important to *improve their energy efficiency at low and moderate utilizations*.

For throughput-oriented, batch workloads such as analytics, there are several ways to improve energy efficiency at low utilization. We can consolidate the load onto a fraction of the servers, turning the rest of them off [86,152]. Alternatively, we can temporarily delay tasks to create sufficiently long periods of idleness so that deep sleep modes are effective [109, 110]. Unfortunately, neither approach works for *on-line, data-intensive (OLDI) workloads* such as search, social networking, or SaaS. Such user-facing services are often scaled across thousands of servers and access distributed state stored across all servers. They also operate with strict service level objectives (SLOs) that are in the range of a few milliseconds or even hundreds of microseconds. OLDI workloads operate frequently at low or medium utilization due to diurnal patterns in user traffic [110]. Nevertheless, server consolidation is not possible, as the state does not fit in a small fraction of the servers and moving the state is expensive. Similarly, delaying tasks for hundreds of milliseconds for deep sleep modes to be practical would lead to unacceptable SLO violations. Even at very low utilization, OLDI servers receive thousands of requests per second. Finally, co-scheduling other workloads on the same servers to utilize spare processing capacity is often impractical as most of the memory is already reserved and interference can lead to unacceptable degradation on latency SLO [28, 73, 105, 163].

A promising method to improve energy efficiency for OLDI workloads at low or medium utilization is to *scale the servers' processing capacity to match the available work*. We can reduce power consumption by scaling voltage and clock frequency (DVFS) or the number of active cores in the server. Traditionally, DVFS is controlled by monitoring CPU utilization, raising the frequency when utilization is high and decreasing it when it is low. We demonstrate that DVFS schemes that use CPU utilization as the only control input are ineffective for OLDI workloads as they can cause SLO violations. We observe that OLDI workloads exhibit different latencies for the same CPU utilization at different CPU frequencies. This makes it particularly difficult to correlate CPU utilization to request latency at different DVFS settings and complicates the design of robust control schemes.

We advocate making OLDI workloads more energy efficient across the utilization spectrum through fine-grain management of the servers' processing capacity based on the observed, end-to-end, request latency. The proposed *iso-latency* power management technique *adjusts server performance so that the OLDI workload "barely meets" its SLO goal*. By directly using the overall request latency and SLO targets, instead of the inaccurate and indirect metric of CPU utilization, we can achieve robust performance (no degradation of the SLO), while saving significant amounts of power during low and medium utilization periods. We show that *iso-latency* power management achieves the highest savings when using a fine-grain CPU power control

mechanism, Running Average Power Limit (RAPL) [60], which allows the enforcement of CPU power limits in increments of 0.125W.

The specific contributions of this chapter are the following. We characterize Google workloads, including search, with real-world anonymized traffic traces to show the high cost of the lack of energy proportionality in WSC systems. We also quantify why power management techniques for batch workloads or utilization-based DVFS management are ineffective for OLDI workloads. We show that latency slack is a better metric compared to CPU utilization when performing power saving decisions. Next, we characterize the potential of *iso-latency* power management using RAPL and show that it improves energy proportionality and can lead to overall power savings of 20% to 40% for low and medium utilization periods of OLDI workloads. Since the cluster is operated at low and medium utilizations for nearly half the time, *iso-latency* translates to significant power savings. The characterization of *iso-latency* demonstrates some non-intuitive results such as: a) aggressive power management works for tail latency and can be applied with minimal extra power at scale; b) ultra-low latency services benefit even more from aggressive power management techniques. Finally, we describe PEGASUS, a feedback-based controller that implements *iso-latency* power management. For search, PEGASUS leads to overall power savings of up to 20% in clusters with thousands of servers without impacting the latency SLO. In addition, PEGASUS makes clusters nearly energy proportional for OLDI workloads in the 20% to 50% utilization range. If we discount the idle power at zero utilization (due to power for fans, power supplies, DRAM refresh etc.), PEGASUS meets and often beats energy proportionality in this range. We also estimate that a distributed version of PEGASUS that identifies less utilized servers in the cluster to further reduce power on can achieve the full potential of *iso-latency* power management, or nearly 40% power savings. To the best of our knowledge, this is the first study to achieve such power savings on an actual warehouse-scale deployment and the first to evaluate fine-grained versus coarse-grained power management tied to application latency SLO metrics.

4.2 On-line, Data Intensive Workloads

4.2.1 Background

On-line, data intensive (OLDI) workloads such as search, social networking, and SaaS represent the vast majority of activity on the Internet. They are driven by user requests that require mining through massive datasets and then returning combined results from many servers in near real-time. Hence, they partition the data across a large number of servers and use multi-tier, high fan-out organizations to process each request. For instance, in web search, processing a user query involves fanning out the query through a large tree of nodes [25]. In addition, DRAM and Flash memory are often used for fast access to data.

OLDI workloads are quite different from large-scale batch workloads like MapReduce. In addition to high throughput requirements, OLDI workloads have strict requirements on end-user latency. In our search example, since the rendered content can only be sent back to the user after all steps have completed, a slowdown in any one server in the tree will lead to either a slowdown for the user or degraded results,

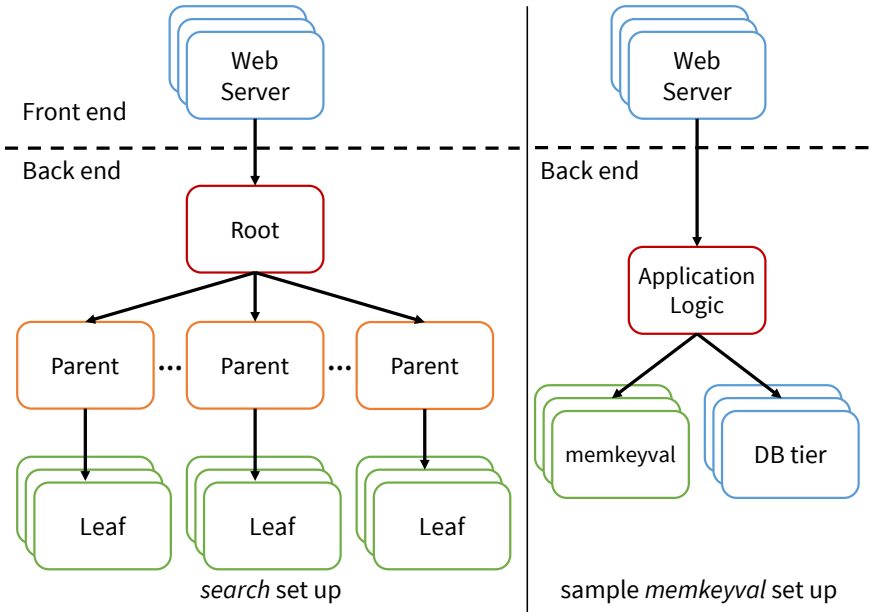

Figure 4.1: Configurations for *search* and *memkeyval*.

either of which result in poor end-user experience. Social networking and SaaS exhibit similar behavior in terms of high fanout and a dependence on the slowest component. It is well understood that an additional server-side delay of just 400msec for page-rendering has a measurable impact on user experience and ad-revenue [137]. Moreover, the large number of users and requests makes it important to optimize tail latency, not just average latency. Achieving low tail latency at the scale and complexity of OLDI workloads is quite difficult [26], making power management challenging. For instance, rendering a social networking news feed involves queries for the user's connections and his/her recent status updates; ranking, filtering, and formatting these updates; retrieving related media files; selecting and formatting relevant advertisements and recommendations; etc. Since the rendered content can only be sent back to the user after all the steps have completed, a slowdown in any one component will lead to either a slowdown for the user or degraded results, either of which result in a poor end-user experience.

4.2.2 OLDI Workloads for This Study

We use two production Google services in this study.

search: We evaluate the query serving portion of a production web search service. *search* requires thousands of leaf nodes all running in parallel in order to meet the stringent SLO, which is on the order of tens of milliseconds. Figure 4.1 shows an example *search* topology: a user query is first processed by a front-end server, which then eventually fans out the query to a large number of leaf nodes [25]. The search index is sharded across all of the leaf nodes and each query is processed by every leaf. Relevant results from each

leaf are then aggregated, scored, ordered, and sent to the front-end to be presented to the user. Most of the processing is in the leaf nodes that mine through their respective shards. Consequently, leaf nodes account for the vast majority of nodes in a search cluster and are responsible for an overwhelming fraction of power consumed. To drive *search*, we use an example serving index from Google. We use an anonymized trace of real user queries for load generation. We can also generate a controlled amount of load by replaying the query log at different QPS (queries per second) levels.

memkeyval: We also evaluate an in-memory key-value store used in production services at Google. Functionally, it is similar to *memcached*, an open source in-memory key-value store [111]. While *memkeyval* is not directly user-facing, it is used in the backends of several Google web services. Other large-scale OLDI services, such as Facebook and Twitter, use *memcached* extensively in user-facing services as well, making this an important workload. Figure 4.1 shows an example of how *memkeyval* is used by user-facing services. *memkeyval* is architected such that each *memkeyval* server is independent from all other *memkeyval* servers. Compared to *search*, there is significantly less processing per request and no direct fan out of requests. Instead, the fan-out occurs at a higher tier, where the web tier or application logic can issue tens or hundreds of requests to satisfy a single user request. Because of this, *memkeyval* has even tighter SLO latency constraints than *search*, typically on the order of tens or hundreds of microseconds. Hence, *memkeyval* adds to our analysis an example of an ultra-low latency workload. To generate load for *memkeyval*, we captured a trace of requests from production services, which we can replay at varying QPS speeds.

4.2.3 Power Management Challenges

Figure 4.2 shows the diurnal load variation for search on an example cluster. Load is normalized to the peak capacity of the cluster and power is normalized to the power consumed at peak capacity. There are several interesting observations. First, the cluster is not overprovisioned as it is highly utilized for roughly half the day, demonstrating that both the number and type of servers are well tuned for the peak of this workload. However, load is not constant. There is a very pronounced trough that represents a long period of low utilization. Second, the cluster exhibits poor energy proportionality during off-peak periods. Ideally, power consumption should closely track load. However, the actual power consumed is much higher: at 30% utilization the cluster draws 70% of its peak power. Since a major reason for lack of proportionality is the non-zero idle power (due to various components such as fans, power supplies, memory refresh, etc.), we also define a relaxed energy proportionality that only looks at the energy proportionality of dynamic power by discounting the idle power draw at 0% utilization. The *Dynamic EP* in Figure 4.2 is defined such that the power at 100% utilization is 100% of peak power, the power at 0% utilization is the idle power of the cluster, and all powers in between fall on a line connecting the two points. *Dynamic EP* represents the expected power draw of a cluster assuming that idle power cannot be removed and is often used to model server power [6]. Even after discounting idle power, the cluster draws far more power than expected at low utilizations. This is the opportunity gap we target: reducing the operating cost of large WSC systems by making them more energy proportional during periods of low or medium utilization.

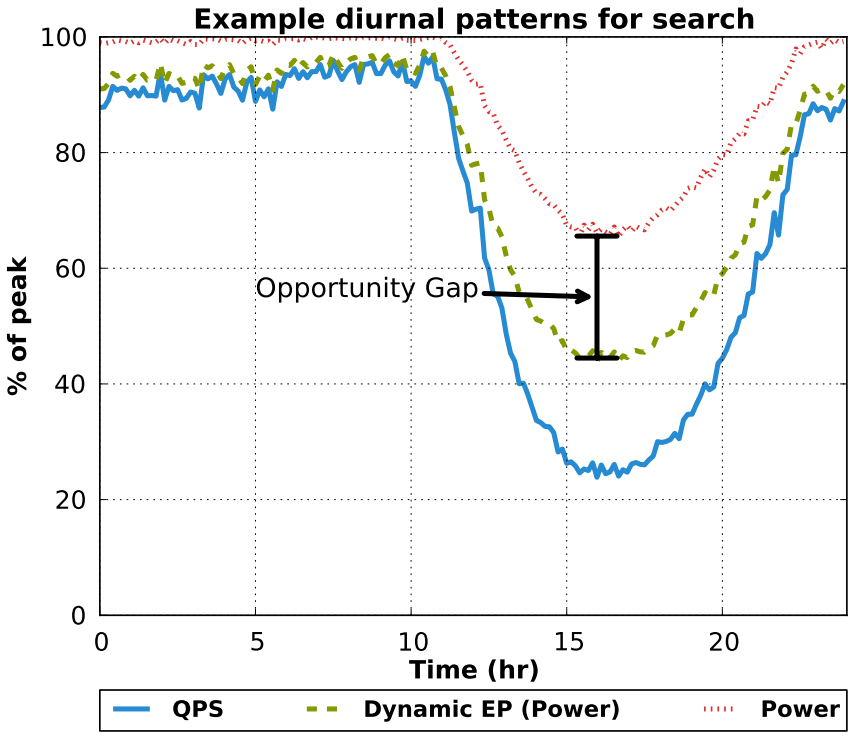

Figure 4.2: Example diurnal load and power draw for a search cluster over 24 hours. For a perfectly energy proportional cluster, power draw would perfectly track load (QPS). *Dynamic EP (Power)* indicates the hypothetical amount of power consumed if the idle power is assumed to be constant and the active power is energy proportional.

Existing power management techniques for WSC systems cannot address this opportunity gap for OLDI workloads. Several techniques advocate consolidating workloads onto a fraction of the available servers during periods of low utilization so that the remaining servers can be turned off [73]. Hence, while each server is not energy proportional, the WSC system as a whole becomes nearly energy proportional. Nevertheless, workload consolidation is difficult for OLDI workloads as the number of servers is set by both peak processing requirements **and** data storage requirements. For instance, a search cluster is sized to hold the entire search index in memory, and individual nodes cannot be powered off without losing part of the search index, which will impact search quality. Even if spare memory storage is available, moving tens of gigabytes of state in and out of servers is expensive and time consuming, making it difficult to react to fast or small changes in load. Other techniques focus on individual servers and attempt to maximize idle periods so that deep sleep power modes can be used. For instance, PowerNap would need to batch tasks on each server in order to create sufficiently long idle periods [109, 110]. Full system idle power modes, such as ACPI S3, have transition times on the order of seconds [110]. Since OLDI workloads have latency requirements in the order of milliseconds or microseconds, use of idle power modes produces frequent SLO violations [110]. Moreover,

OLDI workloads usually have a large fan-out (see Figure 4.1) when processing user queries. A single user query to the front-end will lead to forwarding of the query to all leaf nodes. As a result, even a small request rate can create a non-trivial amount of work on each server. For instance, consider a cluster sized to handle a peak load of 10,000 queries per second (QPS) using 1000 servers. Even at 10% load, each of the 1000 nodes are seeing on average one query per millisecond. There is simply not enough idleness to invoke some of the more effective low power modes.

4.3 Energy Proportionality Analysis for OLDI

4.3.1 Methodology

To understand the challenges of improving energy efficiency for OLDI workloads during low utilization periods, we collected power and latency measurements from a cluster with Sandy Bridge CPUs running production workloads. The power measured is full system power of the cluster and is equivalent to the power draw at the wall socket. For *search*, latency was measured at the root of the fan-out tree as opposed to the latency at each individual leaf node. By measuring as close to the end-user as possible, we have a more accurate assessment of the latency of the entire cluster. For *search*, we use the 30 second moving average latency (μ/30s) as one of the latency SLO metrics. Since we measure latency at the root where the effects of slow leafs are already seen, using mean latency at the root is an acceptable metric. We also collected 95%-ile and 99.9%-ile tail latencies at the root for *search* as a sensitivity analysis for further insights. For *memkeyval*, we measure mean latency, as well as 95%-ile and 99%-ile tail latencies. This is because *memkeyval* is typically used in such a way that the higher-level service waits for several parallel *memkeyval* requests to several servers to complete before being able to return a result. Thus, the overall latency of the entire *memkeyval* service is dependent on the slowest server, which is estimated by the tail latency of an individual server.

4.3.2 Analysis of Energy Inefficiencies

Figures 4.3 and Figure 4.4 show the total cluster power and the CPU-only power respectively at varying loads for *search* and *memkeyval*. As expected, the total cluster power consumed is far higher than the power consumed by an ideal, energy proportional cluster. We also plot the power draw of a cluster that exhibits energy proportional behavior on its active power (*Dynamic EP*). Eliminating idle draw due to fans, power supplies, and leakage power is quite difficult in the absence of sufficiently long idle periods. However, we expect that the cluster should be fairly close to energy proportional once idle power is removed. Figure 4.3 shows this is not the case in practice. The total cluster power consumed is still much higher than the *Dynamic EP power* across all utilization points for both workloads. While idle power is a major contributor to the energy proportionality problem, it alone does not account for the large gap between the power behavior of current clusters and the behavior of energy proportional clusters. To improve energy proportionality, we focus

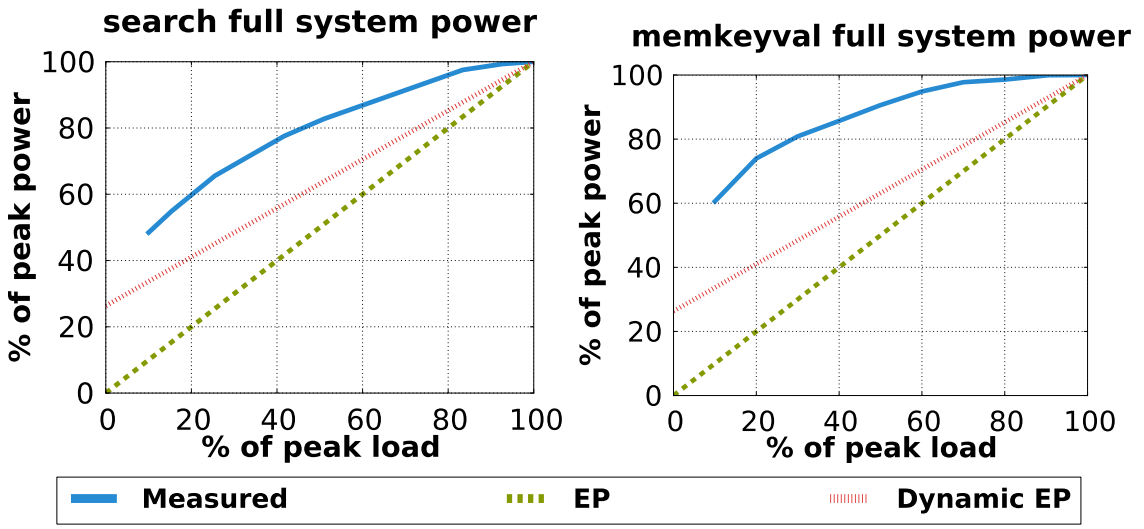

Figure 4.3: Total cluster power for *search* and *memkeyval* at various loads, normalized to peak power at 100% load.

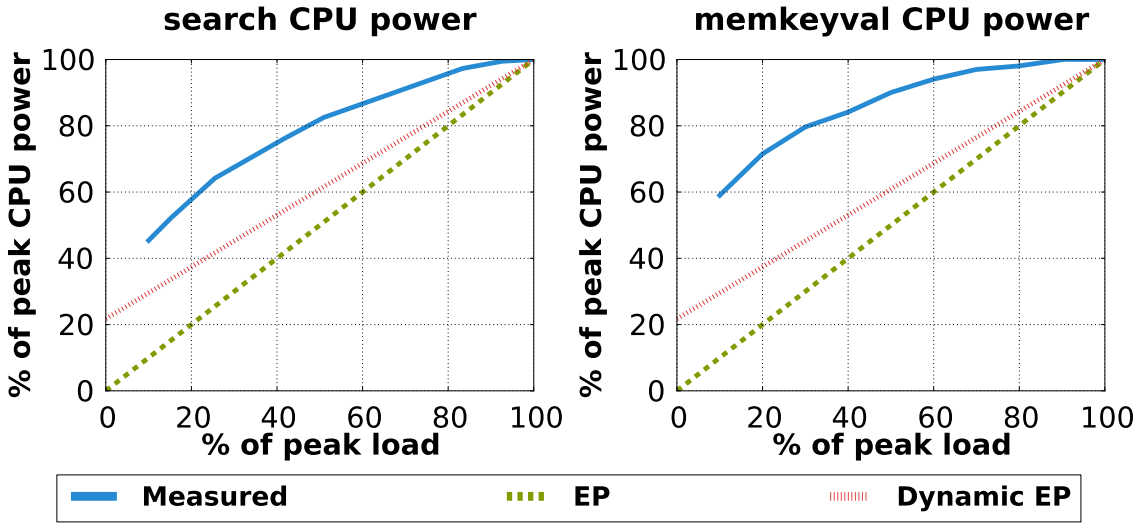

Figure 4.4: CPU power for *search* and *memkeyval* at various loads, normalized to peak CPU power at 100% load.

on addressing active power draw when the cluster is underutilized. We leave the improvement of idle power to future work.

Since the CPUs are the largest contributors to server power in modern servers (40% of total power at idle and 66% at peak [6]), we focus on CPU power as measured directly using on-board sensors in the servers (Figure 4.4). The power consumed by the CPU is not energy proportional and has the same shape as the

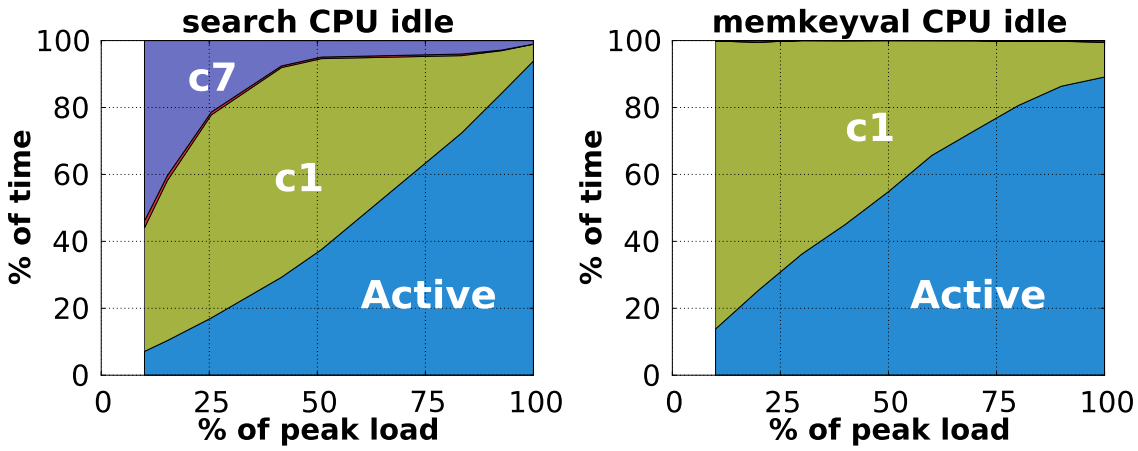

Figure 4.5: Characterization of CPU sleep states for *search* and *memkeyval* at various utilizations.

power curves of the entire cluster (Figure 4.3). This establishes that the CPU is a major contributor to the non-energy proportionality for these OLDI workloads, even if idle power is ignored. Therefore, we focus on understanding the cause of non-energy proportionality on the CPU and how to reduce the power consumed by the CPU in the context of making the entire WSC system more energy proportional.

The default CPU power management approach for the servers we study is to execute at the highest available CPU active power state (p-state), followed by idling in some sleep state. Namely, the power saving driver in use is *intel_idle* [56]. We characterized the fraction of time each core spends active and the fraction of time it spends in various sleep states (c1, c3, c7) in Figure 4.5. In c1, the core is clock gated. In c3, the L1 and L2 caches are flushed and clock gated. In c7, the core is power gated [134]. c1, c3, and c7 are ordered in increasing order of power savings [59]. c1, c3, and c7 have wake up latencies of almost zero, 10μs, and 100μs [59, 110]. We observe that both *search* and *memkeyval* do not spend very much time in the low power c7 sleep state. The vast majority of idle time is spent in the c1 sleep state, which does not save very much power but has almost zero exit latency. This is because in OLDI workloads, idle periods are particularly short even at low utilization, providing little opportunity to exploit deeper sleep states with higher exit latencies [110]. The idle behavior of OLDI workloads contrasts sharply with application behavior for mobile and client devices, where racing to idle is effective because of long idle times between short bursts of activity [127]. These observations motivate us to improve proportionality by improving active mode power consumption and by reducing the (ineffective) CPU idle time for OLDI workloads.

Figure 4.6 provides a clue towards achieving this goal. It shows how the various latencies of *search* and *memkeyval* are increasing with the amount of load on the cluster. It is important to remember that SLO targets for user or internal requests are set at a fixed value. These targets are independent of the immediate load on the cluster. Furthermore, SLO targets are typically set right at the knee of the latency/throughput curve. At loads below these inflection points, we observe that: a) there is still significant headroom between the measured latency and the SLO target; b) workload developers and system operators only care about avoiding

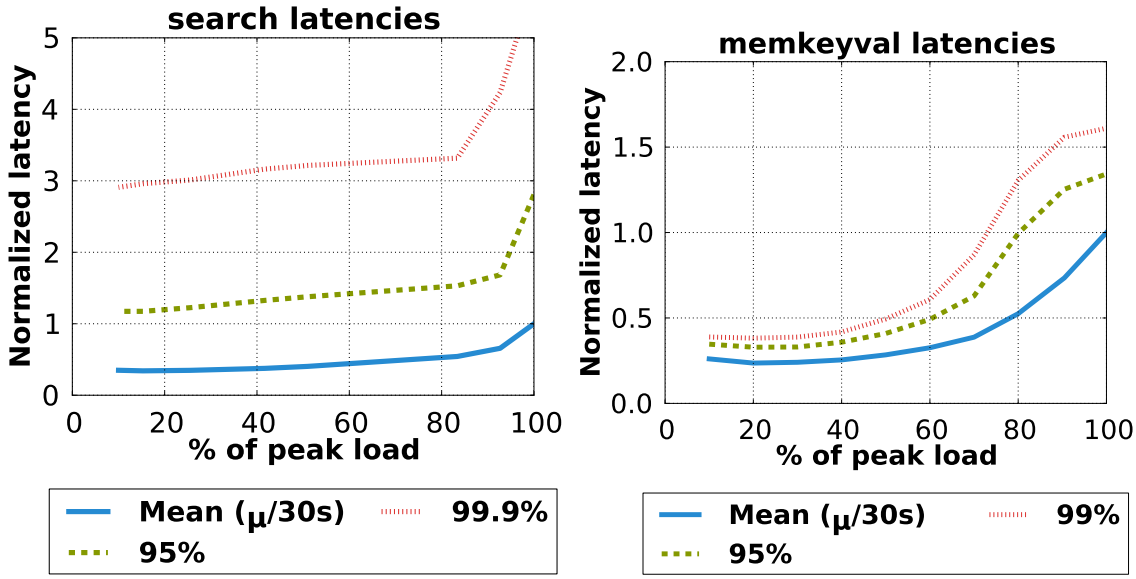

Figure 4.6: Characterization of latencies of *search* and *memkeyval* at various utilizations. The latency for each service is normalized to the average latency of the service at max load.

SLO latency violations. This stems from the fact that SLO targets represent performance that is acceptable to the operator. The gap between the measured latency and the SLO target suggests that there are energy inefficiencies caused by the cluster unnecessarily overachieving on its SLO latency targets. We exploit this observation to reduce power: we slow down the CPU as much as possible under the current load in order to save power without violating the overall workload SLO target.

4.3.3 Shortcomings of Current DVFS Schemes

It is important to understand why existing power management systems based on Dynamic Voltage Frequency Scaling (DVFS), such as Linux's built-in *cpufreq* driver, cannot be used exploit the latency slack at medium and low utilization in order to save power for OLDI workloads. These systems operate by keeping the CPU utilization within a fixed range by changing the CPU's operating frequency through p-states. For example, the *conservative* governor in Linux's *cpufreq* driver keeps the CPU utilization within 20% to 95%. When CPU utilization goes below/above the low/high threshold for a certain amount of time, the driver will transition to the next lower/higher p-state. However, this approach leads to frequent latency spikes for OLDI workloads. We ran *search* with the 24-hour trace with *cpufreq* enabled. Figure 4.7 shows significant latency spikes and SLO violations as *cpufreq* fails to transition to the proper p-state in several cases. This is the reason that the baseline power management policy in the search cluster does not use *cpufreq* and DVFS control.

We demonstrate that the inability of *cpufreq* to lower power without causing SLO violations is because CPU utilization is a poor choice of control input for latency critical workloads. Figure 4.8 shows that the

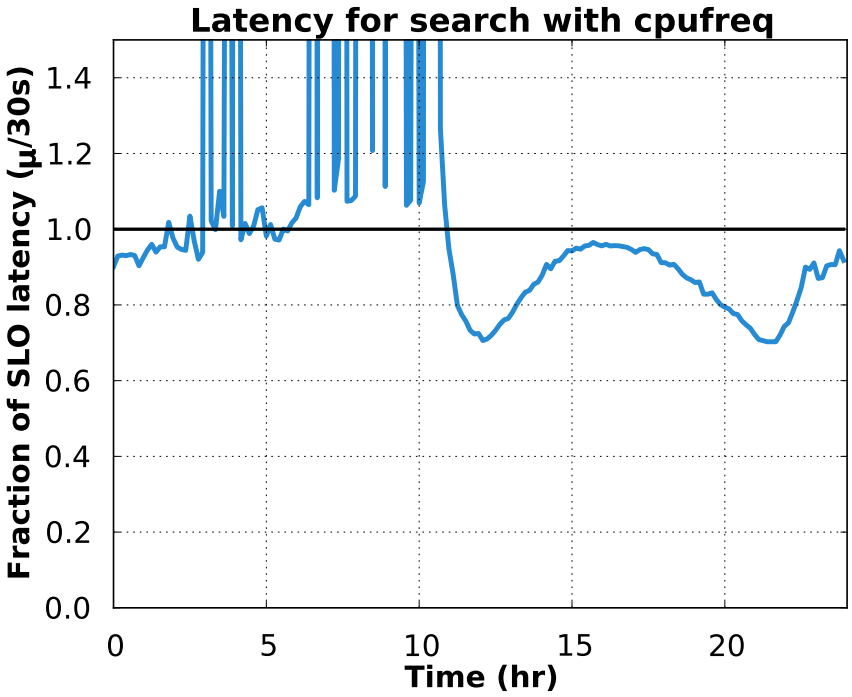

Figure 4.7: Latency of *search* with *cpufreq*, showing SLA violations. The solid horizontal line shows the target SLO latency.

latency of *search* is different at the same CPU utilization across different p-states. Therefore, CPU utilization alone is fundamentally insufficient to estimate latency. No amount of tuning CPU utilization thresholds would allow a DVFS controller to achieve optimal power savings without SLO violations. Depending on the workload complexity and its SLO targets, the thresholds will be different and would vary for each p-state. Thus, we argue that to save power without SLO violations, we need to directly use application-level latency as the input to power control. Note that the use of CPU utilization as the only control input is a shortcoming not only limited to *cpufreq*: several research proposals [36, 53, 124, 129], Intel's demand-based switching mechanism [54], and most OS implementations also use CPU utilization as the sole control input.

Another shortcoming of existing DVFS systems is that they use p-states to manage the trade-off between power and performance. However, p-state based power management is extremely coarse grained. For instance, dropping from p0 to p1 would disable TurboBoost, which can result in a significant frequency drop, up to 700MHz for an example Xeon E5-2667v2 CPU [55]. This means that using p-states alone misses on opportunities for power savings. For instance, in Figure 4.8, at utilization ranges between 65%-85%, the highest power p-state (p0) must be used, as the use of p1 would cause SLO violations. This motivates the need for fine-grain CPU power management in hardware.

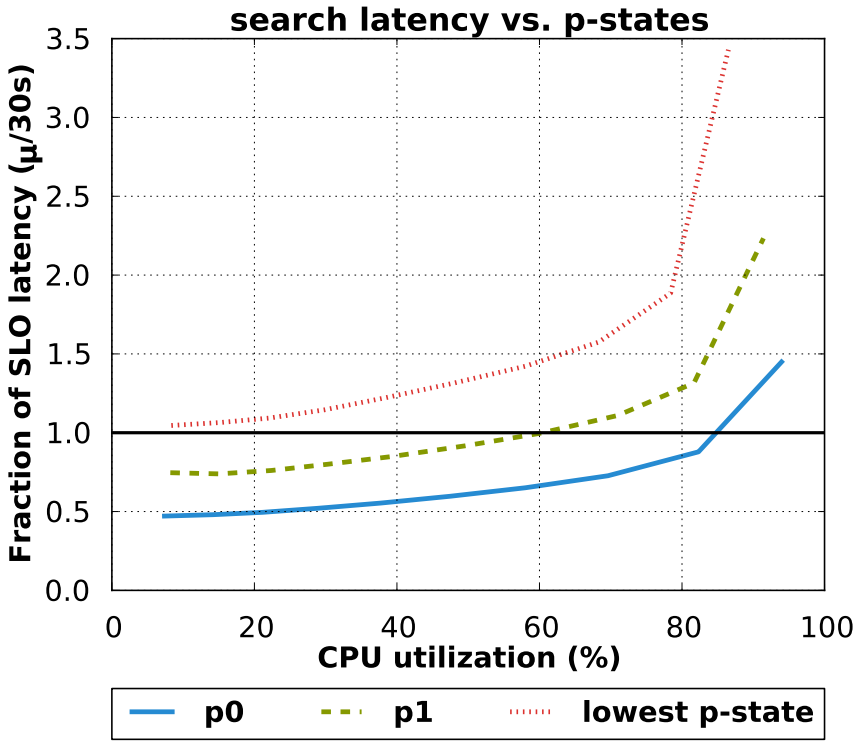

Figure 4.8: Characterization of *search*'s latency dependency on both p-state and CPU utilization. The solid horizontal line shows the target SLO latency.

4.4 Iso-latency Power Management

We propose a power management policy called *iso-latency* that addresses the shortcomings of existing DVFS systems. At a high level, it monitors the end-to-end request latencies of an OLDI service and adjusts the power settings of all servers so that SLO targets are barely met under any load. *Iso-latency* is inherently a dynamic policy as there is no one CPU p-state that will give optimal power savings while preventing SLO violations for all loads and all workloads. Intuitively, *iso-latency* is making a trade-off between latency and power. Figure 4.6 shows that, at low and medium utilization, there is latency headroom that can be exchanged for power savings without impacting SLO targets.

4.4.1 Iso-latency Potential

Before we discuss our implementation of *iso-latency*, we analyze the potential benefits for our OLDI workloads and servers.

To adjust the power settings of servers, we use a fine-grain power management feature introduced in recent Intel chips named *Running Average Power Limit (RAPL)* [60]. The RAPL interface allows the user to set an average power limit that the CPU should never exceed. On the servers we evaluate, we used the default time

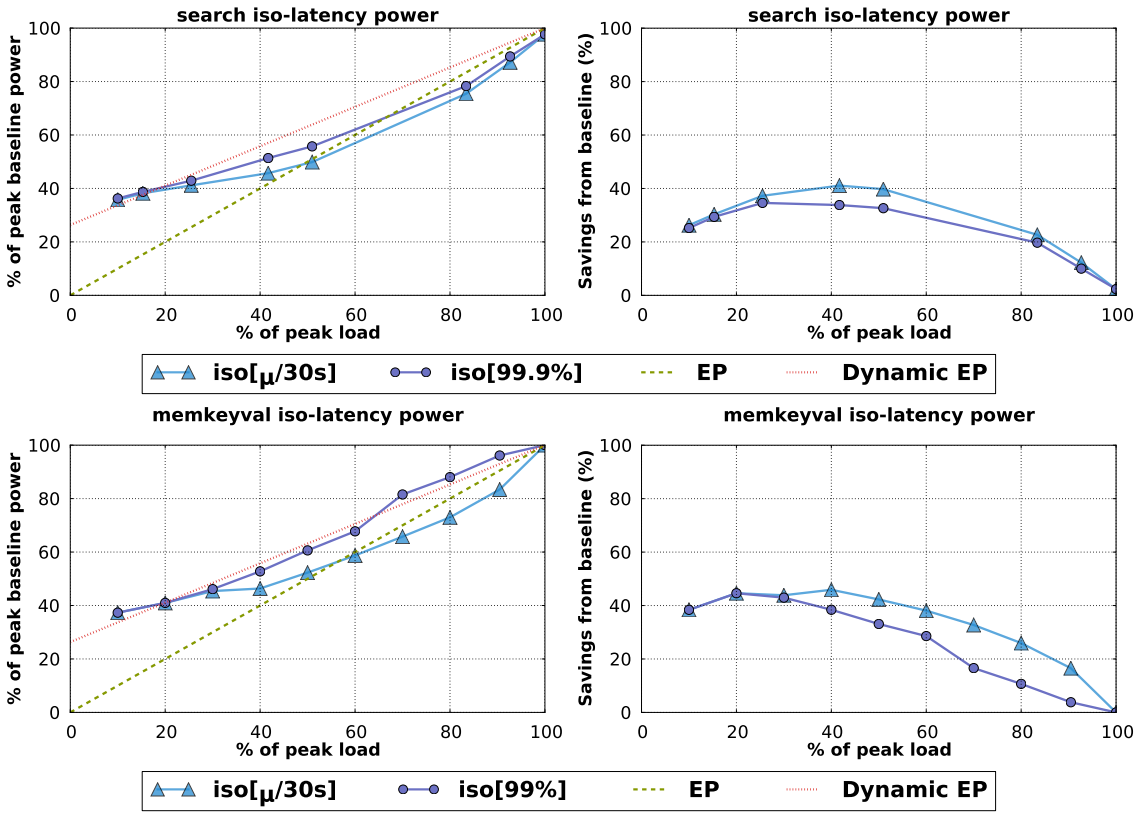

Figure 4.9: Characterization of power consumption for *search* and *memkeyval* for **iso-latency** with various latency SLO metrics. The SLO target is the latency at peak load (**relaxed**)

period to average over (45ms). RAPL can be programmed dynamically by writing a model specific register (MSR), and changes to the power limit take effect within less than 1 millisecond. The interface exports a fine grained power control knob, as the power limit can be set in increments of 0.125W. RAPL enforces this power limit mainly by scaling the voltage and frequency but can also modulate the CPU frequency to achieve average frequencies in between p-state frequencies. Compared to p-states, RAPL allows us to exploit a far wider spectrum of power-performance trade-offs, which is critical to determining the optimal operating point for *iso-latency*.

To understand the potential of *iso-latency* for *search* and *memkeyval*, we sweep the RAPL power limit at a given load to find the point of minimum cluster power that satisfies the SLO target. For sensitivity analysis, we use several SLO targets. The first SLO target is the latency of the workload at maximum utilization. This is a more relaxed constraint, as latency is high at peak throughput (past the knee of the latency-load curve). The second SLO target is more aggressive, as it is the latency measured at the knee of the curve. For *search*, the knee is at 80% of peak utilization, while for *memkeyval*, the knee is at 60% of peak utilization.

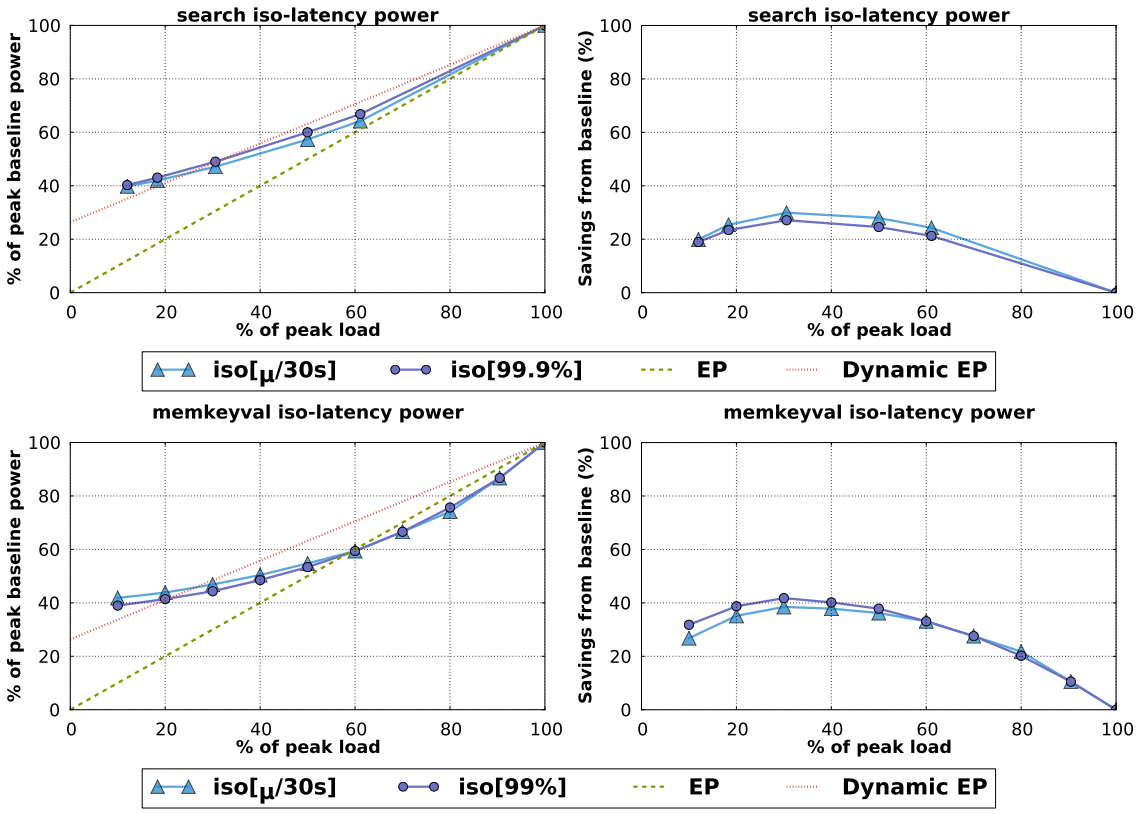

Figure 4.10: Characterization of power consumption for *search* and *memkeyval* for **iso-latency** with various latency SLO metrics. The SLO target used is more **aggressive** compared to Figure 4.9.

Figures 4.9 and 4.10 compare the baseline power consumption to that of a cluster managed by an ideal *iso-latency* controller that always finds the minimum power setting that avoids SLO violations. The right column of the figures shows the power savings using *iso-latency* over the baseline. For clarity, we omit the 95%-ile tail latency result for both *search* and *memkeyval*, as it is almost indistinguishable from the 99.9%-ile latency and 99%-ile latency curves for *search* and *memkeyval*, respectively.

The most salient observation is that *iso-latency* is able to save a significant amount of power compared to the baseline. In the utilization range of 20% to 80%, *iso-latency* can save 20% to 40% power and serve the same load **without** SLO violations. This result holds for both OLDI workloads, even for the aggressive SLO target (Figure 4.10), demonstrating that even a relatively small amount of latency headroom can be turned into large power savings. A physical analogy can be made to explain this result. The baseline can be compared to driving a car with sudden stops and starts. *iso-latency* would then be driving the car at a slower speed to avoid accelerating hard and braking hard. The second way of operating a car is much more fuel efficient than the first, which is akin to the results we have observed.

Another interesting observation from Figures 4.9 and 4.10 is that *iso-latency* can save significant amounts

of power even when the SLO target is enforced on tail latency instead of on mean latency. For both *search* and *memkeyval*, *iso-latency* does not need to spend too much additional power to meet tail latency constraints, such as low 99.9%-ile latency. This is because most of the latency is due to queueing delay, which is responsible for the sharp knee in the latency curves [26]. *Iso-latency* needs to run the cluster just fast enough to avoid excessive queueing delays. While it does take a little more power to avoid queueing delay effects in tail latency, it is not significantly more power than to avoid excessive increases in mean latency.

It is important to note that *iso-latency* compares well to idealized, energy proportional clusters. For the relaxed SLO target (Figure 4.9), *iso-latency* leads to lower power consumption than an energy proportional (EP) cluster at utilizations higher than 50%. The explanation is fairly simple: by using DFVS to reduce the CPU speed, *iso-latency* achieves better than linear reductions in power ($P = CV^2F$) by reducing F almost linearly and V by significant amounts as well. At utilizations lower than 50%, the ideal EP cluster does better than *iso-latency* because the total power consumed is dominated by idle power. When idle power is removed (Dynamic EP), *iso-latency* performs as well as, if not better, than Dynamic EP at all utilizations. When we consider aggressive SLO targets (Figure 4.10), *iso-latency* matches the ideal EP curve above 60% utilization and outperforms the Dynamic EP curve above 30% utilization. A tighter SLO latency causes the power curves to be shifted up; nevertheless, *iso-latency* still saves a significant amount of power over the baseline.

Iso-latency leads to higher power savings for *memkeyval* compared to *search*, even though the former has tighter absolute latency constraints (μsec compared to msec). Recall the characterization of idle times from Figure 4.5. We see that *memkeyval* cannot take advantage of deeper sleep states and can only use c1 because of the high request arrival rate, even at 10% load. On the other hand, because *search* has a lower request arrival rate, the baseline can take advantage of more power efficient sleep states. Thus, we expect *iso-latency* to benefit ultra-low-latency, high throughput workloads more, because it can convert the "race to (inefficient) idle" scenario to a more energy efficient "operate at a moderate but constant rate".

4.4.2 Using Other Power Management Schemes

As mentioned earlier, we can use the *iso-latency* policy with other power management mechanisms such as p-states. While we believe that RAPL is a better management mechanism because it allows for fine-grain control, it is not currently available on all CPU chips. Another power management mechanism is to consolidate the workload onto a sufficient subset of the cores in each CPU during times of low utilization. The remaining cores can be powered off (i.e., put into c7 sleep state) so that power is saved without experiencing SLO violations. We characterize *iso-latency* with CPU consolidation in Figure 4.11. Instead of sweeping RAPL settings to find the most appropriate for each utilization level, we now sweep the number of active cores per server. We leave the CPU operating at its highest p-state in order to maximize the number of cores that can be turned off. The results in Figure 4.11 are for *search* using the relaxed SLO target on the mean latency. These are the easiest constraints one can put on *iso-latency* to obtain maximum power savings.

Figure 4.11 shows that core consolidation is not as effective as RAPL when used as a power management

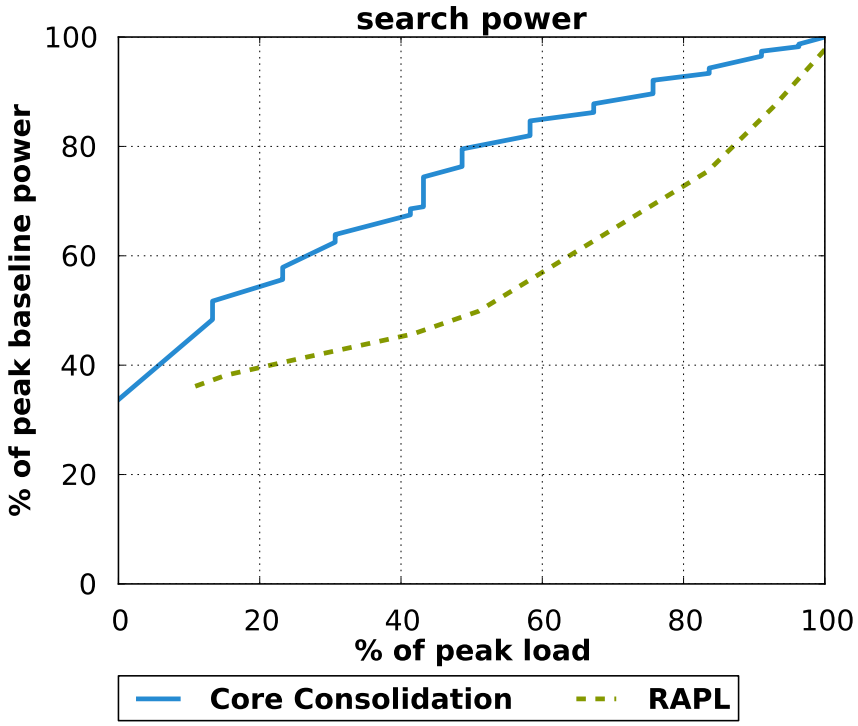

Figure 4.11: Comparison of **iso-latency** with core consolidation to RAPL. Measured total cluster power consumed by *search* at various utilizations, normalized to peak power at 100% load.

scheme for *iso-latency*. The static power savings achieved by shutting down cores are eclipsed by the far larger dynamic power required to operate the remaining cores at a high frequency. This is the basic phenomenon driving the multi-core evolution: assuming sufficient parallelism, many slow cores is more energy efficient than fewer faster cores. Nevertheless, it is still interesting to explore how core consolidation can be combined with RAPL (DVFS control) to create a better power management mechanism. Depending on the exact trade-offs between static and dynamic power at low frequencies, it may be better to have a few moderately fast cores as opposed to many slow cores. This is an interesting trade-off to examine in future work.

4.5 A Dynamic Controller for Iso-latency

Having established the potential of *iso-latency* as a power management policy, we now discuss the implementation of a cluster-wide, *iso-latency* controller for OLDI workloads.

4.5.1 PEGASUS Description

PEGASUS (**P**ower and **E**nergy **G**ains **A**utomatically **S**aved from **U**nderutilized **S**ystems) is a dynamic, feedback-based controller that enforces the *iso-latency* policy. At a high level, PEGASUS is a feedback-based controller that uses both the measured latency from the OLDI workload and the SLO target to adjust the RAPL settings in a fine-grain manner across all servers. During periods with significant latency headroom, PEGASUS will automatically lower the power limit until the latency headroom has been reduced. Conversely, when measured latency is getting close to the SLO target, PEGASUS will raise the power limit until there is sufficient latency headroom. PEGASUS always keeps a small latency headroom in order to ensure stability and robust handling of load increases. This latency headroom is configurable and determined based on the gradient of load spikes. Our current implementation of PEGASUS assumes a uniform cluster and thus applies the same RAPL setting across all servers. We discuss the implications of this assumption in Section 4.5.2.

Figure 4.12 shows a diagram of PEGASUS. The *Application Performance Monitor* monitors workload latency and reports the amount of headroom to the *PEGASUS controller*. This component can piggyback on performance monitoring infrastructure already in OLDI workloads. The *PEGASUS controller* in turn is responsible for determining the proper power adjustment based on the latency headroom, which it then periodically communicates to each of the *local agents* running on each server. The power adjustment is informed by the power savings policy, which is tailored to the OLDI workload. The frequency at which the *PEGASUS controller* sends updated power limits to the *local agent* is determined by how long it takes before the effects of the new power limit are seen in the application latency. This delay is application dependent, due to many workload specific factors such as the inertia of queries already in flight in the cluster, the delay in the latency measurement system, etc. The *PEGASUS controller* will send updates at a fixed frequency to the *local agents*, even if the power limit is staying constant. Finally, the *local agents* set the power limit from the *PEGASUS controller* using the RAPL interface. In case of a communication breakdown between the *PEGASUS controller* and the *local agents*, the *local agents* will automatically default to maximum power. Hence, PEGASUS failures cannot jeopardize the SLO for the workload.

The *PEGASUS controller* is very simple, around 200 lines of code, and has modest resource requirements. In its current form, it is based on a multi-step bang-bang controller that outputs a $\Delta(PowerLimit\%)$ depending on the latency headroom. The thresholds and the control outputs are workload dependent and are determined empirically. We describe control parameters for *search* in Table 4.1 For our experiments, we ran the *PEGASUS controller* on a single core of a single server. In our experiments, running on one core is more than enough to control the thousands of servers in the cluster. We profiled the performance of the *PEGASUS controller*, and determined that most of the time ($> 90\%$) is spent on transmitting the network packets to the *local agents*. When scaled to thousands of servers, the *PEGASUS controller* takes approximately 500 milliseconds to send out the command packet to all of the *local agents*. This delay can be shortened by parallelizing the networking portion of the *PEGASUS controller* to use multiple cores. However, for our experiments, the 500 millisecond delay does not appear to negatively impact the control scheme nor the

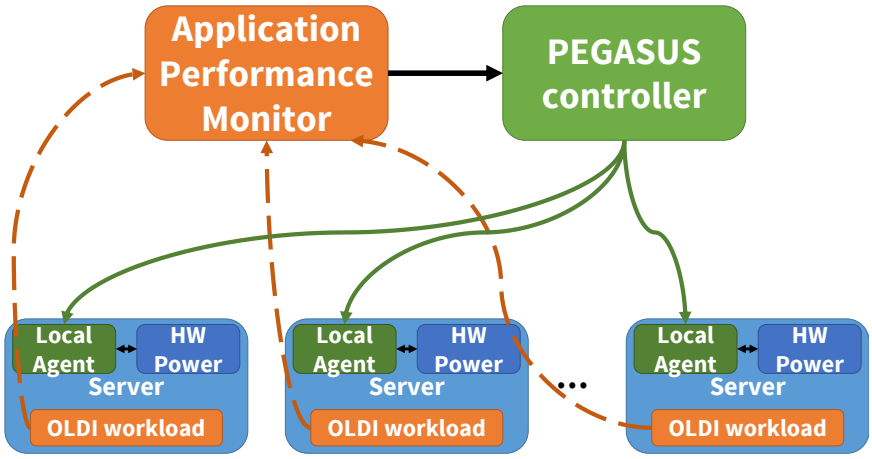

Figure 4.12: Block diagram showing high level operation and communication paths for PEGASUS.

performance of the OLDI workload.

We designed PEGASUS to be a general controller that works with any OLDI workload. PEGASUS is separated into two distinct components: policy (control parameters) and enforcement (actuation). The policy component is responsible for determining how much to adjust the CPU power limit. The policy portion is workload specific, and is dependent on the characteristics of the workload, such as the latency SLO metric (mean or tail latency) as well as the sensitivity of the workload to CPU power. For instance, *search* with its SLO target measured as the mean latency over 30 seconds will need to make smaller power adjustments compared to the same workload with its SLO target measured as the mean latency over 60 seconds. This is because PEGASUS needs to be more conservative when managing workloads with tighter SLO constraints, as there is less room for error. The enforcement portion is workload agnostic. It applies the CPU power limit determined by the policy of PEGASUS uniformly across all nodes in the cluster. Once the local agent receives a request from the central controller, it only takes milliseconds before the new power limit is enforced by RAPL.

4.5.2 PEGASUS Evaluation

We evaluate PEGASUS on the more challenging of the two OLDI workloads, *search*. We chose *search* because it is a complete, large-scale, OLDI workload with high fan-out across multiple tiers. In addition, because *search* is a complete service, measuring the overall latency of a user query is straightforward, as it is the latency at the root of the distribution tree. Moreover, the power savings potential for *search* is lower than that for *memkeyval* (see Figure 4.10). Thus, evaluating PEGASUS on *search* paints a more conservative and realistic picture of its capabilities.

The evaluation setup closely approximates production clusters and their load for *search*. We use the same kind of servers and the same number of servers used for production websearch. We then populate

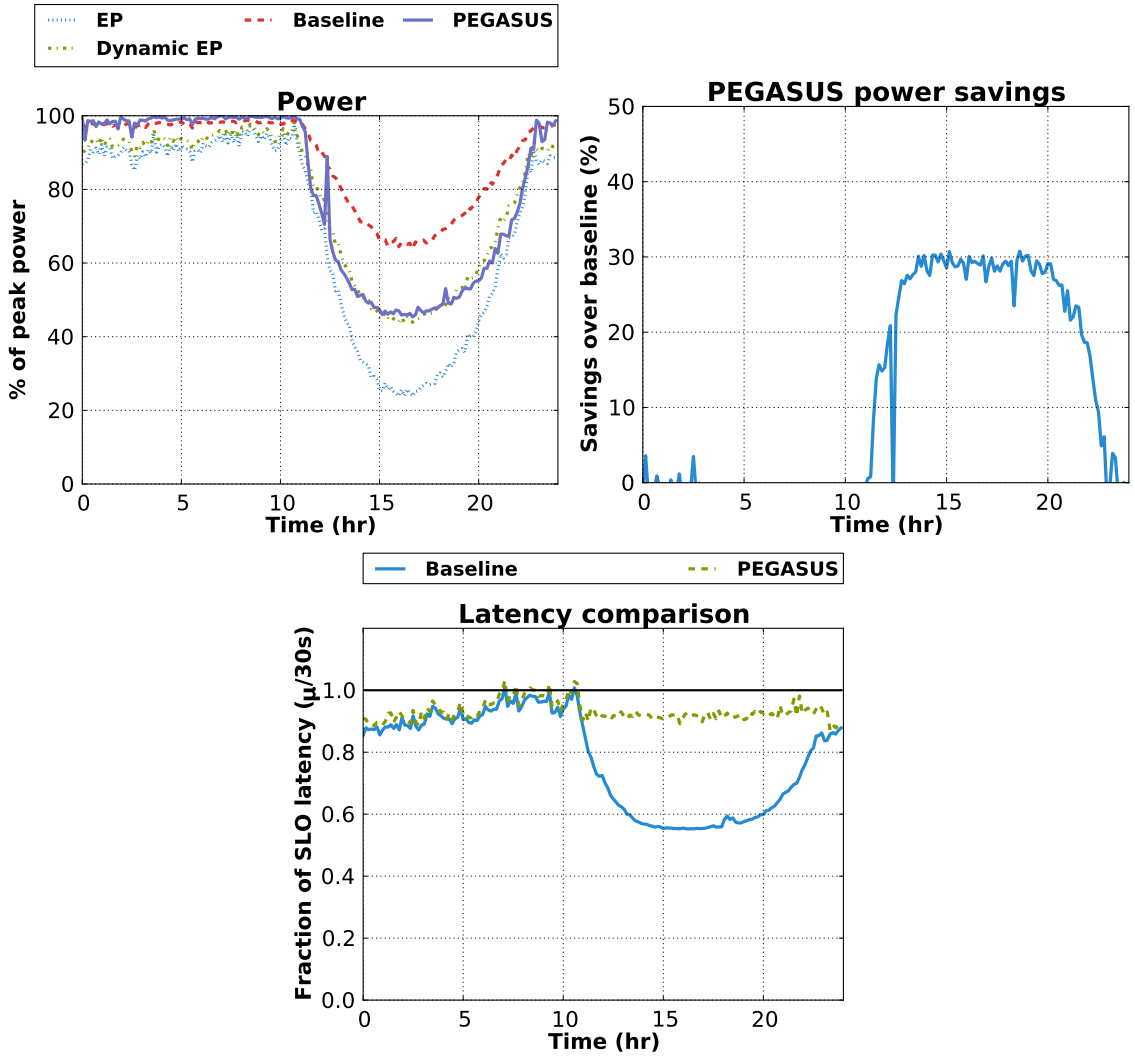

Figure 4.13: Results of running PEGASUS for *search* on the small cluster.

these servers with portions of the Google search index. We generate search queries using an anonymized search query log containing searches from actual users. To evaluate a realistic mix of high and low utilization periods, we use a 24-hour load trace shown in Figure 4.2. Since we measure latency as close as possible to the user (root of the tree), we use the mean latency over a rolling 30-second window as the latency SLO metric. The SLO target is defined as the latency of *search* when operating at 90% of the maximum possible load supported by the cluster. To provide the necessary headroom for stability and load changes, we set the target latency for PEGASUS at 95% of the actual SLO target. For *search*, we only manage the leaf nodes, as they are by far the largest contributor to power consumption.

We describe the PEGASUS policy we used for *search*. It is a *very conservative* policy that aims to slowly

Let $X = Measured\ SLO\ Latency, Y = Measured\ Instantaneous\ Latency, T = SLO\ target$

Input	Action
$X > T$	Set max power, wait 5 minutes
$Y > 1.35T$	Set max power
$Y > T$	Increase power by 7%
$0.85T \leq Y \leq T$	Keep current power
$Y < 0.85T$	Lower power by 1%
$Y < 0.60T$	Lower power by 3%

Table 4.1: PEGASUS policy for *search*.

reduce the power limit without causing any SLO violations along the way. The policy uses both the SLO latency (30 second moving average) and the instantaneous latency as inputs. The actions the policy takes based on the latency headroom is summarized in Table 4.1. The table lists rules in decreasing priority, i.e. only the first matching rule is applied. The rationale for using both SLO latency and instantaneous latency is that the instantaneous latency is a good early warning signal that lets PEGASUS know if an SLO violation might occur. This gives PEGASUS the opportunity to gracefully increase the power limit to stave off SLO violations before they happen. In addition, using the instantaneous latency allows PEGASUS to update the power limit more frequently, as opposed to waiting for the 30 second moving average to change. In our experiments, using the instantaneous latency allowed PEGASUS to update the power limit approximately once every 5 seconds. However, the measured SLO latency is still used as an emergency stop. If PEGASUS causes the SLO to be violated, then it should back off and not interfere with the OLDI workload. The reasoning behind this is that SLO violations are typically caused by excessive load and, in these situations, PEGASUS should not attempt to save power. When adjusting to save power, our policy for *search* takes very tiny steps to avoid riding the steep slope of the latency curve near the knee. Large perturbations near the knee can cause an order of magnitude increase in latency. Therefore, PEGASUS adopts a very cautious wait-and-see control scheme when the latency headroom is small. The policy also includes a built-in margin for the latency headroom where it will keep the current power setting. This margin is to account for noise in the latency measurement caused by variations in load as well as the differences between each search query.

As before, the baseline point for comparison uses the default power manager that races to idle, *cpuidle*. We measure full system power for the entire cluster as well as query latency throughout the entire duration of the run.

Small Cluster Results:

We first evaluate PEGASUS on an experimentation cluster that contains tens of servers. We scale the portion of the *search* index used to the memory capacity of the cluster. Because we are using a smaller dataset (index) and a smaller fan-out, the SLO target used in this experiment is a fraction of the SLO target of the production cluster.

Figure 4.13 shows the results of running the 24-hour trace described previously with and without PEGASUS. First, we note from the latency comparison graph that PEGASUS is able to meet the SLO target just as well as the baseline. In addition, the query latency with PEGASUS is flat, showing that PEGASUS is operating the cluster no faster than it deems necessary. Note that both the baseline and PEGASUS occasionally has small SLO violations (latency above 1.0). However, PEGASUS introduces no new SLO violations: it fails to meet the SLO in exactly the same cases as the baseline. These SLO violations are unavoidable as they are caused by load spikes exceeding the provisioned capacity of the cluster. Indeed, PEGASUS was not even attempting to save power at those points. Looking at the power graph for the first half of the experiment where SLO violations occur, the baseline and PEGASUS curves are identical. PEGASUS recognized that there was not sufficient latency headroom to attempt power reduction measures.

The power savings graph in Figure 4.13 shows that PEGASUS achieves most of the theoretical potential of *iso-latency*. During the low utilization portion of the diurnal load pattern, PEGASUS saves 30% power compared to the baseline. This result establishes that the potential of *iso-latency* can be achieved with a relatively simple controller. Moreover, the power consumption graph shows that PEGASUS turns the cluster into an energy proportional one for *search*, if idle power is excluded. PEGASUS successfully trades off latency headroom for power savings. Over the entire 24 hour run, PEGASUS was able to save 11% total energy compared to the baseline. The overall energy savings are capped by the portion of time *search* operates close to peak capacity in the trace (roughly half of the time). Nevertheless, the power and energy savings from PEGASUS are essentially free, as these savings do not result in additional SLO violations.

Production Cluster Results:

We also evaluated PEGASUS on a full scale, production cluster for *search* at Google, which includes thousands of servers. The salient differences between the full production cluster and the small cluster are that many more servers are available and that the entire search index is used. We also use the production level SLO latency target. For the production cluster experiments, we re-used the 24-hour trace discussed above in order to obtain an apples-to-apples comparison between the baseline and PEGASUS (two runs). We only use the 12 hours of the trace that contain the load trough and run it both with PEGASUS and the baseline approach because we are confident from the small cluster results that PEGASUS can successfully detect periods of peak utilization and operate the cluster at peak performance when needed. The 12 hours containing the trough characterize how effectively PEGASUS can turn the theoretical power savings of *iso-latency* into practical ones.

Figure 4.14 presents the results on the production cluster. The latency graph shows that PEGASUS did not cause any additional SLO violations compared to the baseline. This demonstrates that the enforcement portion of PEGASUS can scale out to thousands of nodes without issues. This result should not be surprising, because *search* must manage thousands of nodes as well. Distributing PEGASUS messages to thousands of servers is not that different from distributing queries to thousands of leafs. It can be done quickly in a coordinated manner. Compared with the traffic that *search* generates itself, PEGASUS messages to servers

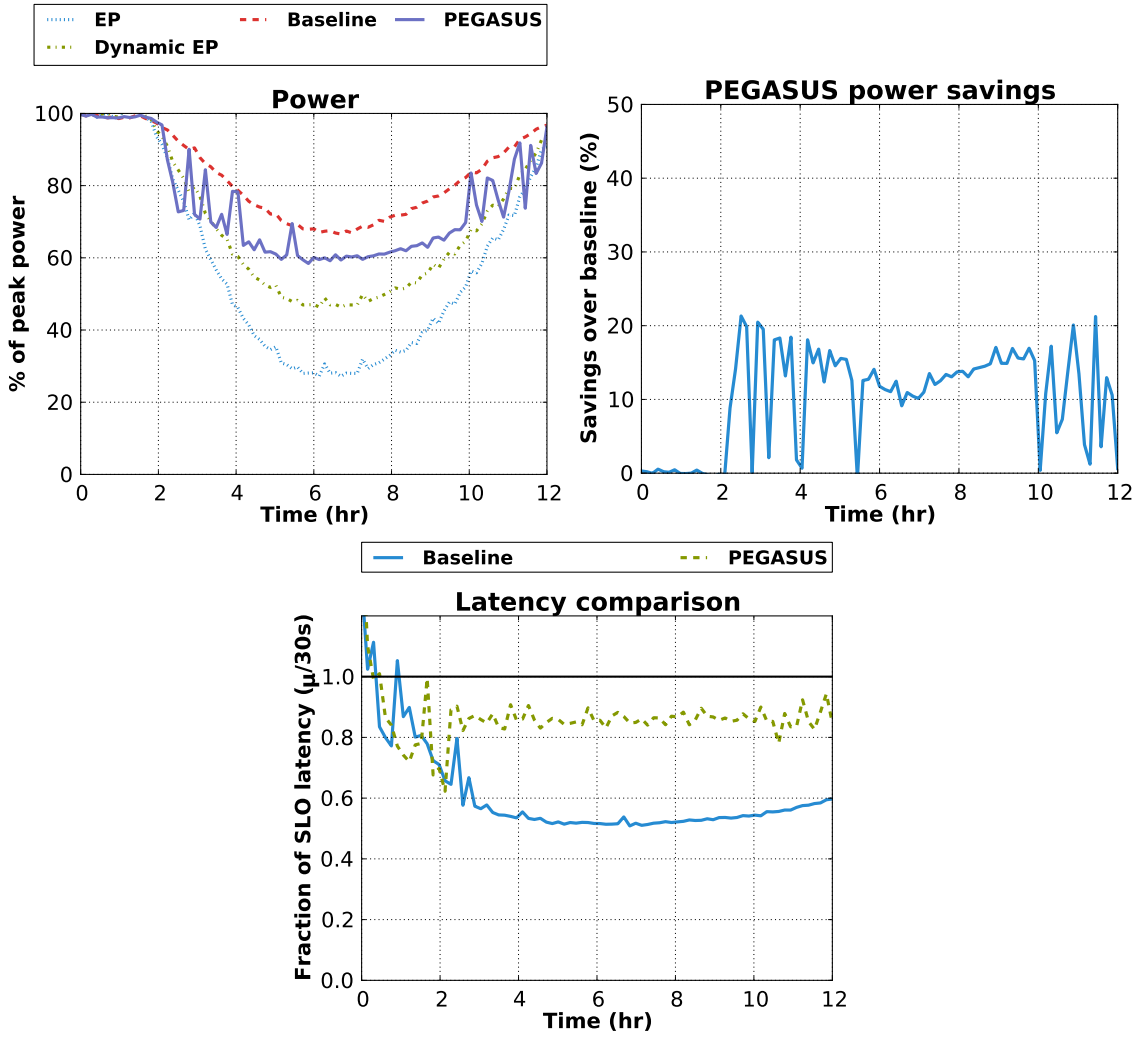

Figure 4.14: Results of running PEGASUS for *search* on the full production cluster.

are rare and are a tiny fraction of overall traffic.

Nevertheless, we do observe several issues that only emerge at scale. The delay between iterations for PEGASUS needed to be increased (from 3 to 4 seconds) due to the increased inertia of queries within the cluster. Namely, when the power limit changed, the observed query latency evolved more slowly compared to that on the small cluster. Another issue is that PEGASUS is not able to save as much power on the full cluster as compared to the small cluster. In Figure 4.14, we observe power savings between 10% and 20% during the period of low utilization, compared to 30% in the small cluster. The reason is that PEGASUS applies uniform RAPL settings across all the servers with the assumption that all servers have the same CPU utilization. However, when scaling to thousands of nodes, this is no longer the case. We examined the distribution of CPU utilizations across the leaf servers and observed a wide variance across the nodes. For

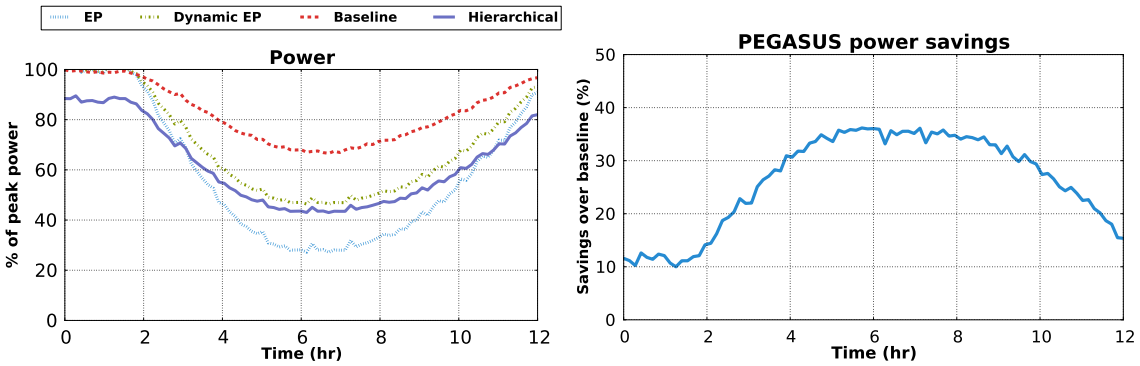

Figure 4.15: Estimation of power when using distributed PEGASUS.

instance, when running at peak utilization, we observed that 50% of the nodes were operating at below 85% peak CPU utilization. At the same time, a tiny fraction (0.2%) of nodes were operating at 100% peak CPU utilization.

The existence of these hot nodes is due to the amount of work per query varying depending on the hotness of the index shard for the leaf node. Because *search* must wait for all leaf nodes to finish processing a single query before it can return results to the user, the entire cluster is bottlenecked by these hot nodes. The use of a single power limit forces all servers to run as fast as the small fraction of hot leaf nodes, significantly reducing the realized power savings. This is a challenge at large-scale that is not obvious from the small cluster results and demonstrates the difficulties in adapting a control scheme that works well for smaller clusters to a cluster with thousands of nodes.

The solution to the hot leaf problem is fairly straightforward: implement a distributed controller on each server that keeps the leaf latency at a certain latency goal. The latency goal would be communicated by the centralized controller that can monitor latency and SLO challenges at the root of the search tree. Using such a distributed approach, only the hot leafs would be run faster to allow the overall SLO target to be met, while the vast majority of leafs would be run at a much lower power. Compared to the simple, centralized version of PEGASUS, the distributed version would be more complicated to implement. However, distributed PEGASUS would be far more efficient at extracting power savings. It would also respond to latency transients faster. For instance, the centralized PEGASUS can only detect an impending latency problem when all of the queues in the search tree start to fill up, while distributed PEGASUS would be able to detect and act on individual queues filling up. Moreover, the distributed controller would be able to deal with heterogeneous server configurations in the cluster.

Unfortunately, due to scheduling constraints for the production cluster, we were unable to evaluate distributed PEGASUS. However, we estimated the power savings that can be achieved with this distributed controller. We measured the distribution of CPU utilization on the search cluster and combined it with the diurnal load curve to estimate how much power the distributed controller would be able to save. We show the results of our estimation in Figure 4.15. The distributed controller is estimated to perform much better than

the uniform PEGASUS controller, saving up to 35% power over the baseline. This is comparable with the results from the small cluster, which shows that an idealized version of distributed PEGASUS can recover all of the power savings that were lost to using a uniform power limit. We also see that distributed PEGASUS has the opportunity to save power during periods of peak utilization, as it can save power on non-hot leaf nodes.

4.6 Related Work

There has been substantial work related to saving power for datacenter workloads. Ranganathan et al. propose a power budgeting approach that budgets for an "ensemble" of servers to take advantage of the rarity of concurrent load spikes in order to increase energy efficiency [131]. Raghavendra et al. propose a coordinated power management architecture for datacenters that integrates several otherwise disparate controllers together without the different controllers interfering internally with each other [128]. PowerNap tackles the energy proportionality problem by having an enhanced "nap" state that is very low power and has low wakeup latencies [109]. Similarly, Blink advocates the use of server low power states that essentially turn off servers [140]. However, OLDI workloads are not amenable to having individual nodes turned off. Meisner et al. showed that coordinated full-system low power modes are needed to achieve energy proportionality for OLDI workloads [110], which is the approach we take. Managing MapReduce clusters for energy efficiency has also been widely explored [18, 82, 85], but these consolidation-based techniques are not applicable for OLDI workloads with tight latency constraints and large dataset footprints.

There are many studies on optimizing energy efficiency of CPUs through the use of DVFS. However, many of those approaches are not applicable to OLDI workloads. Many proposals are geared towards batch workloads without latency requirements. Namely, these DVFS systems improve the energy efficiency of throughput oriented jobs, but they do not make any guarantees on the absolute latency of the job nor do they use the observed latency to inform the DVFS decision [37, 62, 81, 84, 129, 142, 160]. This is not acceptable for OLDI workloads, where the SLO latency is critical. There are also DVFS schemes that aim to maximize energy efficiency of real-time systems where jobs have deadlines [4, 93, 122, 135, 141]. However, these systems have several limitations that make them impractical for OLDI workloads. The first is that both the number and length of jobs must be known ahead of time, which conflicts with the dynamic nature of OLDI workloads. The second is that these control schemes are designed for single node systems; this is not a good fit for OLDI workloads, which run on potentially thousands of servers.

Another way to improve energy efficiency is to use otherwise idle resources on OLDI servers to perform useful work. For example, if *search* operates at 50% utilization, we can fill up the remainder of the cluster with batch workloads that would otherwise be running on other servers. This approach improves energy efficiency by operating servers in their most power efficient mode and can save on capital expenses for batch servers. However, workload co-location has several challenges, including resource provisioning (e.g., removing memory from the search index so that batch workloads can use it) and interference management so

that SLO violations are avoided [21,28,68,105,126,136,163]. Investigation of the interactions of co-location with *iso-latency* will be thoroughly investigated in Chapter 5.

4.7 Conclusions

We presented PEGASUS, a feedback-based controller that implements *iso-latency* power management policy for large-scale, latency-critical workloads: it adjusts the power-performance settings of servers in a fine-grain manner so that the overall workload barely meets its latency constraints for user queries at any load. We demonstrated PEGASUS on a Google search cluster. We showed that it preserves SLO latency guarantees and can achieve significant power savings during periods of low or medium utilization (20% to 40% savings). We also established that overall workload latency is a better control signal for power management compared to CPU utilization. Overall, *iso-latency* provides a significant step forward towards the goal of energy proportionality for one of the challenging classes of large-scale, low-latency workloads.

Chapter 5

Heracles: Improving Resource Efficiency at Scale

Improving energy efficiency for periods of low utilization lowers the OpEX of operating a datacenter. However, the dominant portion of the TCO of datacenters lies in CapEX. The most straightforward way to improving CapEX efficiency is to have high utilization of servers. Unfortunately, user-facing, latency-sensitive services, such as websearch, underutilize their computing resources during daily periods of low traffic. Reusing those resources for other tasks is rarely done in production services since the contention for shared resources can cause latency spikes that violate the service-level objectives of latency-sensitive tasks. The resulting under-utilization hurts both the affordability and energy-efficiency of large-scale datacenters. With technology scaling slowing down, it becomes important to address this opportunity.

We present Heracles, a feedback-based controller that enables the safe colocation of best-effort tasks alongside a latency-critical service. Heracles dynamically manages multiple hardware and software isolation mechanisms, such as CPU, memory, and network isolation, to ensure that the latency-sensitive job meets latency targets while maximizing the resources given to best-effort tasks. We evaluate Heracles using production latency-critical and batch workloads from Google and demonstrate average server utilizations of 90% without latency violations across all the load and colocation scenarios that we evaluated.[1]

5.1 Introduction

Public and private cloud frameworks allow us to host an increasing number of workloads in large-scale datacenters with tens of thousands of servers. The business models for cloud services emphasize reduced infrastructure costs. Of the total cost of ownership (TCO) for modern energy-efficient datacenters, servers are the largest fraction (50-70%) [6]. Maximizing server utilization is therefore important for continued

[1] This chapter is based on work that will be published in [99].

scaling.

Until recently, scaling from Moore's law provided higher compute per dollar with every server generation, allowing datacenters to scale without raising the cost. However, with several imminent challenges in technology scaling [32, 48], alternate approaches are needed. Some efforts seek to reduce the server cost through balanced designs or cost-effective components [71, 92, 101]. An orthogonal approach is to improve the return on investment and utility of datacenters by raising server utilization. Low utilization negatively impacts both operational and capital components of cost efficiency. Energy proportionality can reduce operational expenses at low utilizations [5], which PEGASUS was able to achieve (Chapter 4). But, to amortize the much larger capital expenses, an increased emphasis on the *effective use of server resources* is warranted.

Several studies have established that the average server utilization in most datacenters is low, ranging between 10% and 50% [6, 16, 29, 108, 132, 153]. A primary reason for the low utilization is the popularity of latency-critical (LC) services such as social media, search engines, software-as-a-service, online maps, webmail, machine translation, online shopping and advertising. These user-facing services are typically scaled across thousands of servers and access distributed state stored in memory or Flash across these servers. While their load varies significantly due to diurnal patterns and unpredictable spikes in user accesses, it is difficult to consolidate load on a subset of highly utilized servers because the application state does not fit in a small number of servers and moving state is expensive. The cost of such underutilization can be significant. For instance, Google websearch servers often have an average idleness of 30% over a 24 hour period [98]. For a hypothetical cluster of 10,000 servers, this idleness translates to a wasted capacity of 3,000 servers.

A promising way to improve efficiency is to launch best-effort batch (BE) tasks on the same servers and exploit any resources underutilized by LC workloads [28, 105, 106]. Batch analytics frameworks can generate numerous BE tasks and derive significant value even if these tasks are occasionally deferred or restarted [12, 16, 22, 29]. The main challenge of this approach is interference between colocated workloads on shared resources such as caches, memory, I/O channels, and network links. LC tasks operate with strict service level objectives (SLOs) on tail latency, and even small amounts of interference can cause significant SLO violations [86, 105, 110]. Hence, some of the past work on workload colocation focused only on throughput workloads [21, 116]. More recent systems predict or detect when a LC task suffers significant interference from the colocated tasks, and *avoid or terminate* the colocation [29, 104, 105, 118, 154, 165]. These systems protect LC workloads, but reduce the opportunities for higher utilization through colocation.

Recently introduced hardware features for cache isolation and fine-grained power control allow us to improve colocation. This work aims to enable aggressive colocation of LC workloads and BE jobs by automatically coordinating multiple hardware and software isolation mechanisms in modern servers. We focus on two hardware mechanisms, shared cache partitioning and fine-grained power/frequency settings, and two software mechanisms, core/thread scheduling and network traffic control. Our goal is to eliminate SLO violations at all levels of load for the LC job while maximizing the throughput for BE tasks.

There are several challenges towards this goal. First, we must carefully share each individual resource; conservative allocation will minimize the throughput for BE tasks, while optimistic allocation will lead to

SLO violations for the LC tasks. Second, the performance of both types of tasks depends on multiple resources, which leads to a large allocation space that must be explored in real-time as load changes. Finally, there are non-obvious interactions between isolated and non-isolated resources in modern servers. For instance, increasing the cache allocation for a LC task to avoid evictions of hot data may create memory bandwidth interference due to the increased misses for BE tasks.

We present *Heracles*[2], a real-time, dynamic controller that manages four hardware and software isolation mechanisms in a coordinated fashion to maintain the SLO for a LC job. Compared to existing systems [29, 105, 164] that *prevent* colocation of interfering workloads, *Heracles enables* a LC task to be colocated with any BE job. It guarantees that the LC workload receives just enough of each shared resource to meet its SLO, thereby maximizing the utility from the BE task. Using online monitoring and some offline profiling information for LC jobs, *Heracles* identifies when shared resources become saturated and are likely to cause SLO violations and configures the appropriate isolation mechanism to proactively prevent that from happening.

The specific contributions of this chapter are the following. First, we characterize the impact of interference on shared resources for a set of production, latency-critical workloads at Google, including websearch, an online machine learning clustering algorithm, and an in-memory key-value store. We show that the impact of interference is non-uniform and workload dependent, thus precluding the possibility of static resource partitioning within a server. Next, we design *Heracles* and show that: a) coordinated management of multiple isolation mechanisms is key to achieving high utilization without SLO violations; b) carefully separating interference into independent subproblems is effective at reducing the complexity of the dynamic control problem; and c) a local, real-time controller that monitors latency in each server is sufficient. We evaluate *Heracles* on production Google servers by using it to colocate production LC and BE tasks . We show that *Heracles* achieves an effective machine utilization of 90% averaged across all colocation combinations and loads for the LC tasks while meeting the latency SLOs. *Heracles* also improves throughput/TCO by 15% to 300%, depending on the initial average utilization of the datacenter. Finally, we establish the need for hardware mechanisms to monitor and isolate DRAM bandwidth, which can improve *Heracles*' accuracy and eliminate the need for offline information.

To the best of our knowledge, this is the first study to make coordinated use of new and existing isolation mechanisms in a real-time controller to demonstrate significant improvements in efficiency for production systems running LC services.

5.2 Shared Resource Interference

When two or more workloads execute concurrently on a server, they compete for shared resources. This section reviews the major sources of interference, the available isolation mechanisms, and the motivation for dynamic management.

[2]The mythical hero that killed the multi-headed monster, Lernaean Hydra.

The primary shared resource in the server are the **cores** in the one or more CPU sockets. We cannot simply *statically* partition cores between the LC and BE tasks using mechanisms such as `cgroups cpuset` [112]. When user-facing services such as search face a load spike, they need all available cores to meet throughput demands without latency SLO violations. Similarly, we cannot simply assign high priority to LC tasks and rely on OS-level scheduling of cores between tasks. Common scheduling algorithms such as Linux's completely fair scheduler (CFS) have vulnerabilities that lead to frequent SLO violations when LC tasks are colocated with BE tasks [86]. Real-time scheduling algorithms (e.g., `SCHED_FIFO`) are not work-preserving and lead to lower utilization. The availability of HyperThreads in Intel cores leads to further complications, as a HyperThread executing a BE task can interfere with a LC HyperThread on instruction bandwidth, shared L1/L2 caches, and TLBs.

Numerous studies have shown that uncontrolled interference on the shared **last-level cache (LLC)** can be detrimental for colocated tasks [29, 43, 86, 104, 136]. To address this issue, Intel has recently introduced LLC cache partitioning in server chips. This functionality is called *Cache Allocation Technology (CAT)*, and it enables way-partitioning of a highly-associative LLC into several subsets of smaller associativity [60]. Cores assigned to one subset can only allocate cache lines in their subset on refills, but are allowed to hit in any part of the LLC. It is already well understood that, even when the colocation is between throughput tasks, it is best to dynamically manage cache partitioning using either hardware [21, 68, 126] or software [94, 116] techniques. In the presence of user-facing workloads, dynamic management is more critical as interference translates to large latency spikes [86]. It is also more challenging as the cache footprint of user-facing workloads changes with load [78].

Most important LC services operate on large datasets that do not fit in on-chip caches. Hence, they put pressure on DRAM bandwidth at high loads and are sensitive to **DRAM bandwidth** interference. Despite significant research on memory bandwidth isolation [68, 72, 114, 117], there are no hardware isolation mechanisms in commercially available chips. In multi-socket servers, one can isolate workloads across NUMA channels [10, 147], but this approach constrains DRAM capacity allocation and address interleaving. The lack of hardware support for memory bandwidth isolation complicates and constrains the efficiency of any system that dynamically manages workload colocation.

Datacenter workloads are scale-out applications that generate **network traffic**. Many datacenters use rich topologies with sufficient bisection bandwidth to avoid routing congestion in the fabric [2, 65]. There are also several networking protocols that prioritize short messages for LC tasks over large messages for BE tasks [3, 158]. Within a server, interference can occur both in the incoming and outgoing direction of the network link. If a BE task causes incast interference, we can throttle its core allocation until networking flow-control mechanisms trigger [123]. In the outgoing direction, we can use traffic control mechanisms in operating systems like Linux to provide bandwidth guarantees to LC tasks and to prioritize their messages ahead of those from BE tasks [15]. Traffic control must be managed dynamically as bandwidth requirements vary with load. Static priorities can cause underutilization and starvation [121]. Similar traffic control can be applied to solid-state storage devices [138].

Power is an additional source of interference between colocated tasks. All modern multi-core chips have some form of dynamic overclocking, such as Turbo Boost in Intel chips and Turbo Core in AMD chips. These techniques opportunistically raise the operating frequency of the processor chip higher than the nominal frequency in the presence of power headroom. Thus, the clock frequency for the cores used by a LC task depends not just on its own load, but also on the intensity of any BE task running on the same socket. In other words, the performance of LC tasks can suffer from unexpected drops in frequency due to colocated tasks. This interference can be mitigated with per-core dynamic voltage frequency scaling, as cores running BE tasks can have their frequency decreased to ensure that the LC jobs maintain a guaranteed frequency. A static policy would run all BE jobs at minimum frequency, thus ensuring that the LC tasks are not power-limited. However, this approach severely penalizes the vast majority of BE tasks. Most BE jobs do not have the profile of a power virus[3] and LC tasks only need the additional frequency boost during periods of high load. Thus, a dynamic solution that adjusts the allocation of power between cores is needed to ensure that LC cores run at a guaranteed minimum frequency while maximizing the frequency of cores for BE tasks.

A major challenge with colocation is **cross-resource interactions**. A BE task can cause interference in all the shared resources discussed. Similarly, many LC tasks are sensitive to interference on multiple resources. Therefore, it is not sufficient to manage one source of interference: all potential sources need to be monitored and carefully isolated if need be. In addition, interference sources interact with each other. For example, LLC contention causes both types of tasks to require more DRAM bandwidth, also creating a DRAM bandwidth bottleneck. Similarly, a task that notices network congestion may attempt to use compression, causing core and power contention. In theory, the number of possible interactions scales with the square of the number of interference sources, making this a very difficult problem.

5.3 Interference Characterization & Analysis

This section characterizes the impact of interference on shared resources for latency-critical services.

5.3.1 Latency-critical Workloads

We use three Google production latency-critical workloads.

websearch is the query serving portion of a production web search service. It is a scale-out workload that provides high throughput with a strict latency SLO by using a large fan-out to thousands of leaf nodes that process each query on their shard of the search index. The SLO for leaf nodes is in the tens of milliseconds for the 99%-ile latency. Load for *websearch* is generated using an anonymized trace of real user queries.

websearch has high memory footprint as it serves shards of the search index stored in DRAM. It also has moderate DRAM bandwidth requirements (40% of available bandwidth at 100% load), as most index accesses miss in the LLC. However, there is a small but significant working set of instructions and data in the hot path. Also, *websearch* is fairly compute intensive, as it needs to score and sort search hits. However, it

[3] A computation that maximizes activity and power consumption of a core.

does not consume a significant amount of network bandwidth. For this study, we reserve a small fraction of DRAM on search servers to enable colocation of BE workloads with *websearch*.

ml_cluster is a standalone service that performs real-time text clustering using machine-learning techniques. Several Google services use *ml_cluster* to assign a cluster to a snippet of text. *ml_cluster* performs this task by locating the closest clusters for the text in a model that was previously learned offline. This model is kept in main memory for performance reasons. The SLO for *ml_cluster* is a 95%-ile latency guarantee of tens of milliseconds. *ml_cluster* is exercised using an anonymized trace of requests captured from production services.

Compared to *websearch*, *ml_cluster* is more memory bandwidth intensive (with 60% DRAM bandwidth usage at peak) but slightly less compute intensive (lower CPU power usage overall). It has low network bandwidth requirements. An interesting property of *ml_cluster* is that each request has a very small cache footprint, but, in the presence of many outstanding requests, this translates into a large amount of cache pressure that spills over to DRAM. This is reflected in our analysis as a super-linear growth in DRAM bandwidth use for *ml_cluster* versus load.

memkeyval is an in-memory key-value store, similar to *memcached* [111]. *memkeyval* is used as a caching service in the backends of several Google web services. Other large-scale web services, such as Facebook and Twitter, use *memcached* extensively. *memkeyval* has significantly less processing per request compared to *websearch*, leading to extremely high throughput in the order of hundreds of thousands of requests per second at peak. Since each request is processed quickly, the SLO latency is very low, in the few hundreds of microseconds for the 99%-ile latency. Load generation for *memkeyval* uses an anonymized trace of requests captured from production services.

At peak load, *memkeyval* is network bandwidth limited. Despite the small amount of network protocol processing done per request, the high request rate makes *memkeyval* compute-bound. In contrast, DRAM bandwidth requirements are low (20% DRAM bandwidth utilization at max load), as requests simply retrieve values from DRAM and put the response on the wire. *memkeyval* has both a static working set in the LLC for instructions, as well as a per-request data working set.

5.3.2 Characterization Methodology

To understand their sensitivity to interference on shared resources, we ran each of the three LC workloads with a synthetic benchmark that stresses each resource in isolation. While these are single node experiments, there can still be significant network traffic as the load is generated remotely. We repeated the characterization at various load points for the LC jobs and recorded the impact of the colocation on tail latency. We used production Google servers with dual-socket Intel Xeons based on the Haswell architecture. Each CPU has a high core-count, with a nominal frequency of 2.3GHz and 2.5MB of LLC per core. The chips have hardware support for way-partitioning of the LLC.

We performed the following characterization experiments:

Cores: As we discussed in §5.2, we cannot share a logical core (a single HyperThread) between a LC and a

BE task because OS scheduling can introduce latency spikes in the order of tens of milliseconds [86]. Hence, we focus on the potential of using separate HyperThreads that run pinned on the same physical core. We characterize the impact of a colocated HyperThread that implements a tight spinloop on the LC task. This experiment captures a *lower bound* of HyperThread interference. A more compute or memory intensive microbenchmark would antagonize the LC HyperThread for more core resources (e.g., execution units) and space in the private caches (L1 and L2). Hence, if this experiment shows high impact on tail latency, we can conclude that core sharing through HyperThreads is not a practical option.

LLC: The interference impact of LLC antagonists is measured by pinning the LC workload to enough cores to satisfy its SLO at the specific load and pinning a cache antagonist that streams through a large data array on the remaining cores of the socket. We use several array sizes that take up a quarter, half, and almost all of the LLC and denote these configurations as LLC small, medium, and big respectively.

DRAM bandwidth: The impact of DRAM bandwidth interference is characterized in a similar fashion to LLC interference, using a significantly larger array for streaming. We use *numactl* to ensure that the DRAM antagonist and the LC task are placed on the same socket(s) and that all memory channels are stressed.

Network traffic: We use *iperf*, an open source TCP streaming benchmark [61], to saturate the network transmit (outgoing) bandwidth. All cores except for one are given to the LC workload. Since the LC workloads we consider serve request from multiple clients connecting to the service they provide, we generate interference in the form of many low-bandwidth "mice" flows. Network interference can also be generated using a few "elephant" flows. However, such flows can be effectively throttled by TCP congestion control [13], while the many "mice" flows of the LC workload will not be impacted.

Power: To characterize the latency impact of a power antagonist, the same division of cores is used as in the cases of generating LLC and DRAM interference. Instead of running a memory access antagonist, a CPU power virus is used. The power virus is designed such that it stresses all the components of the core, leading to high power draw and lower CPU core frequencies.

OS Isolation: For completeness, we evaluate the overall impact of running a BE task along with a LC workload using only the isolation mechanisms available in the OS. Namely, we execute the two workloads in separate Linux containers and set the BE workload to be low priority. The scheduling policy is enforced by CFS using the `shares` parameter, where the BE task receives very few `shares` compared to the LC workload. No other isolation mechanisms are used in this case. The BE task is the Google *brain* workload [83, 133], which we will describe further in §5.5.1.

5.3.3 Interference Analysis

Figure 5.1 presents the impact of the interference microbenchmarks on the tail latency of the three LC workloads. Each row in the table shows tail latency at a certain load for the LC workload when colocated with the corresponding microbenchmark. The interference impact is acceptable if and only if the tail latency is less than 100% of the target SLO. We color-code red/yellow all cases where SLO latency is violated.

websearch

	10%	20%	30%	40%	50%	60%	70%	80%	90%
LLC (small)	103%	96%	102%	96%	104%	100%	100%	103%	103%
LLC (med)	106%	99%	111%	103%	116%	108%	110%	125%	111%
LLC (big)	>300%	>300%	>300%	>300%	>300%	>300%	>300%	264%	123%
DRAM	>300%	>300%	>300%	>300%	>300%	>300%	>300%	270%	122%
HyperThread	109%	106%	113%	114%	105%	117%	119%	136%	>300%
CPU power	124%	107%	115%	108%	114%	105%	101%	100%	99%
Network	35%	36%	36%	37%	38%	41%	48%	55%	64%
brain	165%	173%	168%	230%	>300%	>300%	>300%	>300%	>300%

ml_cluster

	10%	20%	30%	40%	50%	60%	70%	80%	90%
LLC (small)	88%	84%	110%	93%	216%	106%	105%	206%	202%
LLC (med)	88%	91%	115%	104%	>300%	212%	220%	212%	205%
LLC (big)	>300%	>300%	>300%	>300%	>300%	>300%	>300%	250%	214%
DRAM	>300%	>300%	>300%	>300%	>300%	>300%	>300%	287%	223%
HyperThread	109%	111%	100%	107%	112%	114%	119%	130%	262%
CPU power	101%	89%	86%	90%	92%	90%	89%	92%	97%
Network	56%	60%	58%	58%	59%	59%	63%	67%	89%
brain	149%	189%	202%	217%	239%	>300%	>300%	>300%	>300%

memkeyval

	10%	20%	30%	40%	50%	60%	70%	80%	90%
LLC (small)	88%	91%	101%	91%	101%	138%	140%	150%	78%
LLC (med)	148%	107%	119%	108%	138%	230%	181%	162%	100%
LLC (big)	>300%	>300%	>300%	>300%	>300%	>300%	280%	222%	79%
DRAM	>300%	>300%	>300%	>300%	>300%	>300%	>300%	234%	103%
HyperThread	31%	32%	32%	35%	43%	51%	62%	119%	153%
CPU power	277%	294%	>300%	>300%	224%	252%	193%	167%	82%
Network	28%	29%	27%	>300%	>300%	>300%	>300%	>300%	>300%
brain	232%	>300%	>300%	>300%	>300%	>300%	>300%	>300%	>300%

Each entry is color-coded as follows: 140% is ≥120%, 110% is between 100% and 120%, and 65% is ≤100%.

Figure 5.1: Impact of interference on shared resources on websearch, ml_cluster, and memkeyval. Each row is an antagonist and each column is a load point for the workload. The values are latencies, normalized to the SLO latency.

By observing the rows for *brain*, we immediately notice that current OS isolation mechanisms are inadequate for colocating LC tasks with BE tasks. Even at low loads, the BE task creates sufficient pressure on shared resources to lead to SLO violations for all three workloads. A large contributor to this is that the OS allows both workloads to run on the same core and even the same HyperThread, further compounding the interference. Tail latency eventually goes above 300% of SLO latency. Proposed interference-aware cluster managers, such as Paragon [28] and Bubble-Up [105], would disallow these colations. To enable aggressive task colocation, not only do we need to disallow different workloads on the same core or HyperThread, we

also need to use stronger isolation mechanisms.

The sensitivity of LC tasks to interference on individual shared resources varies. For instance, *memkeyval* is quite sensitive to network interference, while *websearch* and *ml_cluster* are not affected at all. *websearch* is uniformly insensitive to small and medium amounts of LLC interference, while the same cannot be said for *memkeyval* or *ml_cluster*. Furthermore, the impact of interference changes depending on the load: *ml_cluster* can tolerate medium amounts of LLC interference at loads ¡50% but is heavily impacted at higher loads. These observations motivate the need for dynamic management of isolation mechanisms in order to adapt to differences across varying loads and different workloads. Any static policy would be either too conservative (missing opportunities for colocation) or overly optimistic (leading to SLO violations).

We now discuss each LC workload separately, in order to understand their particular resource requirements.

websearch: This workload has a small footprint and LLC (small) and LLC (med) interference do not impact its tail latency. Nevertheless, the impact is significant with LLC (big) interference. The degradation is caused by two factors. First, the inclusive nature of the LLC in this particular chip means that high LLC interference leads to misses in the working set of instructions. Second, contention for the LLC causes significant DRAM pressure as well. *websearch* is particularly sensitive to interference caused by DRAM bandwidth saturation. As the load of *websearch* increases, the impact of LLC and DRAM interference decreases. At higher loads, *websearch* uses more cores while the interference generator is given fewer cores. Thus, *websearch* can defend its share of resources better.

websearch is moderately impacted by HyperThread interference until high loads. This indicates that the core has sufficient instruction issue bandwidth for both the spinloop and the *websearch* until around 80% load. Since the spinloop only accesses registers, it doesn't cause interference in the L1 or L2 caches. However, since the HyperThread antagonist has the smallest possible effect, more intensive antagonists will cause far larger performance problems. Thus, HyperThread interference in practice should be avoided. Power interference has a significant impact on *websearch* at lower utilization, as more cores are executing the power virus. As expected, the network antagonist does not impact *websearch*, due to *websearch*'s low bandwidth needs.

ml_cluster *ml_cluster* is sensitive to LLC interference of smaller size, due to the small but significant per-request working set. This manifests itself as a large jump in latency at 80% load for LLC (small) and 50% load for LLC (medium). With larger LLC interference, *ml_cluster* experiences major latency degradation. *ml_cluster* is also sensitive to DRAM bandwidth interference, primarily at lower loads (see explanation for *websearch*). *ml_cluster* is moderately resistant to HyperThread interference until high loads, suggesting that it only reaches high instruction issue rates at high loads. Power interference has a lesser impact on *ml_cluster* since it is less compute intensive than *websearch*. Finally, *ml_cluster* is not impacted at all by network interference.

memkeyval: Due to its significantly stricter latency SLO, *memkeyval* is sensitive to all types of interference. At high load, *memkeyval* becomes sensitive even to small LLC interference as the small per-request working

sets add up. When faced with medium LLC interference, there are two latency peaks. The first peak at low load is caused by the antagonist removing instructions from the cache. When *memkeyval* obtains enough cores at high load, it avoids these evictions. The second peak is at higher loads, when the antagonist interferes with the per-request working set. At high levels of LLC interference, *memkeyval* is unable to meet its SLO. Even though *memkeyval* has low DRAM bandwidth requirements, it is strongly affected by a DRAM streaming antagonist. Ironically, the few memory requests from *memkeyval* are overwhelmed by the DRAM antagonist.

memkeyval is not sensitive to the HyperThread antagonist except at high loads. In contrast, it is very sensitive to the power antagonist, as it is compute-bound. *memkeyval* does consume a large amount of network bandwidth, and thus is highly susceptible to competing network flows. Even at small loads, it is completely overrun by the many small "mice" flows of the antagonist and is unable to meet its SLO.

5.4 Heracles Design

We have established the need for isolation mechanisms beyond OS-level scheduling and for a dynamic controller that manages resource sharing between LC and BE tasks. *Heracles* is a dynamic, feedback-based controller that manages in real-time four hardware and software mechanisms in order to isolate colocated workloads. *Heracles* implements a different kind of *iso-latency* policy compared to the power saving policy from Chapter 4. Instead of lowering power, the iso-latency policy in Heracles attempts to increase resource efficiency as long as the SLO is being met. This policy allows for increasing server utilization through tolerating some interference caused by colocation, as long as the the difference between the SLO latency target for the LC workload and the actual latency observed (latency slack) is positive. In its current version, *Heracles* manages one LC workload with many BE tasks. Since BE tasks are abundant, this is sufficient to raise utilization in many datacenters. We leave colocation of multiple LC workloads to future work.

5.4.1 Isolation Mechanisms

Heracles manages 4 mechanisms to mitigate interference.

For **core isolation**, *Heracles* uses Linux's `cpuset cgroups` to pin the LC workload to one set of cores and BE tasks to another set (software mechanism) [112]. This mechanism is necessary, since in §5.3 we showed that core sharing is detrimental to latency SLO. Moreover, the number of cores per server is increasing, making core segregation finer-grained. The allocation of cores to tasks is done dynamically. The speed of core (re)allocation is limited by how fast Linux can migrate tasks to other cores, typically in the tens of milliseconds.

For **LLC isolation**, *Heracles* uses the Cache Allocation Technology (CAT) available in recent Intel chips (hardware mechanism) [60]. CAT implements way-partitioning of the shared LLC. In a highly-associative LLC, this allows us to define non-overlapping partitions at the granularity of a few percent of the total LLC capacity. We use one partition for the LC workload and a second partition for all BE tasks. Partition sizes

can be adjusted dynamically by programming model specific registers (MSRs), with changes taking effect in a few milliseconds.

There are no commercially available DRAM bandwidth isolation mechanisms. We enforce DRAM bandwidth limits in the following manner: we implement a software monitor that periodically tracks the total bandwidth usage through performance counters and estimates the bandwidth used by the LC and BE jobs. If the LC workload does not receive sufficient bandwidth, *Heracles* scales down the number of cores that BE jobs use. We discuss the limitations of this coarse-grained approach in §5.4.2.

For **power isolation**, *Heracles* uses CPU frequency monitoring, Running Average Power Limit (RAPL), and per-core DVFS (hardware features) [60, 80]. RAPL is used to monitor CPU power at the per-socket level, while per-core DVFS is used to redistribute power amongst cores. Per-core DVFS setting changes go into effect within a few milliseconds. The frequency steps are in 100MHz and span the entire operating frequency range of the processor, including Turbo Boost frequencies.

For **network traffic isolation**, *Heracles* uses Linux traffic control (software mechanism). Specifically we use the `qdisc` [15] scheduler with hierarchical token bucket queueing discipline (HTB) to enforce bandwidth limits for outgoing traffic from the BE tasks. The bandwidth limits are set by limiting the maximum traffic burst rate for the BE jobs (`ceil` parameter in HTB parlance). The LC job does not have any limits set on it. HTB can be updated very frequently, with the new bandwidth limits taking effect in less than hundreds of milliseconds. Managing ingress network interference has been examined in numerous previous work [74].

5.4.2 Design Approach

Each hardware or software isolation mechanism allows reasonably precise control of an individual resource. Given that, the controller must dynamically solve the high dimensional problem of finding the right settings for all these mechanisms at any load for the LC workload and any set of BE tasks. *Heracles* solves this as an *optimization problem*, where the *objective* is to maximize utilization with the *constraint* that the SLO must be met.

Heracles reduces the optimization complexity by decoupling interference sources. The key insight that enables this reduction is that *interference is problematic only when a shared resource becomes saturated*, i.e. its utilization is so high that latency problems occur. This insight is derived by the analysis in §5.3: the antagonists do not cause significant SLO violations until an inflection point, at which point the tail latency degrades extremely rapidly. Hence, if *Heracles* can prevent any shared resource from saturating, then *it can decompose the high-dimensional optimization problem into many smaller and independent problems of one or two dimensions each*. Then each sub-problem can be solved using sound optimization methods, such as gradient descent.

Since *Heracles* must ensure that the target SLO is met for the LC workload, it continuously monitors latency and latency slack and uses both as key inputs in its decisions. When the latency slack is large, *Heracles* treats this as a signal that it is safe to be more aggressive with colocation; conversely, when the slack is small, it should back off to avoid an SLO violation. *Heracles* also monitors the load (queries per

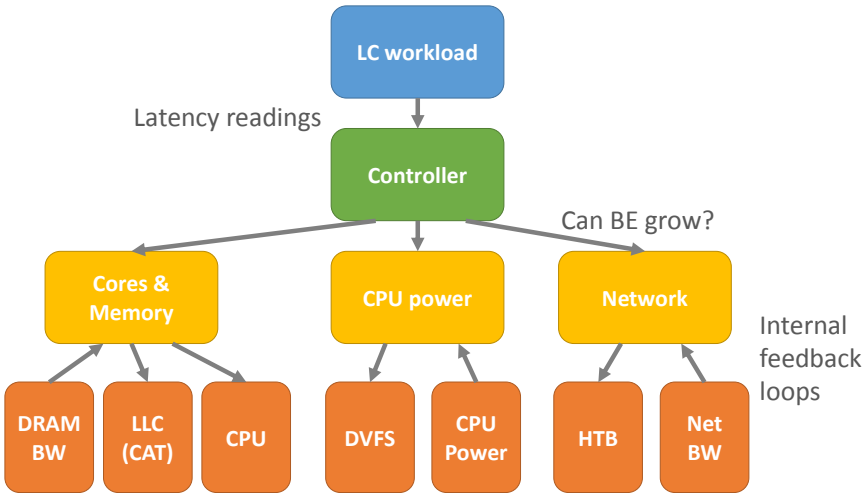

Figure 5.2: The system diagram of *Heracles*.

second), and during periods of high load, it disables colocation due to a high risk of SLO violations. In Chapter 4, we demonstrated that indirect performance metrics, such as CPU utilization, are insufficient to guarantee that the SLO is met.

Ideally, *Heracles* should require no offline information other than SLO targets. Unfortunately, one shortcoming of current hardware makes this difficult. The Intel chips we used do not provide accurate mechanisms for measuring (or limiting) DRAM bandwidth usage at a per-core granularity. To understand how *Heracles*' decisions affect the DRAM bandwidth usage of latency-sensitive and BE tasks and to manage bandwidth saturation, we require some offline information. Specifically, *Heracles* uses an offline model that describes the DRAM bandwidth used by the latency-sensitive workloads at various loads, core, and LLC allocations. We verified that this model needs to be regenerated only when there are significant changes in the workload structure and that small deviations are fine. There is no need for any offline profiling of the BE tasks, which can vary widely compared to the better managed and understood LC workloads. There is also no need for offline analysis of interactions between latency-sensitive and best effort tasks. Once we have hardware support for per-core DRAM bandwidth accounting [68], we can eliminate this offline model.

5.4.3 Heracles Controller

Heracles runs as a separate instance on each server, managing the local interactions between the LC and BE jobs. As shown in Figure 5.2, it is organized as three subcontrollers (cores & memory, power, network traffic) coordinated by a top-level controller. The subcontrollers operate fairly independently of each other and ensure that their respective shared resources are not saturated.

Top-level controller: The pseudo-code for the controller is shown in Algorithm 5.1. The controller polls the tail latency and load of the LC workload every 15 seconds. This allows for sufficient queries to calculate

```
1  while True:
2      latency=PollLCAppLatency()
3      load=PollLCAppLoad()
4      slack=(target-latency)/target
5      if slack<0:
6          DisableBE()
7          EnterCooldown()
8      elif load>0.85:
9          DisableBE()
10     elif load<0.80:
11         EnableBE()
12     elif slack<0.10:
13         DisallowBEGrowth()
14         if slack<0.05:
15             be_cores.Remove(be_cores.Size()-2)
16     sleep(15)
```

Algorithm 5.1: High-level controller.

statistically meaningful tail latencies. If the load for the LC workload exceeds 85% of its peak on the server, the controller disables the execution of BE workloads. This empirical safeguard avoids the difficulties of latency management on highly utilized systems for minor gains in utilization. For hysteresis purposes, BE execution is enabled when the load drops below 80%. BE execution is also disabled when the latency slack, the difference between the SLO target and the current measured tail latency, is negative. This typically happens when there is a sharp spike in load for the latency-sensitive workload. We give all resources to the latency critical workload for a while (e.g., 5 minutes) before attempting colocation again. The constants used here were determined through empirical tuning.

When these two safeguards are not active, the controller uses slack to guide the subcontrollers in providing resources to BE tasks. If slack is less than 10%, the subcontrollers are instructed to disallow growth for BE tasks in order to maintain a safety margin. If slack drops below 5%, the subcontroller for cores is instructed to switch cores from BE tasks to the LC workload. This improves the latency of the LC workload and reduces the ability of the BE job to cause interference on any resources. If slack is above 10%, the subcontrollers are instructed to allow BE tasks to acquire a larger share of system resources. Each subcontroller makes allocation decisions independently, provided of course that its resources are not saturated.

Core & memory subcontroller: *Heracles* uses a single subcontroller for core and cache allocation due to the strong coupling between core count, LLC needs, and memory bandwidth needs. If there was a direct way to isolate memory bandwidth, we would use independent controllers. The pseudo-code for this subcontroller is shown in Algorithm 5.2. Its output is the allocation of cores and LLC to the LC and BE jobs (2 dimensions).

The first constraint for the subcontroller is to avoid memory bandwidth saturation. The DRAM controllers provide registers that track bandwidth usage, making it easy to detect when they reach 90% of peak streaming DRAM bandwidth. In this case, the subcontroller removes as many cores as needed from BE tasks to avoid

saturation. *Heracles* estimates the bandwidth usage of each BE task using a model of bandwidth needs for the LC workload and a set of hardware counters that are proportional to the per-core memory traffic to the NUMA-local memory controllers. For the latter counters to be useful, we limit each BE task to a single socket for both cores and memory allocations using Linux `numactl`. Different BE jobs can run on either socket and LC workloads can span across sockets for cores and memory.

When the top-level controller signals BE growth and there is no DRAM bandwidth saturation, the subcontroller uses gradient descent to find the maximum number of cores and cache partitions that can be given to BE tasks. Offline analysis of LC applications (Figure 5.3) shows that their performance is a convex function of core and cache resources, thus guaranteeing that gradient descent will find a global optimum. We perform the gradient descent in one dimension at a time, switching between increasing the cores and increasing the cache given to BE tasks. Initially, a BE job is given one core and 10% of the LLC and starts in the *GROW_LLC* phase. Its LLC allocation is increased as long as the LC workload meets its SLO, bandwidth saturation is avoided, and the BE task benefits. The next phase (*GROW_CORES*) grows the number of cores for the BE job. *Heracles* will reassign cores from the LC to the BE job one at a time, each time checking for DRAM bandwidth saturation and SLO violations for the LC workload. If bandwidth saturation occurs first, the subcontroller will return to the *GROW_LLC* phase. The process repeats until an optimal configuration has been converged upon. The search also terminates on a signal from the top-level controller indicating the end to growth or the disabling of BE jobs. The typical convergence time is about 30 seconds.

During gradient descent, the subcontroller must avoid trying suboptimal allocations that will either trigger DRAM bandwidth saturation or a signal from the top-level controller to disable BE tasks. To estimate the DRAM bandwidth usage of an allocation prior to trying it, the subcontroller uses the derivative of the DRAM bandwidth from the last reallocation of cache or cores. *Heracles* estimates whether it is close to an SLO violation for the LC task based on the amount of latency slack.

Power subcontroller: The simple subcontroller described in Algorithm 5.3 ensures that there is sufficient power slack to run the LC workload at a minimum guaranteed frequency. This frequency is determined by measuring the frequency used when the LC workload runs alone at full load. *Heracles* uses RAPL to determine the operating power of the CPU and its maximum design power, or thermal dissipation power (TDP). It also uses CPU frequency monitoring facilities on each core. When the operating power is close to the TDP **and** the frequency of the cores running the LC workload is too low, it uses per-core DVFS to lower the frequency of cores running BE tasks in order to shift the power budget to cores running LC tasks. Both conditions must be met in order to avoid confusion when the LC cores enter active-idle modes, which also tends to lower frequency readings. If there is sufficient operating power headroom, *Heracles* will increase the frequency limit for the BE cores in order to maximize their performance. The control loop runs independently for each of the two sockets and has a cycle time of two seconds.

Network subcontroller: This subcontroller prevents saturation of network transmit bandwidth as shown in Algorithm 5.4. It monitors the total egress bandwidth of flows associated with the LC workload ($LCBandwidth$) and sets the total bandwidth limit of all other flows as

```
def PredictedTotalBW():
    return LcBwModel()+BeBw()+bw_derivative
while True:
    MeasureDRAMBw()
    if total_bw>DRAM_LIMIT:
        overage=total_bw-DRAM_LIMIT
        be_cores.Remove(overage/BeBwPerCore())
        continue
    if not CanGrowBE():
        continue
    if state==GROW_LLC:
        if PredictedTotalBW()>DRAM_LIMIT:
            state=GROW_CORES
        else:
            GrowCacheForBE()
            MeasureDRAMBw()
            if bw_derivative≥0:
                Rollback()
                state=GROW_CORES
            if not BeBenefit():
                state=GROW_CORES
    elif state==GROW_CORES:
        needed=LcBwModel()+BeBw()+BeBwPerCore()
        if needed>DRAM_LIMIT:
            state=GROW_LLC
        elif slack>0.10:
            be_cores.Add(1)
    sleep(2)
```

Algorithm 5.2: Core & memory sub-controller.

$LinkRate - LCBandwidth - max(0.05LinkRate, 0.10LCBandwidth)$. A small headroom of 10% of the current $LCBandwidth$ or 5% of the LinkRate is added into the reservation for the LC workload in order to handle spikes. The bandwidth limit is enforced via HTB qdiscs in the Linux kernel. This control loop is run once every second, which provides sufficient time for the bandwidth enforcer to settle.

5.5 Heracles Evaluation

5.5.1 Methodology

We evaluated *Heracles* with the three production, latency-critical workloads from Google analyzed in §5.3. We first performed experiments with *Heracles* on a single leaf server, introducing BE tasks as we run the LC workload at different levels of load. Next, we used *Heracles* on a *websearch* cluster with tens of servers, measuring end-to-end workload latency across the fan-out tree while BE tasks are also running. In the cluster

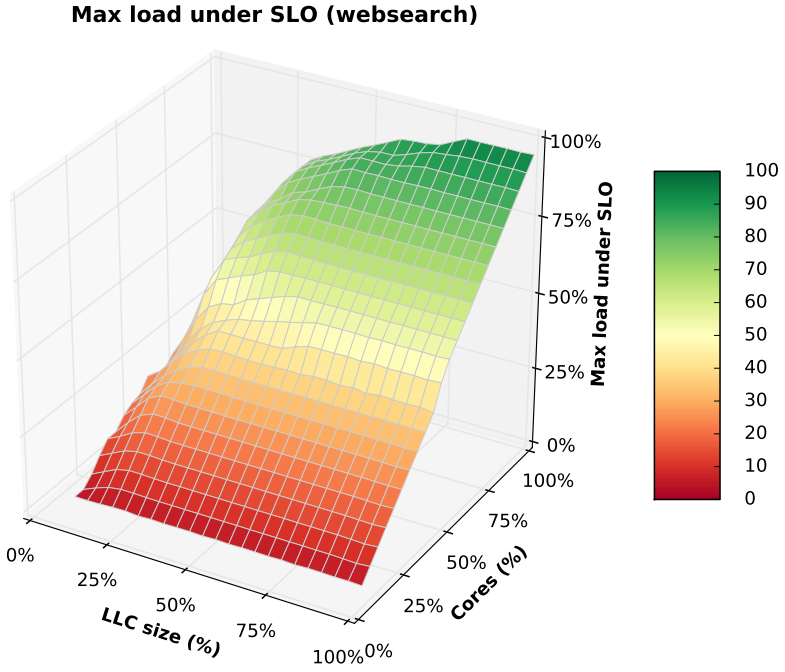

Figure 5.3: Characterization of *websearch* showing that its performance is a convex function of cores and LLC.

experiments, we used a load trace that represents the traffic throughout a day, capturing diurnal load variation. In all cases, we used production Google servers.

For the LC workloads we focus on SLO latency. Since the SLO is defined over 60-second windows, we report the worst-case latency that was seen during experiments. For the production batch workloads, we compute the throughput rate of the batch workload with *Heracles* and normalize it to the throughput of the batch workload running alone on a single server. We then define the **Effective Machine Utilization (EMU)** = LC Throughput + BE Throughput. Note that **Effective Machine Utilization** can be above 100% due to better binpacking of shared resources. We also report the utilization of shared resources when necessary to highlight detailed aspects of the system.

The BE workloads we use are chosen from a set containing both production batch workloads and the synthetic tasks that stress a single shared resource. The specific workloads are:

stream-LLC streams through data sized to fit in about half of the LLC and is the same as LLC (med) from §5.3.2. **stream-DRAM** streams through an extremely large array that cannot fit in the LLC (DRAM from the same section). We use these workloads to verify that *Heracles* is able to maximize the use of LLC partitions and avoid DRAM bandwidth saturation.

cpu_pwr is the CPU power virus from §5.3.2. It is used to verify that *Heracles* will redistribute power to ensure that the LC workload maintains its guaranteed frequency.

```
1 while True:
2     power=PollRAPL()
3     ls_freq=PollFrequency(ls_cores)
4     if power>0.90*TDP and ls_freq<guaranteed:
5         LowerFrequency(be_cores)
6     elif power≤0.90*TDP and ls_freq≥guaranteed:
7         IncreaseFrequency(be_cores)
8     sleep(2)
```

Algorithm 5.3: CPU power sub-controller.

```
1 while True:
2     ls_bw=GetLCTxBandwidth()
3     be_bw=LINK_RATE-ls_bw-max(0.05*LINK_RATE, 0.10*ls_bw)
4     SetBETxBandwidth(be_bw)
5     sleep(1)
```

Algorithm 5.4: Network sub-controller.

iperf is an open source network streaming benchmark used to verify that *Heracles* partitions network transmit bandwidth correctly to protect the LC workload.

brain is a Google production batch workload that performs deep learning on images for automatic labelling [83, 133]. This workload is very computationally intensive, is sensitive to LLC size, and also has high DRAM bandwidth requirements.

streetview is a production batch job that stitches together multiple images to form the panoramas for Google Street View. This workload is highly demanding on the DRAM subsystem.

5.5.2 Individual Server Results

Latency SLO: Figure 5.4 presents the impact of colocating each of the three LC workloads with BE workloads across all possible loads under the control of *Heracles*. Note that *Heracles* attempts to run as many copies of the BE task as possible and maximize the resources they receive. At all loads and in all colocation cases, there are *no SLO violations* with *Heracles*. This is true even for *brain*, a workload that even with the state-of-the-art OS isolation mechanisms would render any LC workload unusable. This validates that the controller keeps shared resources from saturating and allocates a sufficient fraction to the LC workload at any load. *Heracles* maintains a small latency slack as a guard band to avoid spikes and control instability. It also validates that local information on tail latency is sufficient for stable control for applications with milliseconds and microseconds range of SLOs. Interestingly, the *websearch* binary and shard changed between generating the offline profiling model for DRAM bandwidth and performing this experiment. Nevertheless, *Heracles* is resilient to these changes and performs well despite the somewhat outdated model.

Heracles reduces the latency slack during periods of low utilization for all workloads. For *websearch* and *ml_cluster*, the slack is cut in half, from 40% to 20%. For *memkeyval*, the reduction is much more dramatic,

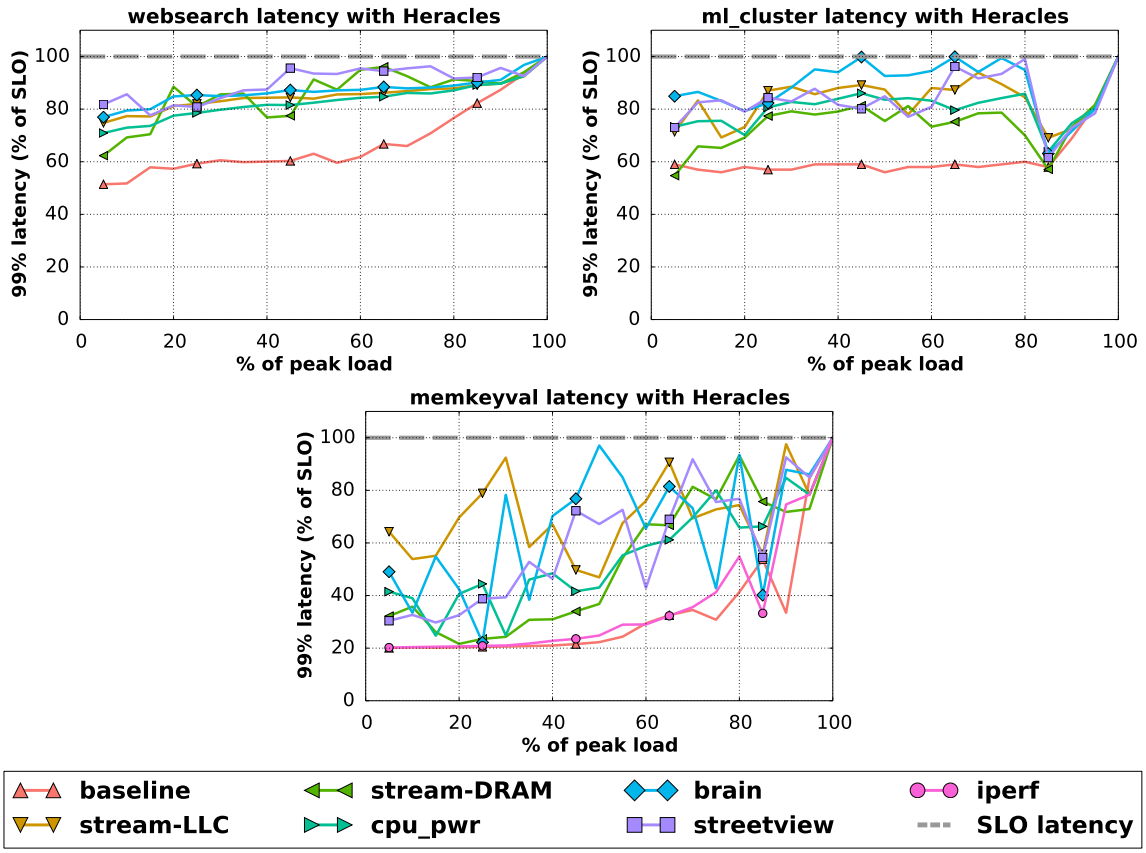

Figure 5.4: Latency of LC applications co-located with BE jobs under *Heracles*. For clarity we omit websearch and ml_cluster with iperf as those workloads are extremely resistant to network interference.

from a slack of 80% to 40% or less. This is because the unloaded latency of *memkeyval* is extremely small compared to the SLO latency. The high variance of the tail latency for *memkeyval* is due to the fact that its SLO is in the hundreds of microseconds, making it more sensitive to interference than the other two workloads.

Server Utilization: Figure 5.5 shows the EMU achieved when colocating production LC and BE tasks with *Heracles*. In all cases, we achieve significant EMU increases. When the two most CPU-intensive and power-hungry workloads are combined, *websearch* and *brain*, *Heracles* still achieves an EMU of at least 75%. When *websearch* is combined with the DRAM bandwidth intensive *streetview*, *Heracles* can extract sufficient resources for a total EMU above 100% at *websearch* loads between 25% and 70%. This is because *websearch* and *streetivew* have complementary resource requirements, where *websearch* is more compute bound and *streetview* is more DRAM bandwidth bound. The EMU results are similarly positive for *ml_cluster* and *memkeyval*. By dynamically managing multiple isolation mechanisms, *Heracles* exposes opportunities to raise EMU that would otherwise be missed with scheduling techniques that avoid interference.

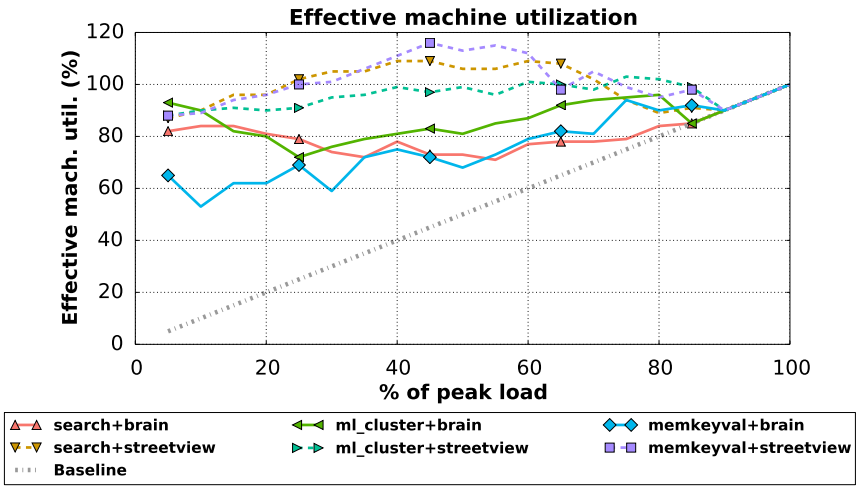

Figure 5.5: EMU achieved by *Heracles*.

Shared Resource Utilization: Figure 5.6, Figure 5.7, and Figure 5.8 plot the utilization of shared resources (DRAM bandwidth, cores, and power) under *Heracles* control. For *memkeyval*, we include measurements of network transmit bandwidth in Figure 5.9.

Across the board, *Heracles* is able to correctly size the BE workloads to avoid saturating DRAM bandwidth. For the stream-LLC BE task, *Heracles* finds the correct cache partitions to decrease total DRAM bandwidth requirements for all workloads. For *ml_cluster*, with its large cache footprint, *Heracles* balances the needs of stream-LLC with *ml_cluster* effectively, with a total DRAM bandwidth slightly above the baseline. For the BE tasks with high DRAM requirements (stream-DRAM, streetview), *Heracles* only allows them to execute on a few cores to avoid saturating DRAM. This is reflected by the lower CPU utilization but high DRAM bandwidth. However, EMU is still high, as the critical resource for those workloads is not compute, but memory bandwidth.

Looking at the power utilization, *Heracles* allows significant improvements to energy efficiency. Consider the 20% load case: EMU was raised by a significant amount, from 20% to 60%-90%. However, the CPU power only increased from 60% to 80%. This translates to an energy efficiency gain of 2.3-3.4x. Overall, *Heracles* achieves significant gains in resource efficiency across all loads for the LC task without causing SLO violations.

5.5.3 Websearch Cluster Results

We also evaluate *Heracles* on a small minicluster for *websearch* with tens of servers as a proxy for the full-scale cluster. The cluster root fans out each user request to all leaf servers and combines their replies. The SLO latency is defined as the average latency at the root over 30 seconds, denoted as $\mu/30s$. The target SLO latency is set as $\mu/30s$ when serving 90% load in the cluster without colocated tasks. *Heracles* runs on every

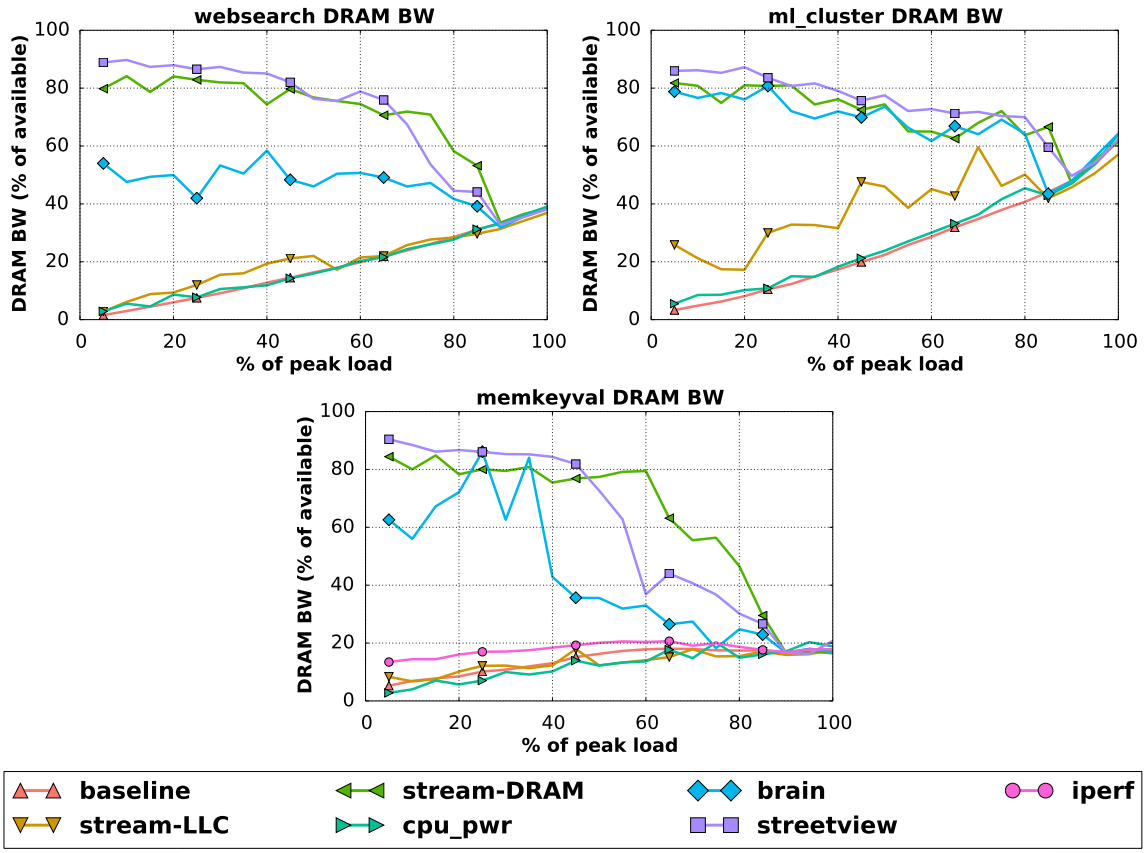

Figure 5.6: DRAM bandwidth of system when LC applications co-located with BE jobs under *Heracles*.

leaf node with a uniform 99%-ile latency target set such that the latency at the root satisfies the SLO. We use *Heracles* to execute *brain* on half of the leafs and *streetview* on the other half. *Heracles* shares the same offline model for the DRAM bandwidth needs of *websearch* across all leaves, even though each leaf has a different shard. We generate load from an anonymized, 12-hour request trace that captures the part of the daily diurnal pattern when *websearch* is not fully loaded and colocation has high potential.

Latency SLO: Figure 5.10 shows the latency SLO with and without *Heracles* for the 12-hour trace. *Heracles* produces no SLO violations while reducing slack by 20-30%. Meeting the 99%-ile tail latency at each leaf is sufficient to guarantee the global SLO. We believe we can further reduce the slack in larger *websearch* clusters by introducing a centralized controller that dynamically sets the per-leaf tail latency targets based on slack at the root. This will allow a future version of *Heracles* to take advantage of slack in higher layers of the fan-out tree.

Server Utilization: Figure 5.10 also shows that *Heracles* successfully converts the latency slack in the baseline case into significantly increased EMU. Throughout the trace, *Heracles* colocates sufficient BE tasks

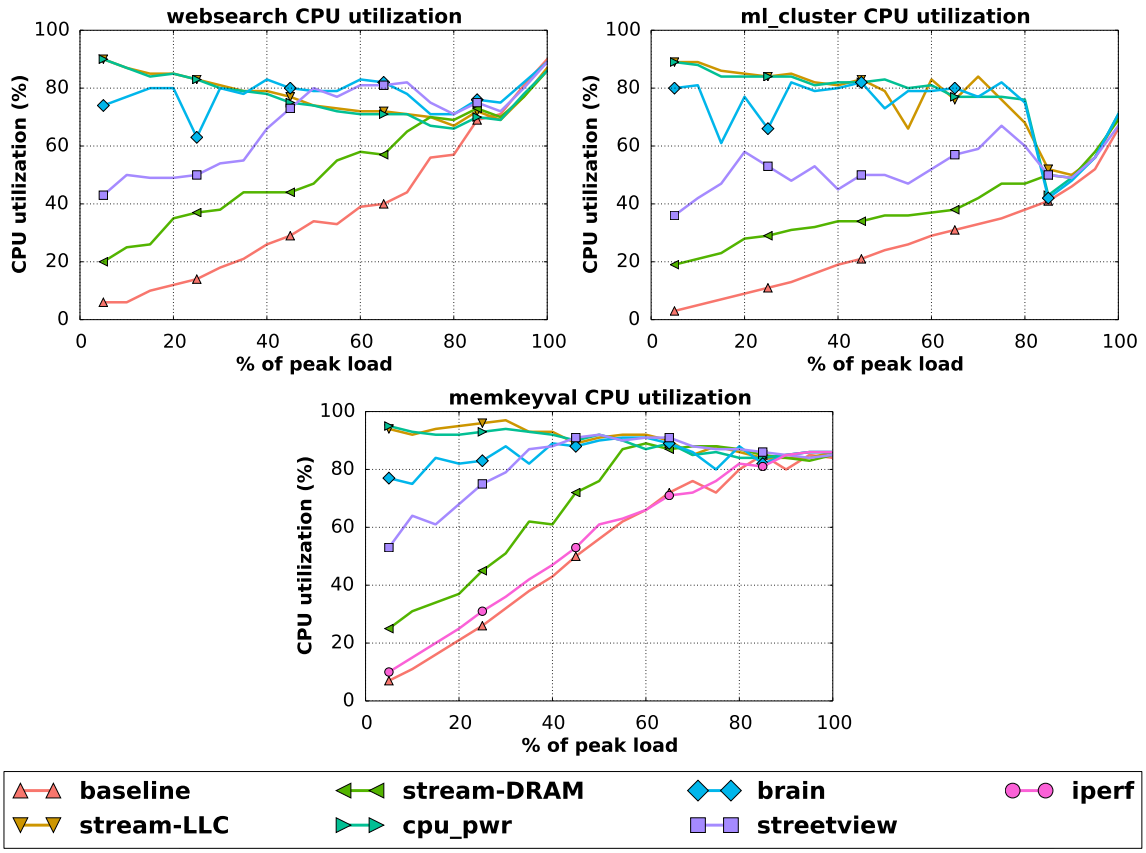

Figure 5.7: CPU utilization of system when LC applications co-located with BE jobs under *Heracles*.

to maintain an average EMU of 90% and a minimum of 80% without causing SLO violations. The *websearch* load varies between 20% and 90% in this trace.

TCO: To estimate the impact on total cost of ownership, we use the TCO calculator by Barroso et al. with the parameters from the case-study of a datacenter with low per-server cost [6]. This model assumes $2000 servers with a PUE of 2.0 and a peak power draw of 500W as well as electricity costs of $0.10/kW-hr. For our calculations, we assume a cluster size of 10,000 servers. Assuming pessimistically that a *websearch* cluster is highly utilized throughout the day, with an average load of 75%, *Heracles*' ability to raise utilization to 90% translates to a 15% throughput/TCO improvement over the baseline. This improvement includes the cost of the additional power consumption at higher utilization. Under the same assumptions, a controller that focuses only on improving energy-proportionality for *websearch*, such as PEGASUS, would achieve throughput/TCO gains of roughly 3%.

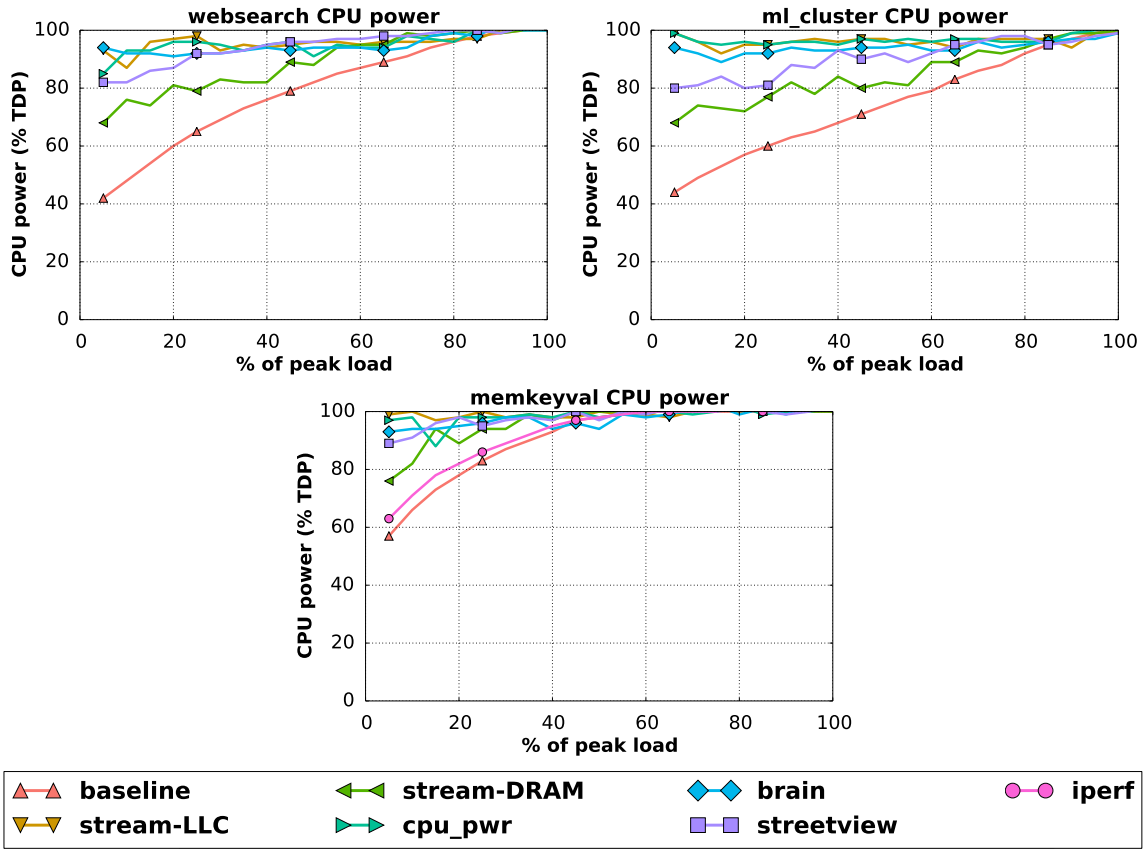

Figure 5.8: CPU power of system when LC applications co-located with BE jobs under *Heracles*.

If we assume a cluster for LC workloads utilized at an average of 20%, as many industry studies suggest [95, 153], *Heracles* can achieve a 306% increase in throughput/TCO. A controller focusing on energy-proportionality would achieve improvements of less than 7%. *Heracles*' advantage is due to the fact that it can raise utilization from 20% to 90% with a small increase to power consumption, which only represents 9% of the initial TCO. As long as there are useful BE tasks available, one should always choose to improve throughput/TCO by colocating them with LC jobs instead of lowering the power consumption of servers in modern datacenters. Also note that the improvements in throughput/TCO are large enough to offset the cost of reserving a small portion of each server's memory or storage for BE tasks.

5.6 Related Work

Isolation mechanisms: There is significant work on shared cache isolation, including soft partitioning based on replacement policies [159, 161], way-partitioning [126, 130], and fine-grained partitioning [102, 136, 143].

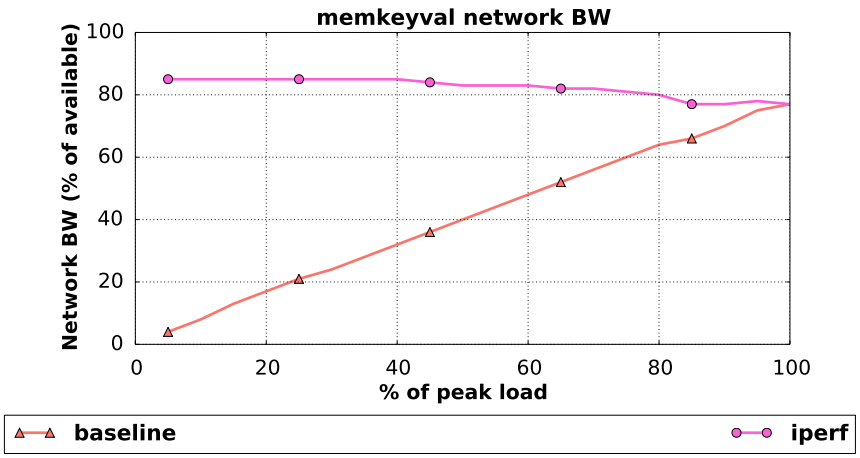

Figure 5.9: Network bandwidth of *memkeyval* under *Heracles*.

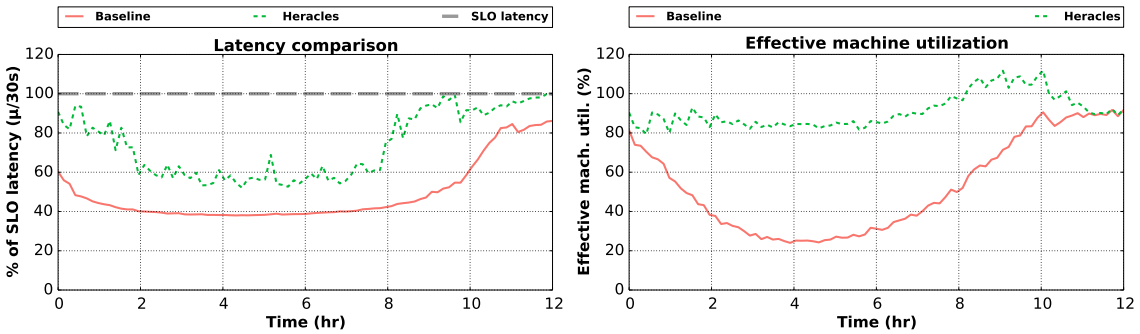

Figure 5.10: Latency SLO and effective machine utilization for a *websearch* cluster managed by *Heracles*.

Tessellation exposes an interface for throughput-based applications to request partitioned resources [96]. Most cache partitioning schemes have been evaluated with a utility-based policy that optimizes for aggregate throughput [126]. *Heracles* manages the coarse-grained, way-partitioning scheme recently added in Intel CPUs, using a search for a right-sized allocation to eliminate latency SLO violations. We expect *Heracles* will work even better with fine-grained partitioning schemes when they are commercially available.

Iyer et al. explores a wide range quality-of-service (QoS) policies for shared cache and memory systems with simulated isolation features [44, 45, 52, 67, 68]. They focus on throughput metrics, such as IPC and MPI, and did not consider latency-critical workloads or other resources such as network traffic. Cook et al. evaluate hardware cache partitioning for throughput based applications and did not consider latency-critical tasks [21]. Wu et al. compare different capacity management schemes for shared caches [159]. The proposed Ubik controller for shared caches with fine-grained partitioning support boosts the allocation for latency-critical workloads during load transition times and requires application level changes to inform the runtime

of load changes [78]. *Heracles* does not require any changes to the LC task, instead relying on a steady-state approach for managing cache partitions that changes partition sizes slowly.

There are several proposals for isolation and QoS features for memory controllers [31, 68, 72, 89, 114, 115, 117, 139]. While our work showcases the need for memory isolation for latency-critical workloads, such features are not commercially available at this point. Several network interface controllers implement bandwidth limiters and priority mechanisms in hardware. Unfortunately, these features are not exposed by device drivers. Hence, *Heracles* and related projects in network performance isolation currently use Linux qdisc [74]. Support for network isolation in hardware should strengthen Heracle's robustness.

The LC workloads we evaluated do not use disks or SSDs in order to meet their aggressive latency targets. Nevertheless, disk and SSD isolation is quite similar to network isolation. Thus, the same principles and controls used to mitigate network interference still apply. For disks, we list several available isolation techniques: 1) the cgroups blkio controller [112], 2) native command queuing (NCQ) priorities [57], 3) prioritization in file-system queues, 4) partitioning LC and BE to different disks, 5) replicating LC data across multiple disks that allows selecting the disk/reply that responds first or has lower load [26]. For SSDs: 1) many SSDs support channel partitions, separate queueing, and prioritization at the queue level, 2) SSDs also support suspending operations to allow LC requests to overtake BE requests.

Interference-aware cluster management: Several cluster-management systems detect interference between colocated workloads and generate schedules that avoid problematic colocations. Nathuji et al. develop a feedback-based scheme that tunes resource assignment to mitigate interference for colocated VMs [116]. Bubble-flux is an online scheme that detects memory pressure and finds colocations that avoid interference on latency-sensitive workloads [105, 163]. Bubble-flux has a backup mechanism to enable problematic co-locations via execution modulation, but such a mechanism would have challenges with applications such as *memkeyval*, as the modulation would need to be done in the granularity of microseconds. DeepDive detects and manages interference between co-scheduled applications in a VM system [118]. CPI2 throttles low-priority workloads that interfere with important services [164]. Finally, Paragon and Quasar use online classification to estimate interference and to colocate workloads that are unlikely to cause interference [28, 29].

The primary difference of *Heracles* is the focus on latency-critical workloads and the use of multiple isolation schemes in order to allow aggressive colocation without SLO violations at scale. Many previous approaches use IPC instead of latency as the performance metric [105, 118, 163, 164]. Nevertheless, one can couple *Heracles* with an interference-aware cluster manager in order to optimize the placement of BE tasks.

Latency-critical workloads: There is also significant work in optimizing various aspects of latency-critical workloads, including energy proportionality [75, 97, 98, 109, 110], networking performance [8, 76], and hardware-acceleration [90, 125, 146]. *Heracles* is largely orthogonal to these projects.

5.7 Conclusions

We present *Heracles*, a heuristic feedback-based system that manages four isolation mechanisms to enable a latency-critical workload to be colocated with batch jobs without SLO violations. We used an empirical characterization of several sources of interference to guide an important heuristic used in *Heracles*: interference effects are large only when a shared resource is saturated. We evaluated *Heracles* and several latency-critical and batch workloads used in production at Google on real hardware and demonstrated an average utilization of 90% across all evaluated scenarios without any SLO violations for the latency-critical job. Through coordinated management of several isolation mechanisms, *Heracles* enables colocation of tasks that previously would cause SLO violations. Compared to power-saving mechanisms alone, *Heracles* increases overall cost efficiency substantially through increased utilization.

Chapter 6

Concluding remarks

This dissertation has presented several practical systems to achieve higher efficiency for datacenters. In particular, we have made the following contributions:

- **Improving peak energy efficiency:** We described autoturbo (Chapter 3), a system that uses machine learning to find the optimal setting of TurboMode for varying efficiency metrics. We demonstrated that a static setting of TurboMode will not be able to capture the optimum energy efficiency for different workloads and metrics. We use a machine learning algorithm to learn the correlation between the optimal setting of TurboMode and performance counters on the CPU and show that such a classifier can substantially improve the energy efficiency of servers.

- **Improving energy proportionality:** In order to achieve energy proportionality for latency-critical workloads, we show that two requirements must be satisfied. The first is that latency feedback information from the application must be used to choose an appropriate trade-off between performance and power. The second is a fine-grained power management mechanism to expose many performance-power operating points. We develop an iso-latency policy to keep the latency-critical workload operating with minimal latency slack to achieve substantial power savings. PEGASUS is a controller that realizes this iso-latency power policy, and we demonstrate its effectiveness on production Google workloads running on real hardware.

- **Improving resource efficiency:** We apply the same principles for iso-latency power management to achieving high utilization in the datacenter. The principal difference is that instead of saving power, we use latency information to manage resource isolation mechanisms to guarantee safe workload co-locations. Heracles is a real-time dynamic controller that manages many isolation mechanisms to achieve high utilization in the datacenter. We demonstrate that Heracles is able to achieve average utilizations of 90% without causing latency SLO violations for latency-critical workloads, even in the face of diurnal load variation. Thus, Heracles is able to significantly raise the resource efficiency of

datacenters by increasing the realizable capacity of datacenters by integer multiples with a marginal increase in the overall cost of operating the datacenter.

We believe that the contributions above open many interesting paths for future research. First, there is significant synergy between all three approaches, as achieving good peak energy efficiency, energy proportionality, and resource efficiency are not mutually exclusive goals. For example, autoturbo can be combined with Heracles to choose the optimal operating frequencies for different workloads running on the same server to achieve better energy efficiency and resource efficiency. Similarly, the principles of iso-latency power management can also be applied to Heracles to further lower the power footprint of a latency-critical workload. In addition, we have demonstrated that an intimate understanding of the workloads, the hardware they run on, and their policies can unlock substantial gains. While past studies to improve efficiency have successfully focused on architectural features such as CPI or cache miss rates, the shift to higher level metrics such as latency SLOs have enabled an entire new class of optimizations. Looking forward, we hope that both software and hardware designers use the same approach to find new opportunities for significant efficiency increases. There is still substantial opportunities left to increase efficiency at a smaller granularity, such as at the level of individual requests. All of our approaches used can be extended to optimally schedule and re-allocate resources at the request level to further increase the efficiency of workloads. We leave these endeavors to future work.

Appendices

Appendix A

OLDIsim: benchmarking scale-out workloads

A.1 Introduction

There are two major classes of workloads running in large-scale datacenters: throughput oriented batch processing workloads (such as analytics, log processing, neural network training) and latency-critical scale-out applications (such as websearch, social networking, ads). The former class of workloads are already well represented with existing benchmarks, ranging from single-node workloads such as SPECCPU [144] and PARSEC [9] to large cluster-scale benchmarks driven by frameworks such as Hadoop [151] and Spark [149]. Unfortunately, there is a dearth of latency-critical scale-out workloads that are capable of emulating the multiple tiers often found in such workloads. While there are several latency-critical that represent one tier, such as memcached [111], Cassandra [150], or SPECWEB [145], there are virtually no publicly available benchmarks for the entire end-to-end stack. For example, there is only one commonly used scale-out workload used by the community, namely, Nutch [79]. Thus, there is a clear and pressing need for additional scale-out benchmarks in order to provide a standard set of workloads to characterize the behavior of large-scale datacenters.

OLDIsim, or **O**n**L**ine **D**ata **I**ntensive **sim**ulator, is designed as an easy-to use open-source framework for developers to construct and benchmark scale-out applications. *OLDIsim* provides a set of Application Programming Interfaces, or APIs, in C++ that abstract away the details of handling node-to-node communication patterns commonly found in scale-out workloads. For instance, *OLDIsim* provides easy to use abstractions for one-to-one, one-to-several, and one-to-all fan-in/fan-out patterns. *OLDIsim* is also optimized for performance and is capable of supporting several million transactions per second on benchmarked hardware. In addition, *OLDIsim* also provides built-in latency and throughput monitoring at all tiers of the scale-out application, thus enabling a transparent view into the behavior of the application. This is important for benchmarking the

behavior of the system, as performance bottlenecks can be easily isolated.

The first public release of *OLDIsim* by Google also includes a sample scale-out workload, *websearch* that simulates the performance of Google websearch. The workload emulates the processing time distribution recorded from production Google websearch to achieve a comparable end-to-end latency distribution. *websearch* is used in Google's open-source cloud performance benchmarker, PerfKitBenchmarker [148], to measure the scaling-efficiency of adding more nodes to horizontally scale a workload. This scaling-efficiency metric captures the inherent server-to-server variations that cause performance degradation in a scale-out setting, as the fan-in/fan-out communication pattern means that the slowest server determines overall query execution time.

This chapter describes the motivation for creating an open-source scale-out benchmarking framework, the APIs that *OLDIsim* exposes, low-level implementation details for *OLDIsim*, and the sample *websearch* workload.

A.2 Motivation

Latency-critical workloads are a growing class of applications in the datacenter. These applications are fueled by the growth of user-facing services such as Google websearch, Facebook, Twitter, various software-as-a-service providers, etc. Despite the large footprint of these workloads in datacenters, there are virtually no public benchmarks that attempt to capture and characterize the behavior of these kinds of workloads. For instance, in the CloudSuite benchmark, only one of the eight benchmarks can be classified as a scale-out workload, namely that of Web Search [35]. The remaining workloads in CloudSuite are either throughput oriented batch workloads (Data Analytics, Graph Analytics, Software Testing) or a single-tier latency-critical workload (Data Caching, Data Serving, Media Streaming, Web Serving). The lack of public benchmarks for multi-tier scale-out applications is quite apparent in the literature, as several recent papers use Nutch (the workload behind CloudSuite's Web Search benchmark) as the sole representative scale-out workload [35, 91, 163].

Unfortunately, representative scale-out workloads used in production datacenters are impossible to come by, as operators of such datacenters have a vested interest in keeping their workloads confidential. Thus, the only clear path forward to obtaining additional scale-out workloads is to enable developers to easily create their own benchmarks. Conceptually, a scale-out workload is not difficult to visualize, as the workload is divided into several tiers, where each tier is responsible for a specific processing task. However, as always, the devil is in the details. Creating a scalable, performant workload is very challenging, as there are many low-level system details that need to be optimized, such as multithreading, load-balancing, networking, etc. Proper design choices and handling of these details are crucial to achieving a high-performance and scalable workload, which are prerequisites to creating a representative scale-out benchmark.

Understandably, most developers have a difficult time managing these details. Facebook and Twitter, two popular examples of scale-out workloads, were originally designed with ease-of-coding as the primary

consideration as opposed to performance. As such, their original incarnations used relatively slow languages such as PHP and Ruby that are single-threaded. Prioritizing ease of development at the expense of performance was ultimately unscalable, as Facebook switched to using HHVM over the default PHP interpreter and Twitter has migrated many core services to Java.

OLDIsim was created to greatly simplify the creation of performant scale-out applications. This is made possible by the observation that scale-out applications have a lot of code and structural reuse. For instance, scale-out workloads all have to manage communications between different tiers, have a reply/response RPC-style communication between different tiers, and use a one-to-one or one-to-many fan-in/fan-out communication pattern. While different scale-out workloads have different processing requirements and actions, there is a big opportunity to abstract out the low-level communication and RPC execution details into a common framework that can be re-used by multiple scale-out applications.

First, *OLDIsim* abstracts away the low-level network communication and protocol parsing into a simple message-based interface. Requests from the user are seen as messages, and different tiers can send their own messages to other tiers for further processing. Messages are sent immediately after being handed off to *OLDIsim* to ensure minimal latency throughout the system. Messages are also labelled with a specific message type that is used to route messages to different message handlers. When a tier is done processing the message, *OLDIsim* provides a simple to use facility to reply to the originator of the message. The tracking of messages and replies is handled internally by *OLDIsim*.

Second, *OLDIsim* is designed with performance as a first-class priority. *OLDIsim* is written in C++11 and was extensively optimized for performance. *OLDIsim* is multi-threaded and uses lock-free concurrent structures as well as intelligent work placement and distribution to achieve high scalability on multi-core systems. We show the scalability of *OLDIsim* in Figure A.1, as measured on a dual-socket Sandy Bridge server with 12 cores (2x Intel Xeon E5-2630) and 10GbE Ethernet sending the smallest possible messages. In addition, *OLDIsim* load-balances work between threads in order to ensure high utilization in the face of irregular workload patterns. More details of the performance optimizations can be found in Section A.4.

A.3 OLDIsim APIs

Since *OLDIsim* is a framework, it is packaged as a C++ library to be linked into *OLDIsim*-enabled applications. Relevant API header files can be found in the `oldisim/include/oldisim/` directory under the source tree.

We now describe commonly used features of the high-level programming model exposed by *OLDIsim*. There are three possible node types: a **driver node** responsible for sending test data into the system, a **parent node** that is used to fan-in/fan-out work to other parts of the system, and a **leaf node** that performs the bulk of the computation to produce a result. The three node types in *OLDIsim* and possible directions of message sending available to each node are shown in Figure A.2. A **ChildConnection** represents the ability to send messages to lower levels in the fan-out tree, while a **ParentConnection** represents the ability to send data

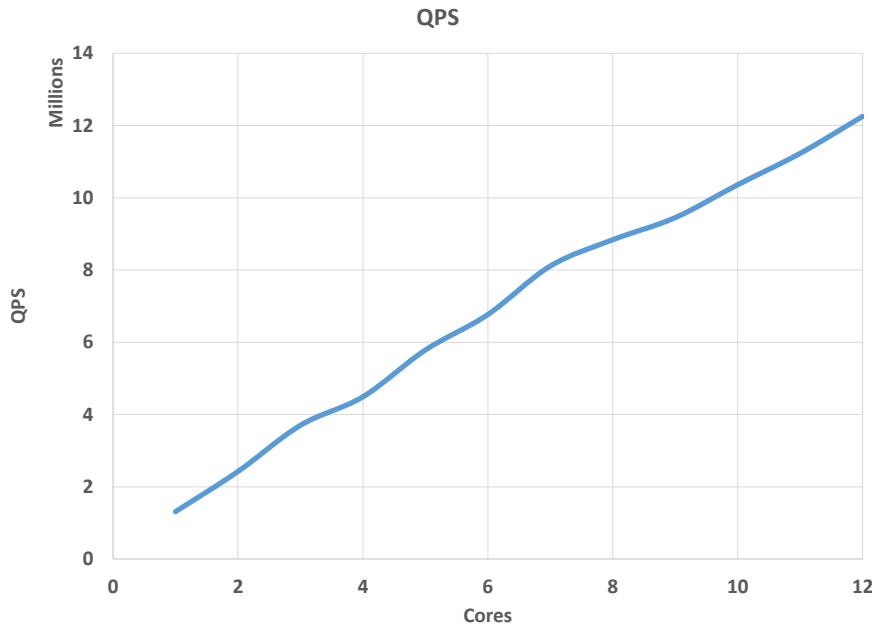

Figure A.1: Scaling behavior of *OLDIsim* on a CMP system. Experiment was run on a dual socket Intel Xeon E5-2630 system with Linux 3.13.0. The benchmark was run with 20 connections per thread and a limit of 25 outstanding requests per thread.

back up to the node that originated the message. In other words, **ChildConnection** and **ParentConnection** represent two parts of the same message flow, where the **ChildConnection** is accessible to the higher level node and the **ParentConnection** to the lower level node. Both **ChildConnection**s and **ParentConnection**s are managed internally by *OLDIsim* and are not exposed in the high-level programming interface.

OLDIsim does not perform any parsing or processing of the payload of messages, as it treats it as a raw stream of bytes. It is up to the developer to use a data serialization format, such as using raw bytes from memory, an ASCII format, protocol buffers [41], etc.

OLDIsim uses many callbacks and continuations throughout its API. One useful trick is to use `std::bind` from the `functional` header in C++11 with placeholder arguments from `std::placeholders` in order to pass state to callbacks and continuations.

A.3.1 DriverNode

The DriverNode produces queries to feed into the system and optionally allows the developer to shape the traffic arrival rates. It also measures the latency response characteristics for the requests it generates, and when the DriverNode is terminated with a SIGINT signal (CTRL+C), it will produce statistics on the QPS, receive and transmit bandwidth for the messages (excluding TCP/IP and Ethernet protocol overheads), as well as the minimum, average, 50%, 90%, 95%, 99%, and 99.9%-ile latencies for each message type. The DriverNode

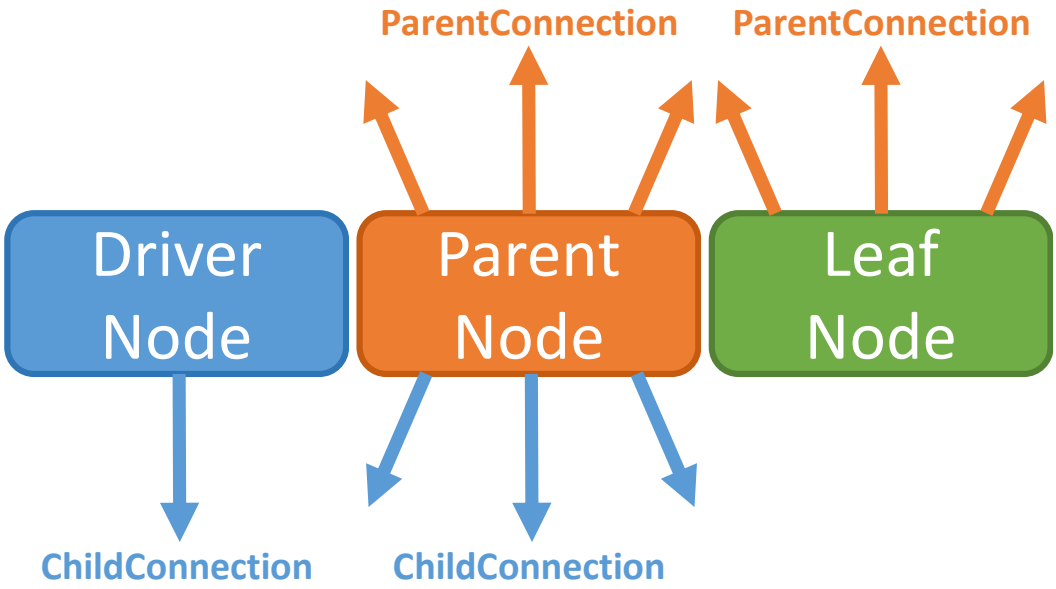

(a) Driver Node (b) ParentNodeServer (c) LeafNodeServer

Figure A.2: Different types of nodes in *OLDIsim*

is multi-threaded to take advantage of multi-core parallelism to generate requests quickly and efficiently. We now describe the operations available to the DriverNode. The relevant definitions and methods can be found in `Callbacks.h`, `DriverNode.h` and `TestDriver.h`.

```
typedef std::function<void(NodeThread&, TestDriver&)>
    DriverNodeThreadStartupCallback;
typedef std::function<void(NodeThread&, ResponseContext&)>
    DriverNodeResponseCallback;
typedef std::function<void(NodeThread&, TestDriver&)>
    DriverNodeMakeRequestCallback;
```

Figure A.3: `Callbacks.h` relevant to DriverNode

```
DriverNode(const std::string& hostname, uint16_t port);

void Run(uint32_t num_threads, bool thread_pinning,
         uint32_t num_connections_per_thread, uint32_t max_connection_depth);

/**
 * Set the callback to run after a thread has started up.
 * It will run in the context of the newly started thread.
 */
void SetThreadStartupCallback(
    const DriverNodeThreadStartupCallback& callback);

/**
 * Set the callback to run when the driver needs a request to send to the
 * service under test. It will run in the context of the driver thread.
 */
void SetMakeRequestCallback(const DriverNodeMakeRequestCallback& callback);

/**
 * Set the callback to run after a reply is received from the workload.
 * It will run in the context of the event thread that is responsible
 * for the connection. The callback will be used for incoming replies
 * of the given type.
 */
void RegisterReplyCallback(uint32_t type,
                           const DriverNodeResponseCallback& callback);

/**
 * Inform the driver node that it can send requests of the specified
 * type
 */
void RegisterRequestType(uint32_t type);

/**
 * Enable remote statistics monitoring at a given port.
 * It exposes a HTTP server with several URLs that provide diagnostic
 * and monitoring information
 */
void EnableMonitoring(uint16_t port);
```

Figure A.4: Relevant methods in DriverNode class

```
void SendRequest(uint32_t type, const void* payload, uint32_t payload_length,
                 uint64_t next_request_delay_us);
```

Figure A.5: Relevant methods in TestDriver class

The constructor is used to specify the hostname:port combination of the *OLDIsim* node to send traffic to. The target node can either be a ParentNodeServer or a LeafNodeServer.

SetThreadStartupCallback is used to allow the developer to perform custom thread initialization steps.

SetMakeRequestCallback specifies a callback that is called when a DriverNode thread needs a message to send to the service under test. This happens under several circumstances: 1) the thread has just started up and needs a message to send 2) the delay has expired from the last message sent on this thread or 3) the maximum number of in-flight messages was previously reached and now a free message slot has opened up. The developer provided callback is provided with the thread-local *TestDriver* instance, which it should call **SendRequest** on to produce a message to send to the service under test. **SendRequest** takes a *next_request_delay_us* parameter to modulate the load that a driver thread sends, if no modulation is desired, this parameter should be set to 0. **SendRequest** does not take ownership of the payload data, as it simply copies it into a network buffer.

RegisterReplyCallback is used to register an optional custom callback to run when a reply to a generated message is received. This could be used to generate and collect statistics on reply quality, for instance.

RegisterRequestType is used to inform the DriverNode that it is capable of sending messages of the specified type. Sending a message type that was not registered is an error.

EnableMonitoring enables a HTTP server running at the given port that exposes the following endpoints: `/topology` and `/child_stats`. Both of these endpoints produce JSON strings that provide monitoring data.

Run is used to actually start the test driver. Run should be called only after all the parameters are set and callback handlers are registered, and is a blocking call that only returns when the DriverNode is shut down. It takes several parameters to control the test driver execution. *num_threads* sets the number of worker threads available to process queries. *thread_pinning* enables pinning each thread to a logical CPU (and is only sensible if *num_threads* is less than the total number of logical CPUs). *num_connections_per_thread* specifies the number of connections to the service under test per thread. If this value is too high, the target node may believe it is under DDoS attack. *max_connection_depth* specifies the maximum number of outstanding messages that can be in-flight per connection. If this value is too high then the latency measurements can be skewed upwards.

```
void MakeRequest(oldisim::NodeThread& thread,
                 oldisim::TestDriver& test_driver) {
  // Send an empty message of type 0 as fast as it can
  test_driver.SendRequest(0, nullptr, 0, 0);
}

int main(int argc, char** argv) {
  // Test the node at testserver:1234
  oldisim::DriverNode driver_node("testserver", 1234);

  driver_node.SetMakeRequestCallback(MakeRequest);
  driver_node.RegisterRequestType(0);

  // Enable remote monitoring at port 8080
  driver_node.EnableMonitoring(8080);

  // Run driver with 4 threads, thread pinning, 10 connections/thread,
  // and request parallelism of 5
  driver_node.Run(4, true, 10, 5);

  return 0;
}
```

Figure A.6: Sample DriverNode code

A.3.2 QueryContext

We now describe the class **QueryContext**, which is used to store the data for a message as well as the meta-data for that message. **QueryContext** is used in both **LeafNodeServer** and **ParentNodeServer**. The relevant definition for the class can be found in `QueryContext.h`.

```
const uint32_t type;
const uint32_t payload_length;
void* const payload;
void SendResponse(const void* data, uint32_t data_length);
```

Figure A.7: Relevant members of QueryContext class

A *QueryContext* object represents a message received from a higher tier. It is composed of a message type and a message payload. The *payload_length* field records the size of the payload, in bytes. The payload data

is owned by the *QueryContext* object and will be automatically freed. When the receiving tier is ready to respond to the message, it can send a reply to the message by calling the *SendResponse* method. *SendResponse* does not take ownership of the reply data, as it simply copies it into a network buffer.

A.3.3 LeafNodeServer

The LeafNodeServer is a multi-threaded server that listens on a port for messages from a higher tier. When it receives a message, it looks up the proper handler for that message type, calls it, and sends back the response that the message handler produces. The LeafNodeServer is optimized for persistent connections opened from higher tiers, and it statically assigns connection parsing duty in a round-robin fashion between its worker threads. We now describe the operations available to the LeafNodeServer. The relevant definitions and methods can be found in `Callbacks.h` and `LeafNodeServer.h`.

```
typedef std::function<void(NodeThread&)> LeafNodeThreadStartupCallback;
typedef std::function<void(NodeThread&, QueryContext&)> LeafNodeQueryCallback;
```

Figure A.8: `Callbacks.h` relevant to LeafNodeServer

```
explicit LeafNodeServer(uint16_t port);

/* Set various configuration parameters for the leaf node server */
void SetNumThreads(uint32_t num_threads);
void SetThreadPinning(bool use_thread_pinning);
void SetThreadLoadBalancing(bool use_thread_lb);
void SetThreadLoadBalancingParams(int lb_process_connections_batch_size,
                                  int lb_process_request_batch_size);

void Run();

/**
 * Set the callback to run after a thread has started up.
 * It will run in the context of the newly started thread.
 */
void SetThreadStartupCallback(const LeafNodeThreadStartupCallback& callback);

/**
 * Set the callback to run after an incoming connection is accepted and a
 * ParentConnection object representing that connection has been made.
 * It will run in the context of the thread that the connection is assigned
 * to.
 */
void SetAcceptCallback(const AcceptCallback& callback);

/**
 * Set the callback to run after an incoming query is received.
 * It will run in the context of the event thread that is responsible
 * for the connection. The callback will be used for incoming queries
 * of a given type
 */
void RegisterQueryCallback(uint32_t type,
                           const LeafNodeQueryCallback& callback);

/**
 * Enable remote statistics monitoring at a given port.
 * It exposes a HTTP server with several URLs that provide diagnostic
 * and monitoring information
 */
void EnableMonitoring(uint16_t port);
```

Figure A.9: Relevant methods in LeafNodeServer class

The constructor takes an argument specifying the port number the LeafNodeServer should listen on.

SetNumThreads sets the number of worker threads available to process queries.

SetThreadPinning enables pinning each thread to a logical CPU (and is only sensible if *num_threads* is less than the total number of logical CPUs).

SetThreadLoadBalancing and **SetThreadLoadBalancingParams** are used to enable and to tune the inter-thread load-balancing parameters. *lb_process_connections_batch_size* is the maximum number of messages that a single thread handles on a connection before waking up other threads to help handle requests, and *lb_process_request_batch_size* represents the maximum number of messages a thread will process when work stealing before checking to see if it has work on its own connections.

SetThreadStartupCallback and **SetAcceptCallback** are used to allow the developer to perform custom thread initialization and connection initialization steps.

RegisterQueryCallback registers a message handler for a given message type that is called when a message of that type is received. The message handler is blocking, so it should avoid calls to long I/O operations. Since a LeafNodeServer does not have any lower tiers it can pass messages to, it must produce a response to the message by the end of the query handler.

EnableMonitoring enables a HTTP server running at the given port that exposes the following endpoints: `/topology` and `/child_stats`. Both of these endpoints produce JSON strings that provide monitoring data.

Run is used to actually start the server. Run should be called only after all the parameters are set and callback handlers are registered, and is a blocking call that only returns when the LeafNodeServer is shut down.

```
void Type0Handler(oldisim::NodeThread& thread, oldisim::QueryContext& context) {
  // Send back a reply with 1 byte
  static const char test_response[] = "0";
  context.SendResponse(test_response, sizeof(test_response));
}

int main(int argc, char** argv) {
  // Listen on port 1234
  oldisim::LeafNodeServer server(1234);

  // Register handler for messages with type 0
  server.RegisterQueryCallback(0, Type0Handler);

  // Run with 4 threads and with thread pinning
  server.SetNumThreads(4);
  server.SetThreadPinning(true);
  server.Run();

  return 0;
}
```

Figure A.10: Sample LeafNodeServer code

A.3.4 ParentNodeServer

The ParentNodeServer represents intermediate nodes in the fan-out tree that can communicate with other ParentNodeServers or LeafNodeServers. ParentNodeServers are the most flexible kind of nodes, and can be used as front-end load balancers, result aggregators, etc. Ideally ParentNodeServers will not perform complex calculations, as those tasks should be delegated to LeafNodeServers. ParentNodeServers are also multi-threaded and also balance connection handling between several worker threads in the same manner as LeafNodeServers. The key different between a ParentNodeServer and a LeafNodeServer is that when a message is received, a ParentNodeServer can issue non-blocking request(s) to one or several nodes in a lower tier of the system, and when the response(s) are received, the ParentNodeServer will resume processing the original message. This is done in a style that closely resembles continuations. We now describe the operations available to the ParentNodeServer. The relevant definitions and methods can be found in `Callbacks.h`, `ParentNodeServer.h`, and `FanoutManager.h`.

```
typedef std::function<void(NodeThread&, FanoutManager&)>
    ParentNodeThreadStartupCallback;
typedef std::function<void(NodeThread&, FanoutManager&, QueryContext&)>
    ParentNodeQueryCallback;
```

Figure A.11: `Callbacks.h` relevant to ParentNodeServer

```
explicit ParentNodeServer(uint16_t port);
void Run(uint32_t num_threads, bool thread_pinning);
/**
 * Set the callback to run after a thread has started up.
 * It will run in the context of the newly started thread.
 */
void SetThreadStartupCallback(
    const ParentNodeThreadStartupCallback& callback);
/**
 * Set the callback to run after an incoming connection from a higher
 * level parent is accepted and a
 * ParentConnection object representing that connection has been made.
 * It will run in the context of main event loop thread.
 */
void SetAcceptCallback(const AcceptCallback& callback);
/**
 * Set the callback to run after an incoming query is received from a parent.
 * It will run in the context of the event thread that is responsible
 * for the connection. The callback will be used for incoming queries
 * of the given type.
 */
void RegisterQueryCallback(uint32_t type,
                           const ParentNodeQueryCallback& callback);
/**
 * Inform the parent node server that it can send requests of the specified
 * type
 */
void RegisterRequestType(uint32_t type);
/**
 * Add a hostname:port as a child node that requests can be sent to.
 * Note that it is up to the thread to create the actual connections.
 */
void AddChildNode(std::string hostname, uint16_t port);
/**
 * Enable remote statistics monitoring at a given port.
 * It exposes a HTTP server with several URLs that provide diagnostic
 * and monitoring information
 */
void EnableMonitoring(uint16_t port);
```

Figure A.12: Relevant methods in ParentNodeServer class

```
struct FanoutRequest {
  uint32_t child_node_id;
  uint32_t request_type;
  const void* request_data;
  uint32_t request_data_length;
};

struct FanoutReply {
  bool timed_out;
  uint32_t child_node_id;
  uint32_t request_type;
  std::unique_ptr<uint8_t[]> reply_data;
  uint32_t reply_data_length;
  float latency_ms;
};

struct FanoutReplyTracker {
  uint64_t starting_request_id;
  int num_requests;
  int num_replies_received;
  std::vector<FanoutReply> replies;
  bool closed;  // Marked as such when timed out or when all replies received
  uint64_t start_time;
};

class FanoutManager {
 public:
  // Methods to create child connections, used by user programs
  void MakeChildConnection(uint32_t child_node_id);
  void MakeChildConnections(uint32_t child_node_id, int num);

  // Methods to perform fanout queries
  typedef std::function<void(QueryContext&, const FanoutReplyTracker&)>
      FanoutDoneCallback;
  void Fanout(QueryContext&& originating_query, const FanoutRequest* requests,
              int num_requests, const FanoutDoneCallback& callback,
              double timeout_ms = 0.0);
  void FanoutAll(QueryContext&& originating_query, const FanoutRequest& request,
                 const FanoutDoneCallback& callback, double timeout_ms = 0.0);
};
```

Figure A.13: Relevant code in `FanoutManager.h`

The ParentNodeServer constructor takes an argument specifying the port number the ParentNodeServer should listen on.

Run is used to actually start the ParentNodeServer. Run should be called only after all the child nodes are added and callback handlers are registered, and is a blocking call that only returns when the ParentNodeServer is shut down. It takes several parameters to control the ParentNodeServer execution. *num_threads* sets the number of worker threads available to process queries. *thread_pinning* enables pinning each thread to a logical CPU (and is only sensible if *num_threads* is less than the total number of logical CPUs).

SetThreadStartupCallback must be used to set a thread initialization callback that opens the connections to the child nodes added with **AddChildNode**. A *FanoutManager* object is provided to this callback with **MakeChildConnection** and **MakeChildConnections** for this purpose. The *child_node_id* parameter corresponds to the order that the child nodes were added, where 0 is the first node added, 1 is the second, and so on.

SetAcceptCallback is used to allow the developer to perform connection initialization steps.

AddChildNode registers a child node that messages can be sent to for processing. The order of which child nodes are added determines the child_id associated with the node: 0 is the first child, 1 is the second, and so on. **AddChildNode** does not create connections to the child nodes, it is up to the thread initialization callback in **SetThreadStartupCallback** to handle that.

EnableMonitoring enables a HTTP server running at the given port that exposes the following endpoints: `/topology` and `/child_stats`. Both of these endpoints produce JSON strings that provide monitoring data.

RegisterQueryCallback registers a message handler for a given message type that is called when a message of that type is received. The message handler is blocking, so it should avoid calls to long I/O operations. The handler can make requests to lower level tiers by using the provided *FanoutManager* object, which will automatically call a user-provided continuation function to continue processing when all the replies have been received or the request times out. The continuation function will also be provided with a *FanoutManager* object if additional requests to lower tiers are required.

The methods in *FanoutManager* to perform fan-in and fan-out communications are **Fanout** and **FanoutAll**. **Fanout** is used to send potentially different messages to a few select child nodes for processing. *originating_query* is the original message from the higher tier that will be passed to the continuation. It must be `std::move`d, as the *FanoutManager* will take ownership of *originating_query*. *requests* is an array of *FanoutRequest* objects, where each object includes the *child_id* of the destination child node, the message type, size of the payload data, and the data itself. The *FanoutManager* does not take ownership of the payload data, as it will copy it into the network buffers. *num_requests* is the size of the *requests* array. *callback* is the continuation function that will be invoked when the fan-out/fan-in is completed. *timeout_ms* is the amount of time in milliseconds to wait for results to return before timing out and invoking the continuation with the partial results. By default this value is 0.0, which means that the request will never time out. **FanoutAll** is similar to **Fanout**, except that it will send the given message to all of the child nodes. The *child_id* field of

the *request* object is ignored in this case.

The continuation function called after the fan-in/fan-out is given the results of the fan-in/fan-out in a *FanoutReplyTracker* object. The *FanoutReplyTracker* object contains information on all the messages sent to the lower tier, including messages without a response because they timed out. The response payload data is owned by the *FanoutReplyTracker* object, and if it is needed later in a future continuation/callback, should be `std::move`d to preserve it. After processing the replies, the continuation function can either continue making requests to the lower tier using the provided *FanoutManager* object or to send a response to the original message from the higher tier with the provided *QueryContext*.

RegisterRequestType is used to inform the ParentServerNode that it is capable of sending messages of the specified type. Sending a message type that was not registered is an error.

```
void ThreadStartup(oldisim::NodeThread& thread,
                   oldisim::FanoutManager& fanout_manager) {
  // Connect to the two children with 20 connections each
  fanout_manager.MakeChildConnections(0, 20);
  fanout_manager.MakeChildConnections(1, 20);
}

void RequestHandler(oldisim::NodeThread& thread,
                    oldisim::FanoutManager& fanout_manager,
                    oldisim::QueryContext& context) {
  // Send a message of type 1 and content "0" to all children
  oldisim::FanoutRequest request;
  request.request_type = 1;
  request.request_data = "0";
  request.request_data_length = 1;

  fanout_manager.FanoutAll(std::move(context), request, FanoutDone);
}

void FanoutDone(oldisim::QueryContext& originating_query,
                const oldisim::FanoutReplyTracker& results) {
  // Send back the data to higher tier
  originating_query.SendResponse("0", 1);
}

int main(int argc, char** argv) {
  oldisim::ParentNodeServer server(1234); // Create server on port 1234
  // Set thread startup callback to create connections
  server.SetThreadStartupCallback(ThreadStartup);
  server.RegisterQueryCallback(0, RequestHandler); // Handle messages of type 0
  server.RegisterRequestType(1); // Can send children messages of type 1
  server.AddChildNode("leaf1", 1234); // Add child nodes
  server.AddChildNode("leaf2", 1234);
  server.EnableMonitoring(8080); // Enable remote monitoring
  server.Run(4, true); // Start with 4 worker threads and with thread pinning

  return 0;
}
```

Figure A.14: Sample ParentNodeServer code

A.4 Implementation details for OLDIsim

In this section we describe the internal implementation details for *OLDIsim*. This information could be useful to developers wishing to further optimize *OLDIsim* or to understand performance subtleties of applications written on top of *OLDIsim*.

A.4.1 Event handling

OLDIsim uses libevent2 [107] to handle events, such as incoming connections, incoming messages, timeout timers, etc. For scalability purposes, there is one *event_base* per worker-thread that handles the events for each thread. The main thread (i.e. the thread that calls **Run**) has one *event_base* to handle new connections. *OLDIsim* uses a connection load balancing model similar to memcached, in that new connections are assigned round-robin to worker threads for connection handling. When a new connection is established, the main thread will select a worker-thread to assign the connection to, put the connection fd into a queue for that thread, and activate an event telling the worker thread that it has a new connection. This is the only explicit locking that occurs between the main thread and the worker threads.

When a worker-thread receives a complete message from a connection, it will take one of two actions depending on whether load balancing is enabled. If load balancing is not enabled, it will immediately call the user-provided callback to process the message. For the load-balancing case, applicable only to LeafNodeServers, refer to Section A.4.2.

A.4.2 LeafNodeServer load-balancing

OLDIsim supports worker-thread load balancing for the LeafNodeServer, as the bulk of the computation should occur there. The load-balancing mechanism is similar to task-stealing parallel runtimes, such as Cilk [11]. When enabled, each worker-thread has a lock-free task queue (provided by Boost C++ library's `lockfree` implementation) that holds outstanding messages. When this task queue has elements in it, an event will be registered with the thread's *event_base* to process messages from its local queue. To enable load-balancing via task-stealing, whenever new messages come in, the thread will also wake other threads to perform task-stealing. If a worker-thread is unable to steal from all other threads, it will go back to sleep until an event wakes it up again. To ensure that worker threads do not spend all their time processing requests, the *lb_process_request_batch_size* parameter controls the maximum number of requests that can be processed before it will check for new work from the connections it is responsible for. Compared to parallel task-stealing runtimes, the task-stealing in *OLDIsim* will steal from the same end of the queue that the owner thread dequeues from, the reason behind this being to drain the queue in the same order that requests arrive in to minimize queueing delay.

We show the benefits of using load-balancing in Figure A.15. For this experiment, we used the **LeafNode** from the *search* example workload (see Section A.5 and measured the latency of requests with and without load-balancing enabled. The benefits of load-balancing are especially pronounced for tail latencies. This is

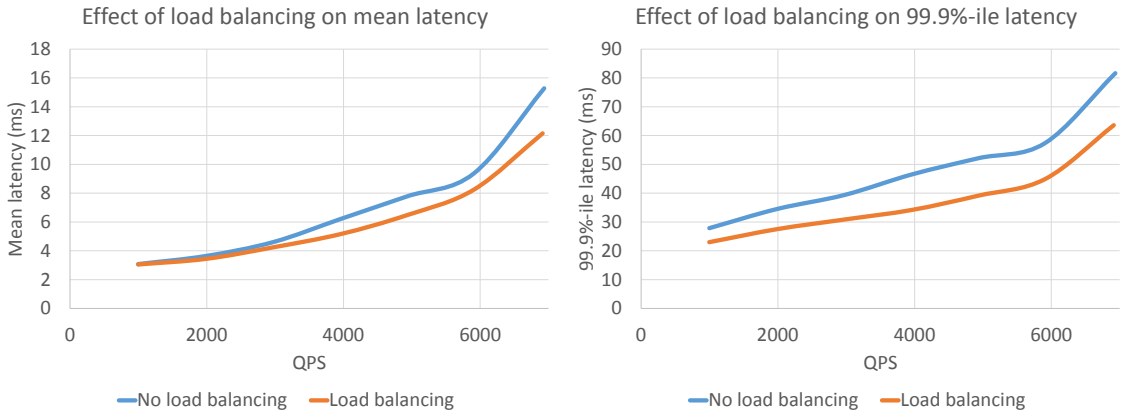

(a) Mean latency comparison

(b) 99.9%-ile latency comparison

Figure A.15: Different types of nodes in *OLDIsim*

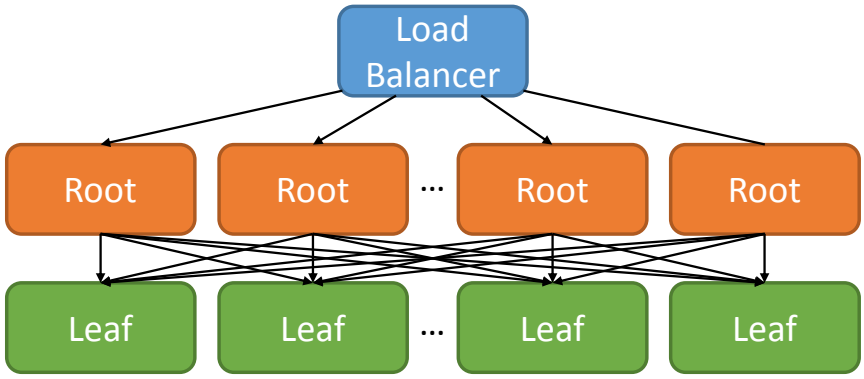

Figure A.16: Workload topology for *websearch*

because of the reduction of queueing delay caused by load-balancing, where messages that would be stuck behind a long-running query are instead processed elsewhere.

A.5 Sample websearch workload

We provide a sample workload for *OLDIsim* modeled off of Google websearch called *search*. It can be found in the `workloads/search` directory. While it does not perform the same computation as actual Google websearch, it has approximately the same communication patterns and normalized request processing latency distributions. *search* showcases the ease of writing *OLDIsim* applications, as the source code for the entire benchmark is less than 1000 lines of code.

We show the topology of *search* in Figure A.16, which closely matches the topology of production Google websearch. There is a top-level **Load Balancer** node that performs round-robin load-balancing between the

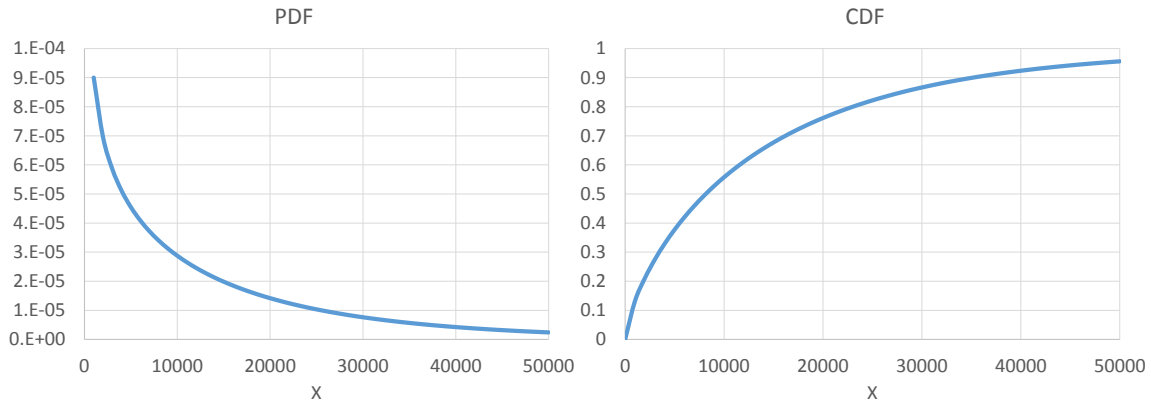

(a) PDF (b) CDF

Figure A.17: PDF and CDF of $\Gamma(\alpha = 0.7, \beta = 20000)$

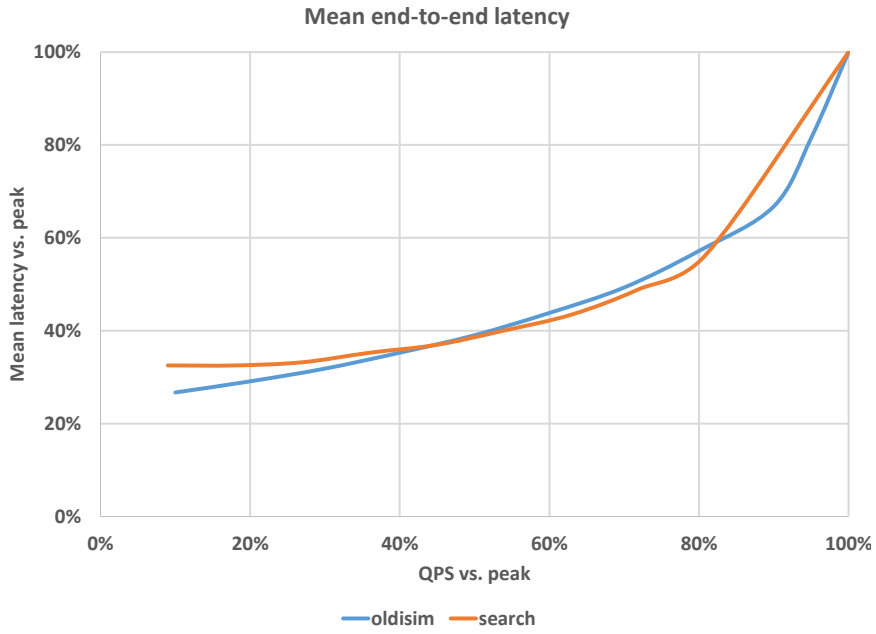

Figure A.18: Comparison of latency between Google websearch and *websearch* on *OLDIsim*.

various **Root** nodes. Each **Root** node then queries all the **Leaf** nodes in the system, only producing a result when all the **Leaf** nodes have responded.

The **Leaf** nodes do not actually perform searches, but they do execute an instruction mix to simulate some microarchitectural aspects of search: a low CPI and a high number of data-cache and instruction-cache misses. The instruction mix is looped sufficient times to produce a request processing time distribution that has the same shape as request processing latencies observed in production Google websearch. While the

absolute values of the distribution obviously do not correspond to absolute latencies, the best fit model we found is a $\Gamma(\alpha = 0.7, \beta = 20000)$ distribution, which we show in Figure A.17. Combined with the topology of *search*, we validate that the end-to-end latencies observed at the test driver closely match the shape of end-to-end latencies observed for production websearch, as shown in Figure A.18.

search is included in the Google PerfKitBenchmarker [40, 148] to benchmark the scaling efficiency of various public clouds. As a metric, scaling efficiency captures the trade-offs of scaling-out the service to handle larger datasets when a workload cannot fit on a single node. To measure scaling efficiency, the benchmark first finds the maximum QPS supported by the system when only running with one leaf node while meeting a latency service level objective (SLO) target (QPS_1). Then the number of leaf nodes (l) is increased and the corresponding maximum QPS that meets the SLO is recorded (QPS_l). The scaling efficiency is computed as $E_l = \frac{QPS_l}{QPS_1}$. As the number of leaf nodes is increased, the scaling efficiency is expected to decrease due to probability: the slowest leaf node will determine the overall query latency, and more leaf nodes means more chances of a slow leaf node. On public clouds, interference caused by co-located workloads, jitter in the network, etc. can decrease the scaling efficiency further. Thus, *search* captures performance variability in scaling efficiency, where an environment with higher performance variability will suffer from lower scaling efficiencies.

A.6 Conclusions

In conclusion, *OLDIsim* is a benchmarking framework that fills the need for a performant yet easy to use toolkit to develop scale-out applications. We show that *OLDIsim* takes advantage of multiple cores and multiple threads to scale up performance on a single node, while exposing APIs to handle communication patterns for scaling-out on several nodes. By abstracting away boilerplate logic for handling networking and multithreading, *OLDIsim* makes it easy for developers to use to write their own scale-out benchmarks. We also include *search*, an example *OLDIsim* benchmark that is also included in the open-source Google PerfKitBenchmarker. *OLDIsim* is released as an open-source project under the Apache 2.0 license.

A.7 Acknowledgements

OLDIsim was developed with the support of several teams at Google while David Lo was an intern there. Rama Govindaraju, Liqun Cheng, and Hui Huang from the Platforms Performance Team and Anthony Voellm, Ivan Filho, and Connor McCoy from the Cloud Performance Team were instrumental in the development of OLDIsim.

Bibliography

[1] ADVANCED MICRO DEVICES, INC. The New AMD Opteron™ Processor Core Technology, 2011.

[2] AL-FARES, M., LOUKISSAS, A., AND VAHDAT, A. A Scalable, Commodity Data Center Network Architecture. In *Proc. of the ACM SIGCOMM 2008 Conference on Data Communication* (New York, NY, 2008), SIGCOMM '08, ACM.

[3] ALIZADEH, M., GREENBERG, A., MALTZ, D. A., PADHYE, J., PATEL, P., PRABHAKAR, B., SENGUPTA, S., AND SRIDHARAN, M. Data Center TCP (DCTCP). In *Proc. of the ACM SIGCOMM 2010 Conference* (New York, NY, 2010), SIGCOMM '10, ACM.

[4] AYDIN, H., MELHEM, R., MOSSE, D., AND MEJIA-ALVAREZ, P. Power-Aware Scheduling for Periodic Real-Time Tasks.

[5] BARROSO, L., AND HLZLE, U. The Case for Energy-Proportional Computing.

[6] BARROSO, L. A., CLIDARAS, J., AND HÖLZLE, U. *The Datacenter as a Computer: An Introduction to the Design of Warehouse-Scale Machines*, second ed. Morgan & Claypool, 2013.

[7] BARROSO, L. A., AND HÖLZLE, U. *The Datacenter as a Computer: An Introduction to the Design of Warehouse-Scale Machines*. Morgan & Claypool, 2009.

[8] BELAY, A., PREKAS, G., KLIMOVIC, A., GROSSMAN, S., KOZYRAKIS, C., AND BUGNION, E. IX: A Protected Dataplane Operating System for High Throughput and Low Latency. In *11th USENIX Symposium on Operating Systems Design and Implementation (OSDI 14)* (10 2014), USENIX Association.

[9] BIENIA, C., KUMAR, S., SINGH, J. P., AND LI, K. The PARSEC benchmark suite: characterization and architectural implications. In *PACT 2008* (2008).

[10] BLAGODUROV, S., ZHURAVLEV, S., DASHTI, M., AND FEDOROVA, A. A Case for NUMA-aware Contention Management on Multicore Systems. In *Proc. of the 2011 USENIX Conference on USENIX Annual Technical Conference* (Berkeley, CA, 2011), USENIXATC'11, USENIX Association.

[11] BLUMOFE, R. D., JOERG, C. F., KUSZMAUL, B. C., LEISERSON, C. E., RANDALL, K. H., AND ZHOU, Y. Cilk: An Efficient Multithreaded Runtime System. *SIGPLAN Not. 30*, 8 (Aug. 1995), 207–216.

[12] BOUTIN, E., EKANAYAKE, J., LIN, W., SHI, B., ZHOU, J., QIAN, Z., WU, M., AND ZHOU, L. Apollo: Scalable and Coordinated Scheduling for Cloud-Scale Computing. In *11th USENIX Symposium on Operating Systems Design and Implementation (OSDI 14)* (2014), USENIX Association.

[13] BRISCOE, B. Flow Rate Fairness: Dismantling a Religion.

[14] BROOKS, D., BOSE, P., SCHUSTER, S., JACOBSON, H., KUDVA, P., BUYUKTOSUNOGLU, A., WELLMAN, J., ZYUBAN, V., GUPTA, M., AND COOK, P. Power-aware microarchitecture: design and modeling challenges for next-generation microprocessors.

[15] BROWN, M. A. Traffic Control HOWTO. http://linux-ip.net/articles/Traffic-Control-HOWTO/.

[16] CARVALHO, M., CIRNE, W., BRASILEIRO, F., AND WILKES, J. Long-term SLOs for Reclaimed Cloud Computing Resources. In *Proc. of SOCC* (12 2014).

[17] CHARLES, J., JASSI, P., ANANTH, N., SADAT, A., AND FEDOROVA, A. Evaluation of the Intel ® Core ™ i7 Turbo Boost feature. In *IISWC 2009* (2009).

[18] CHEN, Y., ALSPAUGH, S., BORTHAKUR, D., AND KATZ, R. Energy efficiency for large-scale mapreduce workloads with significant interactive analysis. In *Proc. of the 7th ACM european Conf. on Computer Systems* (2012).

[19] CHUN, B.-G., IANNACCONE, G., IANNACCONE, G., KATZ, R., LEE, G., AND NICCOLINI, L. An energy case for hybrid datacenters.

[20] CISCO SYSTEMS, INC. Cisco Global Cloud Index: Forecast and Methodology 20132018 White Paper. http://www.cisco.com/c/en/us/solutions/collateral/service-provider/global-cloud-index-gci/Cloud_Index_White_Paper.html, 2013.

[21] COOK, H., MORETO, M., BIRD, S., DAO, K., PATTERSON, D. A., AND ASANOVIC, K. A Hardware Evaluation of Cache Partitioning to Improve Utilization and Energy-efficiency While Preserving Responsiveness. In *Proc. of the 40th Annual Intl. Symp. on Computer Architecture* (2013), ISCA '13.

[22] CURINO, C., DIFALLAH, D. E., DOUGLAS, C., KRISHNAN, S., RAMAKRISHNAN, R., AND RAO, S. Reservation-based Scheduling: If Youre Late Dont Blame Us! In *Proc. of the 5th annual Symposium on Cloud Computing* (2014).

[23] CURK, T., DEMSAR, J., XU, Q., LEBAN, G., PETROVIC, U., BRATKO, I., SHAULSKY, G., AND ZUPAN, B. Microarray data mining with visual programming.

[24] DE KUNDER, M. WorldWideWebSize.com — The size of the World Wide Web (The Internet). http://www.worldwidewebsize.com/, 2015.

[25] DEAN, J. Challenges in Building Large-scale Information Retrieval Systems: Invited Talk. In *Proc. of the 2nd ACM Intl. Conf. on Web Search and Data Mining* (2009), WSDM '09.

[26] DEAN, J., AND BARROSO, L. A. The tail at scale.

[27] DEGRANDIS, W. Power Considerations in Siting Data Centers. http://www.datacenterknowledge.com/archives/2011/02/08/power-considerations-in-siting-data-centers/, 2011.

[28] DELIMITROU, C., AND KOZYRAKIS, C. Paragon: QoS-Aware Scheduling for Heterogeneous Datacenters. In *Proc. of the 18th Intl. Conf. on Architectural Support for Programming Languages and Operating Systems (ASPLOS)* (2013), Houston, TX, USA, 2013.

[29] DELIMITROU, C., AND KOZYRAKIS, C. Quasar: Resource-Efficient and QoS-Aware Cluster Management. In *Proc. of the Nineteenth International Conference on Architectural Support for Programming Languages and Operating Systems (ASPLOS)* (2014).

[30] DENNARD, R. H., CAI, J., AND KUMAR, A. A perspective on todays scaling challenges and possible future directions. *Solid-State Electronics 51*, 4 (2007), 518–525.

[31] EBRAHIMI, E., LEE, C. J., MUTLU, O., AND PATT, Y. N. Fairness via Source Throttling: A Configurable and High-performance Fairness Substrate for Multi-core Memory Systems. In *Proc. of the Fifteenth Edition of ASPLOS on Architectural Support for Programming Languages and Operating Systems* (New York, NY, 2010), ASPLOS XV, ACM.

[32] ESMAEILZADEH, H., BLEM, E., ST.AMANT, R., SANKARALINGAM, K., AND BURGER, D. Dark silicon and the end of multicore scaling. In *Computer Architecture (ISCA), 2011 38th Annual International Symposium on* (June 2011).

[33] EYERMAN, S., AND EECKHOUT, L. A Counter Architecture for Online DVFS Profitability Estimation.

[34] FAN, X., WEBER, W.-D., AND BARROSO, L. A. Power Provisioning for a Warehouse-sized Computer. In *The 34th ACM International Symposium on Computer Architecture* (2007).

[35] FERDMAN, M., ADILEH, A., KOCBERBER, O., VOLOS, S., ALISAFAEE, M., JEVDJIC, D., KAYNAK, C., POPESCU, A. D., AILAMAKI, A., AND FALSAFI, B. Clearing the clouds: a study of emerging scale-out workloads on modern hardware. In *ASPLOS 2012* (2012).

[36] FLAUTNER, K., AND MUDGE, T. Vertigo: Automatic Performance-setting for Linux.

[37] GE, R., FENG, X., CHUN FENG, W., AND CAMERON, K. CPU MISER: A Performance-Directed, Run-Time System for Power-Aware Clusters. In *Parallel Processing, 2007. ICPP 2007. Intl. Conf. on* (2007).

[38] GLANZ, J. Power, Pollution and the Internet.

[39] GOODFELLOW, I. J., BULATOV, Y., IBARZ, J., ARNOUD, S., AND SHET, V. Multi-digit number recognition from street view imagery using deep convolutional neural networks. *arXiv preprint arXiv:1312.6082* (2013).

[40] GOOGLE INC. GoogleCloudPlatform/PerfKitBenchmarker. https://github.com/GoogleCloudPlatform/PerfKitBenchmarker.

[41] GOOGLE INC. Protocol Buffers. https://developers.google.com/protocol-buffers/.

[42] GOOGLE INC. Efficiency: How we do it. https://www.google.com/about/datacenters/efficiency/internal/, 2015.

[43] GOVINDAN, S., LIU, J., KANSAL, A., AND SIVASUBRAMANIAM, A. Cuanta: quantifying effects of shared on-chip resource interference for consolidated virtual machines. In *Proc. of the 2nd ACM Symposium on Cloud Computing* (2011).

[44] GUO, F., KANNAN, H., ZHAO, L., ILLIKKAL, R., IYER, R., NEWELL, D., SOLIHIN, Y., AND KOZYRAKIS, C. From Chaos to QoS: Case Studies in CMP Resource Management.

[45] GUO, F., SOLIHIN, Y., ZHAO, L., AND IYER, R. A Framework for Providing Quality of Service in Chip Multi-Processors. In *Proc. of the 40th Annual IEEE/ACM International Symposium on Microarchitecture* (2007), MICRO 40, IEEE Computer Society.

[46] HAMILTON, J. Overall Data Center Costs. http://perspectives.mvdirona.com/2010/09/18/OverallDataCenterCosts.aspx, 2010.

[47] HAMILTON, J. Keynote. In *ISCA 2011* (2011).

[48] HARDAVELLAS, N., FERDMAN, M., FALSAFI, B., AND AILAMAKI, A. Toward Dark Silicon in Servers.

[49] HARRIS, S. Microsoft Reinvents Datacenter Power Backup with New Open Compute Project Specification. http://blogs.technet.com/b/server-cloud/archive/2015/03/10/microsoft-reinvents-datacenter-power-backup-with-new-open-compute-project-speci aspx, 2015.

[50] HERDRICH, A., ILLIKKAL, R., IYER, R., NEWELL, D., CHADHA, V., AND MOSES, J. Rate-based QoS Techniques for Cache/Memory in CMP Platforms. In *ICS-23* (2009).

[51] HINDMAN, B., KONWINSKI, A., ZAHARIA, M., GHODSI, A., JOSEPH, A. D., KATZ, R., SHENKER, S., AND STOICA, I. Mesos: a platform for fine-grained resource sharing in the data center. In *Proc. of the 8th USENIX Conf. on Networked systems design and implementation* (2011), NSDI'11.

[52] HSU, L. R., REINHARDT, S. K., IYER, R., AND MAKINENI, S. Communist, Utilitarian, and Capitalist Cache Policies on CMPs: Caches As a Shared Resource. In *Proc. of the 15th International Conference on Parallel Architectures and Compilation Techniques* (New York, NY, 2006), PACT '06, ACM.

[53] HUANG, M., RENAU, J., YOO, S.-M., AND TORRELLAS, J. A Framework for Dynamic Energy Efficiency and Temperature Management. In *Proc. of the 33rd Annual ACM/IEEE Intl. Symp. on Microarchitecture* (2000), MICRO 33.

[54] INTEL CORPORATION. Addressing power and thermal challenges in the datacenter,.

[55] INTEL CORPORATION. Intel®Xeon®Processor E5-2667 v2 (25M Cache, 3.30GHz). http://ark.intel.com/products/75273/Intel-Xeon-Processor-E5-2667-v2-25M-Cache-3_30-GHz.

[56] INTEL CORPORATION. Linux/drivers/idle/intel_idle.c. http://lxr.free-electrons.com/source/drivers/idle/intel_idle.c.

[57] INTEL CORPORATION. Serial ATA II Native Command Queuing Overview. http://download.intel.com/support/chipsets/imsm/sb/sata2_ncq_overview.pdf, 2003.

[58] INTEL CORPORATION. Intel® Turbo Boost Technology in Intel® Core™ Microarchitecture (Nehalem) Based Processors, 2008.

[59] INTEL CORPORATION. Intel®Core™i7 Processor Family for the LGA-2011 Socket.

[60] INTEL CORPORATION. Intel®64 and IA-32 Architectures Software Developer's Manual.

[61] IPERF. Iperf - The TCP/UDP Bandwidth Measurement Tool. https://iperf.fr/.

[62] ISCI, C., BUYUKTOSUNOGLU, A., CHER, C.-Y., BOSE, P., AND MARTONOSI, M. An Analysis of Efficient Multi-Core Global Power Management Policies: Maximizing Performance for a Given Power Budget. In *MICRO-39* (2006).

[63] ISCI, C., BUYUKTOSUNOGLU, A., AND MARTONOSI, M. Long-term workload phases: duration predictions and applications to DVFS. In *MICRO-38* (2005).

[64] ISCI, C., AND MARTONOSI, M. Runtime power monitoring in high-end processors: methodology and empirical data. In *MICRO-36* (2003).

[65] ISSARIYAKUL, T., AND HOSSAIN, E. *Introduction to Network Simulator NS2*, 1st ed. Springer Publishing Company, Incorporated, 2010.

[66] ITU. Number of worldwide internet users from 2000 to 2014 (in millions). http://www.statista.com/statistics/273018/number-of-internet-users-worldwide/, 2015.

[67] IYER, R. CQoS: A Framework for Enabling QoS in Shared Caches of CMP Platforms. In *Proc. of the 18th Annual International Conference on Supercomputing* (New York, NY, 2004), ICS '04, ACM.

[68] IYER, R., ZHAO, L., GUO, F., ILLIKKAL, R., MAKINENI, S., NEWELL, D., SOLIHIN, Y., HSU, L., AND REINHARDT, S. QoS Policies and Architecture for Cache/Memory in CMP Platforms. In *Proc. of the 2007 ACM SIGMETRICS Intl. Conf. on Measurement and Modeling of Computer Systems* (2007), SIGMETRICS '07.

[69] JAHRE, M., GRANNAES, M., AND NATVIG, L. A Quantitative Study of Memory System Interference in Chip Multiprocessor Architectures. In *HPCC 2009* (2009).

[70] JALEEL, A., HASENPLAUGH, W., QURESHI, M., SEBOT, J., STEELY, JR., S., AND EMER, J. Adaptive insertion policies for managing shared caches. In *PCT 2008* (2008).

[71] JANAPA REDDI, V., LEE, B. C., CHILIMBI, T., AND VAID, K. Web search using mobile cores: quantifying and mitigating the price of efficiency.

[72] JEONG, M. K., EREZ, M., SUDANTHI, C., AND PAVER, N. A QoS-aware Memory Controller for Dynamically Balancing GPU and CPU Bandwidth Use in an MPSoC. In *Proc. of the 49th Annual Design Automation Conference* (New York, NY, 2012), DAC '12, ACM.

[73] JERGER, N., VANTREASE, D., AND LIPASTI, M. An Evaluation of Server Consolidation Workloads for Multi-Core Designs. In *Workload Characterization, 2007. IISWC 2007. IEEE 10th Intl. Symp. on* (2007).

[74] JEYAKUMAR, V., ALIZADEH, M., MAZIRES, D., PRABHAKAR, B., KIM, C., AND GREENBERG, A. EyeQ: Practical Network Performance Isolation at the Edge. In *Proc. of the 10th USENIX Conference on Networked Systems Design and Implementation* (Berkeley, CA, 2013), nsdi'13, USENIX Association.

[75] KANEV, S., HAZELWOOD, K., WEI, G.-Y., AND BROOKS, D. Tradeoffs between Power Management and Tail Latency in Warehouse-Scale Applications. In *IISWC* (2014).

[76] KAPOOR, R., PORTER, G., TEWARI, M., VOELKER, G. M., AND VAHDAT, A. Chronos: Predictable Low Latency for Data Center Applications. In *Proc. of the Third ACM Symposium on Cloud Computing* (New York, NY, 2012), SoCC '12, ACM.

[77] KARPATHY, A., AND FEI-FEI, L. Deep visual-semantic alignments for generating image descriptions. *arXiv preprint arXiv:1412.2306* (2014).

[78] KASTURE, H., AND SANCHEZ, D. Ubik: Efficient Cache Sharing with Strict QoS for Latency-Critical Workloads. In *Proc. of the 19th international conference on Architectural Support for Programming Languages and Operating Systems (ASPLOS-XIX)* (March 2014).

[79] KHARE, R., AND CUTTING, D. Nutch: A flexible and scalable open-source web search engine.

[80] KIM, W., GUPTA, M., WEI, G.-Y., AND BROOKS, D. System level analysis of fast, per-core DVFS using on-chip switching regulators. In *HPCA 2008* (2008).

[81] KONDO, M., SASAKI, H., AND NAKAMURA, H. Improving Fairness, Throughput and Energy-efficiency on a Chip Multiprocessor Through DVFS.

[82] LANG, W., AND PATEL, J. M. Energy management for mapreduce clusters.

[83] LE, Q., RANZATO, M., MONGA, R., DEVIN, M., CHEN, K., CORRADO, G., DEAN, J., AND NG, A. Building high-level features using large scale unsupervised learning. In *International Conference in Machine Learning* (2012).

[84] LEE, J., AND KIM, N. S. Optimizing Throughput of Power- and Thermal-constrained Multicore Processors Using DVFS and Per-core Power-gating. In *Proc. of the 46th Annual Design Automation Conf.* (2009), DAC '09.

[85] LEVERICH, J., AND KOZYRAKIS, C. On the Energy (in)Efficiency of Hadoop Clusters.

[86] LEVERICH, J., AND KOZYRAKIS, C. Reconciling High Server Utilization and Sub-millisecond Quality-of-Service. In *SIGOPS European Conf. on Computer Systems (EuroSys)* (2014).

[87] LEVERICH, J., MONCHIERO, M., TALWAR, V., RANGANATHAN, P., AND KOZYRAKIS, C. Power Management of Datacenter Workloads Using Per-Core Power Gating.

[88] LEVERICH, J. B. *Future Scaling of Datacenter Power-efficiency*. PhD thesis, Stanford University, 2014.

[89] LI, B., ZHAO, L., IYER, R., PEH, L.-S., LEDDIGE, M., ESPIG, M., LEE, S. E., AND NEWELL, D. CoQoS: Coordinating QoS-aware Shared Resources in NoC-based SoCs.

[90] LIM, K., MEISNER, D., SAIDI, A. G., RANGANATHAN, P., AND WENISCH, T. F. Thin Servers with Smart Pipes: Designing SoC Accelerators for Memcached. In *Proc. of the 40th Annual International Symposium on Computer Architecture* (2013).

[91] LIM, K., RANGANATHAN, P., CHANG, J., PATEL, C., MUDGE, T., AND REINHARDT, S. Understanding and Designing New Server Architectures for Emerging Warehouse-Computing Environments.

[92] LIM, K., TURNER, Y., SANTOS, J. R., AUYOUNG, A., CHANG, J., RANGANATHAN, P., AND WENISCH, T. F. System-level Implications of Disaggregated Memory. In *Proc. of the 2012 IEEE 18th International Symposium on High-Performance Computer Architecture* (2012), HPCA '12, IEEE Computer Society.

[93] LIN, C., AND BRANDT, S. A. Improving Soft Real-Time Performance Through Better Slack Reclaiming. In *Proc. of the 26th IEEE Intl. Real-Time Systems Symp.* (2005), RTSS '05.

[94] LIN, J., LU, Q., DING, X., ZHANG, Z., ZHANG, X., AND SADAYAPPAN, P. Gaining insights into multicore cache partitioning: Bridging the gap between simulation and real systems. In *High Performance Computer Architecture, 2008. HPCA 2008. IEEE 14th International Symposium on* (Feb 2008).

[95] LIU, H. A Measurement Study of Server Utilization in Public Clouds. In *Dependable, Autonomic and Secure Computing (DASC), 2011 IEEE Ninth Intl. Conf. on* (2011).

[96] LIU, R., KLUES, K., BIRD, S., HOFMEYR, S., ASANOVI, K., AND KUBIATOWICZ, J. Tessellation: Space-time Partitioning in a Manycore Client OS. In *Proc. of the First USENIX Conference on Hot Topics in Parallelism* (Berkeley, CA, 2009), HotPar'09, USENIX Association.

[97] LIU, Y., DRAPER, S. C., AND KIM, N. S. SleepScale: Runtime Joint Speed Scaling and Sleep States Management for Power Efficient Data Centers. In *Proceeding of the 41st Annual International Symposium on Computer Architecuture* (Piscataway, NJ, 2014), ISCA '14, IEEE Press.

[98] LO, D., CHENG, L., GOVINDARAJU, R., BARROSO, L. A., AND KOZYRAKIS, C. Towards energy proportionality for large-scale latency-critical workloads. *2014 ACM/IEEE 41st International Symposium on Computer Architecture (ISCA) 0* (2014), 301–312. ©2014 IEEE. Reprinted with permission.

[99] LO, D., CHENG, L., GOVINDARAJU, R., RANGANATHAN, P., AND KOZYRAKIS, C. Heracles: Improving Resource Efficiency at Scale. *2015 ACM/IEEE 42nd International Symposium on Computer Architecture (ISCA)* (2015).

[100] LO, D., AND KOZYRAKIS, C. Dynamic management of TurboMode in modern multi-core chips. In *High Performance Computer Architecture (HPCA), 2014 IEEE 20th International Symposium on* (Feb 2014), pp. 603–613. ©2014 IEEE. Reprinted with permission.

[101] MALLADI, K. T., LEE, B. C., NOTHAFT, F. A., KOZYRAKIS, C., PERIYATHAMBI, K., AND HOROWITZ, M. Towards Energy-proportional Datacenter Memory with Mobile DRAM.

[102] MANIKANTAN, R., RAJAN, K., AND GOVINDARAJAN, R. Probabilistic Shared Cache Management (PriSM). In *Proc. of the 39th Annual International Symposium on Computer Architecture* (Washington, DC, 2012), ISCA '12, IEEE Computer Society.

[103] MANYIKA, J., AND ROXBURGH, C. The great transformer: The impact of the Internet on economic growth and prosperity. *McKinsey Global Institute, October 1* (2011).

[104] MARS, J., TANG, L., SKADRON, K., SOFFA, M., AND HUNDT, R. Increasing Utilization in Modern Warehouse-Scale Computers Using Bubble-Up.

[105] MARS, J., TANG, L., AND SOFFA, M. L. Directly characterizing cross core interference through contention synthesis. In *HiPEAC 2011* (2011), ACM.

[106] MARSHALL, P., KEAHEY, K., AND FREEMAN, T. Improving Utilization of Infrastructure Clouds. In *Proc. of the 2011 11th IEEE/ACM International Symposium on Cluster, Cloud and Grid Computing* (2011).

[107] MATHEWSON, N., AND PROVOS, N. libevent an event notification library. http://libevent.org/.

[108] MCKINSEY & COMPANY. Revolutionizing data center efficiency.

[109] MEISNER, D., GOLD, B. T., AND WENISCH, T. F. PowerNap: Eliminating Server Idle Power. In *Proc. of the 14th Intl. Conf. on Architectural Support for Programming Languages and Operating Systems* (2009), ASPLOS XIV.

[110] MEISNER, D., SADLER, C. M., BARROSO, L. A., WEBER, W.-D., AND WENISCH, T. F. Power Management of Online Data-Intensive Services. In *Proc. of the 38th ACM Intl. Symp. on Computer Architecture* (2011).

[111] MEMCACHED. memcached. http://memcached.org/.

[112] MENAGE, P. CGROUPS. https://www.kernel.org/doc/Documentation/cgroups/cgroups.txt.

[113] MERKEL, A., STOESS, J., AND BELLOSA, F. Resource-conscious scheduling for energy efficiency on multicore processors. In *EuroSys 2010* (2010).

[114] MURALIDHARA, S. P., SUBRAMANIAN, L., MUTLU, O., KANDEMIR, M., AND MOSCIBRODA, T. Reducing Memory Interference in Multicore Systems via Application-aware Memory Channel Partitioning. In *Proc. of the 44th Annual IEEE/ACM International Symposium on Microarchitecture* (New York, NY, 2011), MICRO-44, ACM.

[115] NAGARAJAN, V., AND GUPTA, R. ECMon: Exposing Cache Events for Monitoring. In *Proc. of the 36th Annual International Symposium on Computer Architecture* (New York, NY, 2009), ISCA '09, ACM.

[116] NATHUJI, R., KANSAL, A., AND GHAFFARKHAH, A. Q-Clouds: Managing Performance Interference Effects for QoS-Aware Clouds. In *Proc. of EuroSys, France* (2010).

[117] NESBIT, K., AGGARWAL, N., LAUDON, J., AND SMITH, J. Fair Queuing Memory Systems. In *Microarchitecture, 2006. MICRO-39. 39th Annual IEEE/ACM International Symposium on* (Dec 2006).

[118] NOVAKOVIC, D., VASIC, N., NOVAKOVIC, S., KOSTIC, D., AND BIANCHINI, R. DeepDive: Transparently Identifying and Managing Performance Interference in Virtualized Environments. In *Proc. of the USENIX Annual Technical Conference (ATC'13)* (2013).

[119] PATEL, C. D., AND RANGANATHAN, P. Enterprise Power and Cooling: A Chip-to-DataCenter Perspective.

[120] PATEL, C. D., AND SHAH, A. J. Cost Model for Planning, Development and Operation of a Data Center.

[121] PATTARA-AUKOM, W., BANERJEE, S., AND KRISHNAMURTHY, P. Starvation prevention and quality of service in wireless LANs. In *Wireless Personal Multimedia Communications, 2002. The 5th International Symposium on* (Oct 2002), vol. 3.

[122] PILLAI, P., AND SHIN, K. G. Real-time Dynamic Voltage Scaling for Low-power Embedded Operating Systems. In *Proc. of the Eighteenth ACM Symp. on Operating Systems Principles* (2001), SOSP '01.

[123] PODLESNY, M., AND WILLIAMSON, C. Solving the TCP-Incast Problem with Application-Level Scheduling. In *Modeling, Analysis Simulation of Computer and Telecommunication Systems (MASCOTS), 2012 IEEE 20th International Symposium on* (Aug 2012).

[124] POUWELSE, J., LANGENDOEN, K., AND SIPS, H. Dynamic Voltage Scaling on a Low-power Microprocessor. In *Proc. of the 7th Annual Intl. Conf. on Mobile Computing and Networking* (2001), MobiCom '01.

[125] PUTNAM, A., CAULFIELD, A. M., CHUNG, E. S., CHIOU, D., CONSTANTINIDES, K., DEMME, J., ESMAEILZADEH, H., FOWERS, J., PRASHANTH, G., JAN, G., MICHAEL, G., HAUCK, H. S., HEIL, S., HORMATI, A., KIM, J.-Y., LANKA, S., LARUS, J., PETERSON, E., POPE, S., SMITH, A., THONG, J., YI, P., AND BURGER, X. D. A Reconfigurable Fabric for Accelerating Large-scale Datacenter Services. In *Proceeding of the 41st Annual International Symposium on Computer Architecuture* (Piscataway, NJ, 2014), ISCA '14, IEEE Press.

[126] QURESHI, M. K., AND PATT, Y. N. Utility-based cache partitioning: A low-overhead, high-performance, runtime mechanism to partition shared caches. In *Proc. of the 39th Annual IEEE/ACM Intl. Symp. on Microarchitecture* (2006).

[127] RAGHAVAN, A., LUO, Y., CHANDAWALLA, A., PAPAEFTHYMIOU, M., PIPE, K. P., WENISCH, T., AND MARTIN, M. Computational sprinting. In *HPCA-2012* (2012).

[128] RAGHAVENDRA, R., RANGANATHAN, P., TALWAR, V., WANG, Z., AND ZHU, X. No "Power" Struggles: Coordinated Multi-level Power Management for the Data Center. In *Proc. of the 13th Intl. Conf. on Architectural Support for Programming Languages and Operating Systems* (2008), ASPLOS XIII.

[129] RAJAMANI, K., RAWSON, F., WARE, M., HANSON, H., CARTER, J., ROSEDAHL, T., GEISSLER, A., SILVA, G., AND HUA, H. Power-performance management on an IBM POWER7 server. In *Low-Power Electronics and Design (ISLPED), 2010 ACM/IEEE Intl. Symp. on* (2010).

[130] RANGANATHAN, P., ADVE, S., AND JOUPPI, N. P. Reconfigurable Caches and Their Application to Media Processing. In *Proc. of the 27th Annual International Symposium on Computer Architecture* (New York, NY, 2000), ISCA '00, ACM.

[131] RANGANATHAN, P., LEECH, P., IRWIN, D., AND CHASE, J. Ensemble-level Power Management for Dense Blade Servers. In *Proc. of the 33rd Annual Intl. Symp. on Computer Architecture* (2006), ISCA '06.

[132] REISS, C., TUMANOV, A., GANGER, G. R., KATZ, R. H., AND KOZUCH, M. A. Heterogeneity and Dynamicity of Clouds at Scale: Google Trace Analysis. In *ACM Symp. on Cloud Computing (SoCC)* (10 2012).

[133] ROSENBERG, C. Improving Photo Search: A Step Across the Semantic Gap. http://googleresearch.blogspot.com/2013/06/improving-photo-search-step-across.html.

[134] ROTEM, E., NAVEH, A., RAJWAN, D., ANANTHAKRISHNAN, A., AND WEISSMANN, E. Power management architecture of the 2nd generation Intel® Core™ microarchitecture, formerly codenamed Sandy Bridge. In *HotChips 23* (2011).

[135] SAHA, S., AND RAVINDRAN, B. An Experimental Evaluation of Real-time DVFS Scheduling Algorithms. In *Proc. of the 5th Annual Intl. Systems and Storage Conf.* (2012), SYSTOR '12.

[136] SANCHEZ, D., AND KOZYRAKIS, C. Scalable and Efficient Fine-Grained Cache Partitioning with Vantage.

[137] SCHURMAN, E., AND BRUTLAG, J. The User and Business Impact of Server Delays, Additional Bytes, and HTTP Chunking in Web Search.

[138] SEONG, Y. J., NAM, E. H., YOON, J. H., KIM, H., YONG CHOI, J., LEE, S., BAE, Y. H., LEE, J., CHO, Y., AND MIN, S. L. Hydra: A Block-Mapped Parallel Flash Memory Solid-State Disk Architecture.

[139] SHARIFI, A., SRIKANTAIAH, S., MISHRA, A. K., KANDEMIR, M., AND DAS, C. R. METE: Meeting End-to-end QoS in Multicores Through System-wide Resource Management. In *Proc. of the ACM SIGMETRICS Joint International Conference on Measurement and Modeling of Computer Systems* (New York, NY, 2011), SIGMETRICS '11, ACM.

[140] SHARMA, N., BARKER, S., IRWIN, D., AND SHENOY, P. Blink: Managing Server Clusters on Intermittent Power. In *Proc. of the 16th Intl. Conf. on Architectural Support for Programming Languages and Operating Systems* (2011), ASPLOS XVI.

[141] SHIN, Y., AND CHOI, K. Power conscious fixed priority scheduling for hard real-time systems. In *Design Automation Conf.* (1999).

[142] SPILIOPOULOS, V., KAXIRAS, S., AND KERAMIDAS, G. Green governors: A framework for Continuously Adaptive DVFS. In *Green Computing Conf. and Workshops (IGCC), 2011 Intl.* (2011).

[143] SRIKANTAIAH, S., KANDEMIR, M., AND WANG, Q. SHARP Control: Controlled Shared Cache Management in Chip Multiprocessors. In *Proc. of the 42Nd Annual IEEE/ACM International Symposium on Microarchitecture* (New York, NY, 2009), MICRO 42, ACM.

[144] STANDARD PERFORMANCE EVALUATION CORPORATION. SPEC CPU™ 2006. http://www.spec.org/cpu2006/.

[145] STANDARD PERFORMANCE EVALUATION CORPORATION. SPECweb2009. http://www.spec.org/web2009/.

[146] TANAKA, S., AND KOZYRAKIS, C. High Performance Hardware-Accelerated Flash Key-Value Store. In *The 2014 Non-volatile Memories Workshop (NVMW)* (2014).

[147] TANG, L., MARS, J., VACHHARAJANI, N., HUNDT, R., AND SOFFA, M. The impact of memory subsystem resource sharing on datacenter applications. In *Computer Architecture (ISCA), 2011 38th Annual International Symposium on* (June 2011).

[148] TEAM, G. C. P. P. New open source tools for measuring cloud performance. http://googlecloudplatform.blogspot.com/2015/02/new-open-source-tools-for-measuring-cloud-performance.html.

[149] THE APACHE SOFTWARE FOUNDATION. Apache Spark® - Lightning-Fast Cluster Computing! https://spark.apache.org/.

[150] THE APACHE SOFTWARE FOUNDATION. The Apache Cassandra Project. https://cassandra.apache.org/.

[151] THE APACHE SOFTWARE FOUNDATION. Welcome to Apache™ Hadoop®! https://hadoop.apache.org/.

[152] TOLIA, N., WANG, Z., MARWAH, M., BASH, C., RANGANATHAN, P., AND ZHU, X. Delivering Energy Proportionality with Non Energy-Proportional Systems-Optimizing the Ensemble.

[153] VASAN, A., SIVASUBRAMANIAM, A., SHIMPI, V., SIVABALAN, T., AND SUBBIAH, R. Worth their watts? - an empirical study of datacenter servers. In *Intl. Symp. on High-Performance Computer Architecture* (2010).

[154] VASI, N., NOVAKOVI, D., MIUIN, S., KOSTI, D., AND BIANCHINI, R. DejaVu: accelerating resource allocation in virtualized environments. In *Proc. of the seventeenth international conference on Architectural Support for Programming Languages and Operating Systems (ASPLOS)* (2012).

[155] VERMA, A., PEDROSA, L., KORUPOLU, M. R., OPPENHEIMER, D., TUNE, E., AND WILKES, J. Large-scale cluster management at Google with Borg. In *Proceedings of the European Conference on Computer Systems (EuroSys)* (Bordeaux, France, 2015).

[156] VINYALS, O., TOSHEV, A., BENGIO, S., AND ERHAN, D. Show and tell: A neural image caption generator. *arXiv preprint arXiv:1411.4555* (2014).

[157] WAKABAYASHI, D. Apple to Build Data Command Center in Arizona.

[158] WILSON, C., BALLANI, H., KARAGIANNIS, T., AND ROWTRON, A. Better Never Than Late: Meeting Deadlines in Datacenter Networks. In *Proc. of the ACM SIGCOMM 2011 Conference* (New York, NY, 2011), SIGCOMM '11, ACM.

[159] WU, C.-J., AND MARTONOSI, M. A Comparison of Capacity Management Schemes for Shared CMP Caches. In *Proc. of the 7th Workshop on Duplicating, Deconstructing, and Debunking* (2008), vol. 15, Citeseer.

[160] WU, Q., MARTONOSI, M., CLARK, D., REDDI, V., CONNORS, D., WU, Y., LEE, J., AND BROOKS, D. Dynamic-Compiler-Driven Control for Microprocessor Energy and Performance.

[161] XIE, Y., AND LOH, G. H. PIPP: Promotion/Insertion Pseudo-partitioning of Multi-core Shared Caches. In *Proc. of the 36th Annual International Symposium on Computer Architecture* (New York, NY, 2009), ISCA '09, ACM.

[162] XIE, Y., AND O'HALLARON, D. Locality in Search Engine Queries and Its Implications for Caching. In *IEEE Infocom 2002* (2002).

[163] YANG, H., BRESLOW, A., MARS, J., AND TANG, L. Bubble-flux: Precise Online QoS Management for Increased Utilization in Warehouse Scale Computers. In *Proc. of the 40th Annual Intl. Symp. on Computer Architecture* (2013), ISCA '13.

[164] ZHANG, X., TUNE, E., HAGMANN, R., JNAGAL, R., GOKHALE, V., AND WILKES, J. CPI2: CPU performance isolation for shared compute clusters. In *Proc. of the 8th ACM European Conference on Computer Systems (EuroSys)* (2013).

[165] ZHANG, Y., LAURENZANO, M. A., MARS, J., AND TANG, L. SMiTe: Precise QoS Prediction on Real-System SMT Processors to Improve Utilization in Warehouse Scale Computers. In *International Symposium on Microarchitecture (MICRO)* (2014).